UNIVERSIDADE ESTADUAL DE MARINGÁ
Centro de Ciências Biológicas
Programa de Pós-Graduação em Ciências Biológicas
Área de Concentração: Biologia Celular e Molecular

JÉSSICA CARREIRA DE PAULA

MORTE CELULAR INDUZIDA PELAS SUBSTÂNCIAS RCC, C5 E A11K3 EM PROTOZOÁRIOS PARASITAS *Leishmania amazonensis* e *Trypanosoma cruzi*

Orientador:

Prof. Dr. Celso Vataru Nakamura

Maringá

Outubro/2019

JÉSSICA CARREIRA DE PAULA

MORTE CELULAR INDUZIDA PELAS SUBSTÂNCIAS RCC, C5 E A11K3 EM PROTOZOÁRIOS PARASITAS *Leishmania amazonensis* e *Trypanosoma cruzi*

Tese de doutorado apresentado ao Programa de Pós-Graduação em Ciências Biológicas (Área de concentração – Biologia Celular e Molecular) da Universidade Estadual de Maringá para obtenção do grau de Doutor em Ciências Biológicas.

Maringá

Outubro de 2019

Dados Internacionais de Catalogação-na-Publicação (CIP)
(Biblioteca Central - UEM, Maringá - PR, Brasil)

P324m

Paula, Jéssica Carreira de

Morte celular induzida pelas substâncias RCC, C5 e A11K3 em protozoários parasitas Leishmania amazonensis e Trypanosoma cruzi / Jéssica Carreira de Paula. -- Maringá, PR, 2019.

94 f.: il. color.

Orientador: Prof. Dr. Celso Vataru Nakamura.

Tese (Doutorado) - Universidade Estadual de Maringá, Centro de Ciências Biológicas, Departamento de Biologia, Programa de Pós-Graduação em Ciências Biológicas (Biologia Celular), 2019.

1. Leishmania amazonensis. 2. Trypanosoma cruzi. 3. Doença de Chagas. 4. Dibenzilidenoacetonas. I. Nakamura, Celso Vataru, orient. II. Universidade Estadual de Maringá. Centro de Ciências Biológicas. Departamento de Biologia. Programa de Pós-Graduação em Ciências Biológicas (Biologia Celular). III. Título.

CDD 23.ed. 616.936

Márcia Regina Paiva de Brito - CRB-9/1267

JÉSSICA CARREIRA DE PAULA

MORTE CELULAR INDUZIDA PELAS SUBSTÂNCIAS RCC, C5 E A11K3 EM PROTOZOÁRIOS PARASITAS *Leishmania amazonensis* E *Trypanosoma cruzi*

Tese de doutorado apresentado ao Programa de Pós-Graduação em Ciências Biológicas (Área de concentração – Biologia Celular e Molecular) da Universidade Estadual de Maringá para obtenção do grau de Doutor em Ciências Biológicas.

Maringá – PR, 21 de outubro de 2019

BANCA EXAMINADORA

Celso Vataru Nakamura – Presidente
(Universidade Estadual de Maringá)

Sueli Fumie Yamada OgattaOgatta
(Universidade Estadual de Londrina)

Danielle Lazarin Bidóia

(Universidade Estadual de Londrina)

Juliana Cogo

(Unicesumar)

Francielle Pelegrin Garcia Geremias

(Universidade Estadual de Maringá)

BIOGRAFIA

Jéssica Carreira de Paula nasceu em Apucarana/PR em 04 de outubro de 1992. Possui graduação em Ciências Biológicas (Licenciatura) pela Universidade Estadual de Maringá (UEM) (2013). Desde a graduação tem se dedicado à pesquisa de compostos naturais e sintéticos com atividade anti-*Trypanosoma cruzi*. Em 2013 iniciou o mestrado no programa de Pós-Graduação em Ciências Biológicas (PBC), onde deu início aos trabalhos com *Leishmania*, *T. cruzi* e células de mamíferos. No ano de 2016, obteve o título de Mestre e iniciou o doutorado logo em seguida. Durante o período de doutorado, executou trabalhos com os protozoários *L. amazonensis* e *T. cruzi*. No ano de 2018, realizou um período de doutorado sanduiche na Universidade de Granada, Espanha, tendo como objetivo inserir novas técnicas no Laboratório de Inovação Tecnológica no Desenvolvimento de Fármacos e Cosméticos relacionadas a biologia molecular desses parasitos.

AGRADECIMENTOS

Ao meu marido **Rafael Ortega** que sempre esteve ao meu lado, me apoiando, incentivando e dando força nas horas de maior desespero e acompanhando nas alegrias, de fato, sem ele o doutorado não teria chegado ao fim.

A minha mãe **Solange Carreira** e ao meu avô **Alfredo Carreira** pelo eterno esforço e estímulo em fazer com que eu tivesse uma educação de qualidade.

Ao meu orientador **Prof. Dr. Celso Vataru Nakamura**, que mostrou confiança em me aceitar como aluna de iniciação científica, mestrado e doutorado incentivando a produção cientifica e acadêmica.

Aos professores **Dra. Tania Ueda-Nakamura, Dra. Maria Helena Sarragiotto** e **Dr. Edson Rodrigues Filho** pelas contribuições técnico-científicas na elaboração dos artigos.

A minha amiga **Dra. Nilma de Souza Fernandes**, pela amizade, por me aguentar e por fazer um árduo trabalho durante as correções de inglês e argumentação dos artigos científicos, além de ser o pivô do doutorado sanduiche, pois me incentivou e encontrou um orientador no exterior.

Aos meus grandes amigos de laboratório, **Juliana Kovalczuk de Oliveira, Rodolfo Bento Balbinot. Danielle Lazarin Bidóia, Thayza K. Karam, Amanda Beatriz Kawano Bakoshi, Natália Storck Ceroni** e **Gustavo Vasconcelos Gomes** pela ajuda nos experimentos e nos momentos de descontração.

Aos meus queridos amigos **Lisiane Bevilacqua**, **Pedro Rogério** e **Gabriela Evaristo** que apesar da distância sempre estamos juntos e unidos nos melhores e piores momentos.

Ao meu orientador do exterior, **Dr. Luis Miguel de Pablos Tórro** pelos ensinamentos científicos e pela oportunidade. Ao professor **Dr. Antônio Osuna** pelo apoio laboratorial. Aos meus amigos de laboratório de Granada - Espanha, **Romina Romero, Alberto Fernandes, Ana K. Ibarrola, Samir Córdova, Alberto Cornet, Alexa Prescilla, Glória Gonzales, Toni Chulia, Sérgio Battaner** e **Mercedes G. Samblás** pela ajuda durante a execução nos experimentos e pela bela recepção.

A CAPES, CNPq e Fundação Araucária pelo apoio financeiro. A Universidade Estadual de Maringá e ao COMCAP pela oportunidade de realizar a Pós-Graduação e utilizar equipamentos de alta qualidade.

E a todos aqueles não mencionados que também contribuíram com este trabalho.

Muito obrigado!

APRESENTAÇÃO

Este texto é composto por um resumo do trabalho (português e inglês) e dois artigos contemplando os principais resultados obtidos durante o doutorado. O primeiro artigo descreve a atividade biológica de duas substâncias sintéticas da classe de β- carbonílicos em formas amastigotas de *L. amazonensis* intitulado: **β-carboniles, p-anisal-RCC-iso and C5, induce autophagy in intracellular amastigotes of *Leishmania amazonensis*** o qual está em fase de submissão. O segundo artigo possui a descrição da atividade biológica de uma dibenzilidenoacetona (**A11K3**), substância sintética frente a *Trypanosoma cruzi*, intitulado como: **Antiproliferative activity of the dibenzilidenoacetone derivate (E)-3-ethyl-4-(4-nitrophenyl)but-3-en-2-one in *Trypanosoma cruzi*** está em processo de finalização e submissão. Além dos resultados apresentados em forma de artigo, será apresentado em apêndices os resultados obtidos durante o doutorado sanduiche.

RESUMO GERAL

INTRODUÇÃO: As doenças negligenciadas são um grupo de doenças infecciosas que afetam principalmente populações de baixa renda e em países em desenvolvimento. Dentre elas podemos citar: a leishmaniose, um complexo de doenças causada por protozoários parasitos do gênero *Leishmania*; e a doença de Chagas, causada pelo protozoário *Trypanosoma cruzi*. O tratamento para ambas as doenças é extremamente limitado, pois os medicamentos disponíveis causam diversos efeitos colaterais nos pacientes. Visto a necessidade de novas alternativas de tratamento, o presente estudo avaliou a atividade de dois β-carbonilicos, **RCC** e **C5** contra *L. amazonensis*, causador da leishmaniose cutânea e uma dibenzilidenoacetona, **A11K3**, em *T. cruzi*. Trabalhos anteriores demonstraram atividade biológica desses grupos de substâncias contra protozoários, bactérias e células tumorais. **METODOLOGIA, RESULTADOS E DISCUSSÃO:** Os β-carbonílicos **RCC** (*N*-{2-[(4,6-bis(isopropilamino)-1,3,5-triazina-2-yl)amino]etil}-1-(4-metoxiphenil)-*β*-carbolina-3-carboxamida) e **C5** (N-benzyl-1-(4-metoxi)fenil-9H-beta-carbolina-3-carboxamida) foram sintetizados pelo grupo da professora Maria Helena Sarragiotto do Departamento de Química da Universidade Estadual de Maringá e testadas frente à amastigotas intracelulares de *L. amazonesis*. Para isso, macrófagos J774A.1 foram infectados com promastigotas e após 24 h tratados e incubados por 48 h. Após, as amostras foram fixadas, coradas e a concentração inibitória para 50% (CI_{50}) dos protozoários foi determinada. As substâncias **RCC** e **C5** foram ativas CI_{50} de 1,2 ± 0,2 e 1,0 ± 0,3 µM, respectivamente. A citotoxicidade foi analisada pelo método de redução do 3-(4,5-dimetil-2-tiazolil)-2, 5-difenil-2H-tetrazólio (MTT) com macrófagos J774A1. As concentrações citotóxicas (CC_{50}) foram de 145,7 ± 10,1 e >1000 µM para o **RCC** e **C5**, respectivamente. As substâncias apresentaram atividade em formas amastigotas e baixa toxicidade em macrófagos, sendo que, a substância **RCC** apresentou um índice de seletividade (IS) de 97,1 e o **C5** de >1000, ou seja, os compostos são mais tóxicos para o protozoário que para os macrófagos. A imagens de MET (Microscopia Eletrônica de Transmissão) e a MEV (Microscopia Eletrônica de Varredura) obtidas em amastigotas intracelulares de *L. amazonensis* tratadas com a CI_{50} de **RCC e C5** mostram que ocorreu uma diminuição na quantidade de amastigotas intracelulares em macrófagos infectados quando comparado ao controle não tratado, sendo possível a visualização de vacúolos parasitoforos completamente vazios. As amastigotas tratadas apresentaram

alterações estruturais como inchaço mitocondrial, desorganização celular e formação de vacúolos. Ainda foram realizados os ensaios bioquímicos para avaliar e analisar os alvos dos β-carbonílicos em amastigotas intracelulares. Com 48 h de tratamento foi possível observar um aumento de corpos lipídicos, vacúolos autofágicos, despolarização mitocondrial seguido de diminuição na produção de ATP e exposição da fosfatidilserina (**RCC**). Não ocorreu geração de espécies reativas de oxigênio (EROS) em nenhum tratamento, porém a geração de EROS pode ocorrer nas primeiras horas de tratamento, sendo as demais alterações decorrentes do estresse oxidativo. Dessa forma, foi possível concluir que o protozoário não prolifera devido a eventos autofágicos. Quanto aos resultados utilizando *T. cruzi*, foi utilizada a substância **A11K3 (**(E)-3-ethyl-4-(4-nitrofenil)but-3-en-2-ona) sintetizada pelo professor Edson Rodrigues Filho do Departamento de Química da Universidade Federal de São Carlos. Foram avaliadas as formas epimastigotas, tripomastigotas e amastigotas de *T.cruzi* (cepa Y). A atividade antiproliferativa em epimastigotas foi realizada pelo método XTT/PMS (2,3-bis-(2-metoxi-4-nitro-5-sulfofenil)-2H-tetrazólio-5-carboxanilida e metilfeenazina metil sulfato) e a CI_{50} obtida foi de 3,3 ± 0,8 µM. As formas tripomastigotas foram coletadas do sobrenadante de células $LLCMK_2$ previamente infectadas e utilizadas para o experimento de viabilidade celular. Para isso, os tripomastigotas foram tratados com **A11K3** e a concentração efetiva (CE_{50}) foi determinada realizando a contagem dos protozoários viáveis em lâmina/lamínula onde o valor encontrado foi de 24,0 ± 4,3 µM. Para análise antiproliferativa de amastigotas intracelulares, células $LLCMK_2$ foram infectadas com tripomastigotas e tratadas com **A11K3.** Após 96 h de incubação, as amostras foram fixadas coradas e a CI_{50} determinada foi de 9,2 ± 0,6 µM. A CC_{50} de **A11K3** para células $LLCMK_2$, determinada pelo método de redução de MTT foi de 239,3 ± 15,7 µM. Com esses valores foi possível calcular o IS para as três formas tratadas com a substância **A11K3**. Para epimastigotas, tripomastigotas e amastigotas intracelulares os IS foram de 72,5, 9,9 e 25,3, respectivamente. A análise ultraestrutural de epimastigotas tratadas com **A11K3** sugere um aumento na vacuolização, excreção de vesículas derivadas com complexo de Golgi, surgimento de membranas concêntricas, alterações de membrana e aumento de corpos lipídicos. Através da MEV foi possível observar epimastigotas com dois flagelos, arredondamento do protozoário e extravasamento de material citoplasmático. Em amastigotas intracelulares tratadas com **A11K3**, os resultados de MET mostraram aumento de vacuolização e excreção nas vesículas do complexo de Golgi, inchaço mitocondrial e ruptura de membrana. Os resultados

encontrados durante a microscopia foram confirmados com a análise bioquímica do parasito. O tratamento de **A11K3** em epimastigotas gerou alterações de membrana, confirmada pela análise com iodeto de propídeo, possivelmente causada pela produção de EROS e peroxidação lipídica. Além disso, o tratamento com **A11K3** ocasionou despolarização de membrana mitocondrial, e consequentemente a diminuição de ATP intracelular. O surgimento de membranas concêntricas é geralmente precursora de vacúolos autofágicos, alteração essa confirmada pela análise com monodancilcadaverina. A análise em amastigotas intracelulares revelou alterações semelhantes ao encontrado em epimastigotas como o surgimento de vacúolos, aumento na excreção de vesículas do complexo de Golgi e ruptura de membrana. Foi possível ainda observar o inchaço mitocondrial em amastigota. Os vacúolos encontrados podem ser corpos lipídicos, devido ao aumento na fluorescência em amastigotas marcadas com vermelho do Nilo. Os resultados sugerem eventos semelhantes à uma morte celular programada, a ferroptose, semelhante à necrose, pois gera alterações de membrana plasmática, membrana mitocondrial e peroxidação lipídica. **CONCLUSÃO E PERSPECTIVAS:** As substâncias **RCC**, **C5** e **A11K3** foram ativas e seletivas contra as amastigotas intracelulares de *L. amazonensis* e *T.cruzi*; Através de microscopia eletrônica e os ensaios bioquímicos foi observado que os β-carbonílicos, **RCC** e **C5,** afetam a mitocôndria e a formação de vesículas lipídica e/ou autofágicas, ou seja, o tratamento leva os protozoários a um estresse onde ocorre o acúmulo de reservas de energia (formação de corpos lipídicos) e geração de vacúolos com origem autofágica; O *T. cruzi* tratado com a substância **A11K3** mostrou alterações celulares que leva o parasito à morte. Os dados sugerem que tal morte de *T. cruzi* pode ser semelhante à ferroptose. No período de doutorado sanduiche foram realizados experimentos para geração de uma cepa fluorescente de *T. cruzi*. A marcação fluorescente foi realizada através da inserção de plasmídeos bacterianos em formas epimastigotas de *T. cruzi*. Esse protozoário gerado poderá auxiliar projetos futuros no Laboratório de Inovação Tecnológica no Desenvolvimento de Fármacos e Cosméticos.

GENERAL ABSTRACT

INTRODUCTION: Neglected diseases are a group of infectious diseases that mainly affect poor and vulnerable populations. These include leishmaniasis, a disease complex caused by protozoa parasites of the genus *Leishmania*; and Chagas disease, caused by the protozoa *Trypanosoma cruzi*. Treatments for both diseases are extremely limited, as the drugs available have various side effects in patients and their effectiveness are limited. Given the need for new treatment alternatives, the present study sought to evaluate the activity of two β-carbonyls, **RCC** and **C5** against *L. amazonensis*, which causes cutaneous leishmaniasis and a dibenzylidenoacetone, **A11K3**, against *T. cruzi*. Previous work has shown biological activity of these groups of substances against protozoa, bacteria and tumor cells. **METHODOLOGY, RESULTS AND DISCUSSION**: The β-carbonyl **RCC** (N- {2 - [(4,6-bis (isopropylamino) -1,3,5-triazin-2-yl) amino] ethyl} -1-(4- methoxyphenyl) -β-carboline-3-carboxamide) and **C5** (N-benzyl-1- (4-methoxy) phenyl-9H-beta-carboline-3-carboxamide) were synthesized by Professor Maria Helena Sarragiotto group from the Department of Chemistry of Maringá State University and tested against intracellular amastigotes of *L. amazonesis.* For this, J774A.1 macrophage were infected with promastigotes, treated and incubated for 48 h. After that, the samples were fixed, stained and the IC_{50} obtained for **RCC** and **C5** substances were IC_{50} of 1.2 ± 0.2 and 1.0 ± 0.3 µM, respectively. Cytotoxicity assay were performed by the method of 3- (4,5-dimethyl-2-thiazolyl) -2,5-diphenyl-2H-tetrazolium (MTT) at a concentration of 2 mg/mL in treated and incubated J774A1 macrophages for 48 h. The CC_{50} were 145.7 ± 10.1 and > 1000 µM for **RCC** and **C5**, respectively. The substances showed activity against amastigote forms and low toxicity in macrophages. **RCC** substance showed a selectivity index (IS) of 97.1 and **C5** of >1000 µM, that is, the compounds are more toxic for protozoan than for the mammal cells. TEM and SEM performed on *L. amazonensis* amastigotes treated for 48 h with the IC_{50} of **RCC** and **C5** showed that occur a decrease in the amount of intracellular amastigotes in infected macrophages when compared to untreated parasites, allowing the visualization of completely empty vacuoles. The amastigotes presented alterations such as mitochondrial swelling, cellular disorganization and vacuole formation. Biochemical assays were also performed to evaluate and analyze the targets of β-carboniles in intracellular amastigotes. After 48 h of treatment it was possible to observe an increase in lipid bodies, autophagic vacuoles, mitochondrial depolarization followed by a decrease in ATP production and phosphatidylserine

exposure (**RCC**). No reactive oxygen species (ROS) generation occurred in any treatment. Based on the results, it was possible to conclude that the protozoan did not proliferate due to autophagic events. The substance **A11K3** ((E) -3-ethyl-4- (4-nitrophenyl) but-3-en-2-one) was synthesized by Professor Edson Rodrigues of the Department of Chemistry, Universidade Federal de São Carlos. **A11K3** were evaluated against epimastigote, trypomastigote and amastigotes forms of *T. cruzi* (Y strain). For epimastigote analysis, protozoa were treated with **A11K3** and incubated for 96 h at 28 °C. Then, 50 µL of 2,3-bis- (2-methoxy-4-nitro-5-sulfophenyl) -2H-tetrazolium-5-carboxanilide solution and methylphenazinium methyl sulfate (XTT / PMS) was added at a concentration of 0.5 and 0.3 mg/mL, respectively and incubated for 4 h. The reading was performed by spectrophotometer at 450 nm and the IC_{50} determined IC_{50} was 3.3 ± 0.8 µM. Trypomastigotes were collected from the supernatant of previously infected $LLCMK_2$ cells and used for cell viability assay. For this, trypomastigotes were treated with **A11K3** and incubated for 24 h. The EC_{50} was determined by direct parasite counting where the value found was 24.0 ± 4.3 µM. For antiproliferative analysis of intracellular amastigotes, $LLCMK_2$ cells were infected with trypomastigotes and then treated with **A11K3**. After 96 h of incubation, the samples were fixed, stained and 50% inhibitory concentration (IC_{50}) was 9.2 ± 0.6 µM. Cytotoxicity in $LLCMK_2$ cells was evaluated by the MTT method and the CC_{50} was 239.3 ± 15.7 µM. With these values it was possible to calculate the IS for the three forms treated with substance **A11K3**. For epimastigotes, trypomastigotes and intracellular amastigotes the IS were 72.5, 9.9 and 25.3, respectively. Ultrastructural analysis of epimastigotes of *T. cruzi* treated with **A11K3** suggest an increase in vacuolization, Golgi complex vesicle excretion, appearance of concentric membranes, membrane alterations, and increase of lipid bodies. Through SEM it was possible to observe epimastigotes with two flagella, protozoa with rounded body and extravasation of cytoplasmic material. TEM of intracellular amastigotes treated with **A11K3** showed increased vacuolization and excretion in Golgi complex vesicles, mitochondrial swelling and membrane rupture. The results found during microscopy were confirmed with the biochemical analysis of the parasite. The treatment with **A11K3** in epimastigotes generated membrane changes, confirmed by propidium iodide analysis, possibly caused by ROS production and lipid peroxidation. In addition, **A11K3** treatment induced mitochondrial membrane depolarization, which decreased the intracellular ATP level. The emergence of concentric membranes is usually a precursor of autophagic vacuoles, as confirmed by monodancylcadaverine assay. Analysis in intracellular

amastigotes revealed changes similar to those found in epimastigotes such as the emergence of vacuoles, increased excretion of Golgi vesicles and membrane rupture. In addition, it was possible to observe mitochondrial swelling in amastigotes. The vacuoles found may be lipid bodies as it was observed an increase in fluorescence in amastigotes labeled with Nile red. The results suggest events similar to a programmed cell death, ferroptosis, similar to necrosis, as generates changes in the plasma membrane, mitochondrial membrane and lipid peroxidation. **CONCLUSION AND PERSPECTIVES: RCC, C5** and **A11K3** were active and selective against the intracellular amastigotes of *L. amazonensis* and *T. cruzi*; through electron microscopy and biochemical assays it was observed that the β-carbonyls, **RCC** and **C5**, affect the mitochondria and the formation of lipid bodies and autophagic vesicles. The treatment leads the protozoa to a stress where the accumulation of energy reserves (formation of lipid bodies) and generation of vacuoles with autophagic origin; *T. cruzi* treated with **A11K3** substance showed cellular changes that lead the parasite to programmed cell death known as ferroptosis. During the sandwich doctorate period, assays were performed in order to generate a fluorescent strain of *T. cruzi*. Fluorescent labeling was performed by inserting bacterial plasmids into epimastigotes *T. cruzi*. This protozoan may help future projects in infection control *in vitro* and *in vivo* studies.

ARTIGO CIENTIFICO 1

Submissão: International Journal Antimicrobial Agents

Fator de impacto: 4,60

β-carbolines, RCC and C5 induce death of *Leishmania amazonensis* intracellular amastigotes

Jéssica Carreira de Paula[1], Nilma de Souza Fernandes[1], Thaysa Ksiaskiewcz Karam[1], Paula Baréa[2], Maria Helena Sarragiotto[2], Tania Ueda-Nakamura[1], Celso Vataru Nakamura[1,a]

[1] Programa de Pós-graduação em Ciências Biológicas, Laboratório de Inovação Tecnológica no Desenvolvimento de Fármacos e Cosméticos, Universidade Estadual de Maringá, Bloco B-08, Av. Colombo 5790, Maringá, PR, 87020-900, Brazil

[2] Departamento de Química, Universidade Estadual de Maringá, Bloco E-90, Av. Colombo 5790, Maringá, PR, 87020-900, Brazil

[a]email address: cvnakamura@gmail.com

Abstract

Leishmaniasis is a complex of diseases that are endemic in several countries. Cutaneous leishmaniasis (CL) is the most common clinical manifestation and affects more than 200,000 people per year. The treatment for CL is with antimonials and miltefosine, however these drugs have high toxicity. This protozoan parasite is a motile flagellate as promastigotes, the form found inside the insect vector, and an immotile intracellular amastigote inside mammalian cells. Compounds with an alkaloid indol and a hydrogenated six-member pyridine ring, known as the β-carbolines, have shown activity against both of these forms. Here, we studied the activity and effects of two of these β-carbolines, **RCC** and **C5**, against *L. amazonensis* intracellular amastigotes in order to analyze their mechanism of action. The results showed that **RCC** and **C5** are active against intracellular amastigotes with IC_{50} values of 1.2 and 1.0 µM, respectively and were more selective for the parasite than the host macrophages. Treatment with these β-carbolines induced ultrastructural alterations leading the parasite to death.

Keywords: *Leishmania amazonensis*; β-carbolines; intracellular amastigotes

1. Introduction

Leishmania spp. are protozoan parasites with two main cell morphologies: the promastigote, a motile, flagellated form present in the sand fly vector; and the amastigote form found inside host mammalian cells. There parasite are responsible for a complex of pathologies in humans, primarily divided into cutaneous (CL), mucocutaneous (MCL) and visceral (VL) leishmaniasis. The cutaneous form is the most common, with 200,000 to 400,000 people infected each year (Clemente et al. 2018). CL can be caused by various *Leishmania* species, such as *L. major*, *L. amazonensis*, *L. guyanensis* and *L. braziliensis.* The majority of those infected (95%) live in the Americas, Mediterranean basin, Middle East and Central Asia (Sunter and Gull 2017*;* WHO, 2019).

CL is characterized by lesions that can vary in number and size depending on the immune state of the patient. Treatment is generally performed with pentavalent antimonials and miltefosine, however, both are highly toxic and can cause several side severe effects. Furthermore, as yet production of an effective vaccine not been possible (Mitropoulos, Konidas, and Durkin-Konidas 2010). Due to this, drug studies are vital in order to find new active compounds against *Leishmania* spp. that have less toxicity and higher efficacy. Our group has previously evaluated different β-carbolines that exhibited activity against both the promastigote and amastigote forms of *L. amazonensis* parasites. (Baréa et al. 2018; Mendes et al. 2016; Valdez et al. 2009; Volpato et al. 2013). The β-carbolines are synthetic substances with an alkaloid indol nucleus and a hydrogenated six-member pyridine ring. These compounds have also shown activity against fungi, cancer cells and other protozoa such as *Trypanosoma cruzi* (Mendes et al. 2016; Pedroso et al. 2011; Volpato et al. 2013). This study aims to analyze the biochemical effects induced by two β-carbolines, RCC and C5, in *L. amazonensis* intracellular amastigotes.

2. Materials and methods

2.1.Chemicals

The following chemicals from Sigma Aldrich were used: carbonyl cyanide m-chlorophenylhydrazone (CCCP), rhodamine 123 (Rh123), dansylcadaverine (MDC), Nile Red, digitonin, methylphenazinium methyl sulfate (PMS), dihydrochlorofluorescein (H_2DCFDA), wortmannin, potassium cyanate (KCN), and hemin and folic acid. 3-[4,5-dimethylthiazol-2-yl]-2,5-diphenyltetrazolium bromide (MTT), 2,3-bis(2-methoxy-4-

nitro-5-sulfophenyl)-2H-tetrazolium-5-carboxanilide (XTT), propidium iodide (PI), DAF-FM diacetate and annexin V conjugated with FITC were obtained from Invitrogen. Roswell Park Memorial Institute (RPMI 1640), fetal bovine serum (FBS) and Giemsa were obtained from Gibco. Sodium cacodylate buffer, 1% osmium tetroxide (OsO_4), 0.8% potassium ferrocyanide, 10 mM calcium chloride ($CaCl_2$), lead citrate, uranyl acetate, 25% glutaraldehyde and EPON resin were obtained from EMS – Electron microscopy Sciences. Diphenyl-1-pyrenylphosphine (DPPP) was from Molecular Probes, CellTiter-Glo® Luminescent Cell Viability Assay from Promega, and dimethylsulfoxide (DMSO) from Reatec. Warren's medium (brain–heart infusion plus hemin and folic acid; pH 7.2).

2.2. Synthesis and preparation of the β-carboline derivatives

The synthesis of the substances was described by Baréa et al. (2018) for the (*N*-{2-[(4,6-bis(isopropylamino)-1,3,5-triazin-2-yl)amino]ethyl}-1-(4-methoxyphenyl)-*β*-carboline-3-carboxamide) known as **RCC,** and by Pedroso et al. (2014) for the (N-benzyl-1-(4-methoxy)phenyl-9H-beta-carboline-3-carboxamide known as **C5**. The molecular structures of the substances are shown in Figure 1. The substances were solubilized with DMSO and the work solution did not overtake1%.

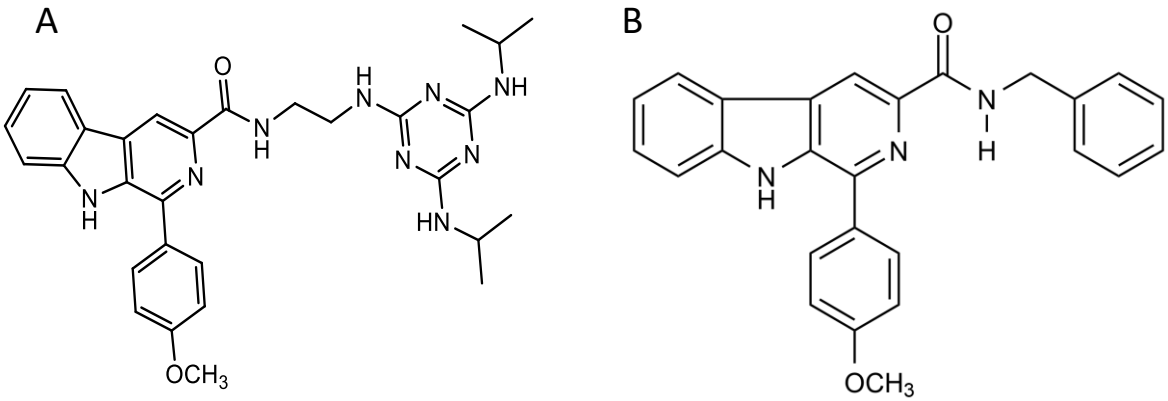

Figure 1. Chemical structures of the β-carbolines derivatives of (A) the (*N*-{2-[(4,6-bis(isopropylamino)-1,3,5-triazin-2-yl)amino]ethyl}-1-(4-methoxyphenyl)-*β*-carboline-3-carboxamide) (**RCC**) and (B) the (N-benzyl-1-(4-methoxy)phenyl-9H-beta-carboline-3-carboxamide (**C5**).

2.3. Parasites and cell culture

J774A.1 macrophage were maintained in RPMI 1640 medium supplemented with 10% FBS and incubated in a 5% CO_2 atmosphere at 37°C. Promastigotes of *L. amazonensis* (MHOM/BR/75/Josefa) were maintained at 25°C in Warren's medium (pH 7.2) supplemented with 10% heat-inactivated FBS. Monolayers of J774A.1 macrophages were infected with *L. amazonensis* promastigotes in the 6th day of culture at a ratio of 10:1 (parasites:macrophages). Infected macrophages were maintained in RPMI 1640 medium supplemented with 2 mM L-glutamine and 10% FBS and buffered with sodium bicarbonate at 5% CO_2 and 34°C.

For the biochemical analysis the J774A.1 macrophage were infected at 1:10 and after 24 h treated with 2.4 µM miltefosine, 1.2 µM **RCC**, or 1 µM **C5** and incubated for 48 h. Intracellular amastigotes were isolated by rupture of the J774A.1 macrophage membrane by syringe and needle and differential centrifugation by 1000 rpm for 3 min. The supernatant was collected and then, centrifuged at 3000 rpm for 5 min. After the isolation, amastigotes were diluted to a concentration of $1x10^6$ parasites/mL for subsequent analysis. Untreated amastigotes were used as a negative control.

2.4. Antiproliferative assay against intracellular amastigotes

For the antiproliferative assay and the inhibitory concentration for 50% of the parasites (IC_{50}) determination against intracellular amastigotes, $5x10^5$ cells/mL of J774A.1 macrophage and $5x10^6$ promastigotes/mL at a ratio 1:10 were added in a plate with coverslips and incubated at 34°C with 5% CO_2 for 24 h. Cells were then treated with the β-carboline derivatives (100, 50, 10, 5 and 1 µM) and incubated for 48 h. Cells were fixed with methanol for 10 min and stained with 10% Giemsa stain for 40 min. On a light microscope, 200 macrophages per coverslip were evaluated. The number of infected macrophages and the number of amastigotes within each infected macrophage were recorded. The survival index (SI = percentage of infected cells x average number of amastigotes per infected macrophage) was determined. The SI of amastigotes from untreated infected macrophages (NC, negative control) was considered as 100% of survival.

2.5. Cytotoxicity in J774A.1 macrophages

J774A.1 macrophage ($5x10^5$ cells/mL) were added to 96-well plates with PRMI plus 10% FBS and incubated at 34°C with 5% CO_2. After 24 h, the cells were treated with **RCC** and **C5** (1, 5, 10, 50 and 100 µM) and incubated for a further 48 h. The cytotoxicity assay was performed using the MTT reduction method (2 mg/mL), in which assesses the ability of viable cells to convert tetrazolium salt (yellow) into a purple compound, formazan (Ewa Grelaa, Joanna Kozłowskab 2018). The optical density was measured in a spectrophotometer (Power Wave XS - Bio-Tek) at 570 nm and the cytotoxicity concentration for 50% of cells (CC_{50}) was determined from a graph comparing percentage of growth inhibition with the concentration of β-carboline derivatives.

2.6. Electron microscopy

Intracellular amastigotes ($1x10^6$ parasites/mL) were left untreated (control) or treated with 2.4 µM miltefosine or the IC_{50} concentration of the compounds, **RCC** and **C5,** for 48 h. After treatment, samples were fixed with 2.5% glutaraldehyde in 0.1 M sodium cacodylate buffer for 1 h. For scanning electron microscopy (SEM), the samples were dehydrated in increasing ethanol concentrations, submitted to critical point drying and metalized with gold. Lastly, the samples were observed on an FEI Quanta 250 SEM.

For ultrastructural analysis, transmission electron microscopy (TEM) was used. After the fixation described above, the samples were post-fixed in a solution of 1% OsO_4, 0.8% potassium ferrocyanide, and 10 mM $CaCl_2$ in 0.1 M sodium cacodylate buffer, dehydrated in increasing acetone concentrations and embedded in EPON resin. Ultrathin sections (60 nm) were obtained, contrasted with uranyl acetate and lead citrate, and observed on a JEOL JM 1400 TEM.

2.7.Detection of nitric oxide (NO)

For the determination of NO produced by macrophages, the J774A.1 macrophage were infected then treated with 1.2 µM **RCC** or 1 µM **C5** for 48 h. The probe DAF-FM was added at 1 µM for 30 min and fluorescence was quantified on a Victor X3 spectrophotometer at λ_{ex} 490 and λ_{em} 520 nm. The positive control used was 4 µM H_2O_2.

2.8. Detection of reactive oxygen species (ROS)

For detection of total ROS, isolated amastigotes ($1x10^6$ parasites/mL) treated with 1.2 µM **RCC** or 1 µM **C5** for 48 h were incubated with 10 µM H_2DCFDA at room temperature in the dark for 45 min. The fluorescence was determined using a Victor X3 spectrophotometer at λ_{ex} 488 and λ_{em} 530 nm. For the positive control 4 µM H_2O_2 was used (Hempel et al. 1999).

2.9. Detection of lipid bodies

For detection of lipid bodies, isolated amastigotes were treated for 48 h with 1.2 µM **RCC** or 1 µM **C5** then labeled with 10 µg/mL Nile Red in the dark for 30 min. The fluorescence was quantified using a Victor X3 spectrophotometer at λ_{ex} 490 and λ_{em} 535 nm. For the positive control 4 µM H_2O_2. was used.

2.10. Determination of cell membrane integrity and phosphatidylserine exposure

For determination of cell membrane integrity and phosphatidylserine (PS) exposure, isolated amastigotes treated with 40 µM digitonin, 1.2 µM **RCC** or 1 µM **C5** for 48 h were labeled with PI and FITC-conjugated annexin V. The read was performed by flow cytometry as described by Lazarin-Bidóia et al. (2016).

2.11. Determination of mitochondrial membrane potential (ΔΨm)

For determination of mitochondrial membrane potential, isolated amastigotes treated with 1.2 µM **RCC** or 1 µM **C5** for 48 h were labeled with 5 µg/mL Rh123 in the dark for 30 min. The positive control was treated with 100 µM CCCP. The read was performed by flow cytometry as described by Lazarin-Bidóia et al. (2016).

2.12. Evaluation of autophagic vacuoles

For determination of autophagic vacuoles, isolated amastigotes were treated with 1.2 µM **RCC** or 1 µM **C5** for 48 h then incubated with 0.05 mM MDC in the dark for 60 min. For the positive control, parasites without serum were used. The fluorescence was quantified on a Victor X3 spectrophotometer at λ_{ex} 380 and λ_{em} 535 nm.

2.13. Detection of intracellular ATP

For determination of ATP production, isolated amastigotes were treated with 1.2 µM **RCC** or 1 µM **C5** for 48 h. After that, the CellTiter-Glo® Luminescent Cell Viability Assay was used and the luminescence was determined on a Victor X3 spectrophotometer. For the positive control, 50 µM KCN and 100 µM CCCP were used.

2.14. Statistical analysis

The data shown in the graphs are expressed as the mean ± standard deviation (SD) of at least three independent assays. The data were analyzed using one or two-way analysis of variance (ANOVA). Significant differences among means were identified with Tukey test. Values of $p \leq 0.05$ were considered statistically significant. The statistical analyses were performed using GraphPad Prism 6 software.

3. RESULTS

3.1 Activity of β-carboline derivatives against *L. amazonensis* intracellular amastigotes

The β-carbolines, **RCC** and **C5** were evaluated against intracellular amastigotes of *L. amazonensis*. The antiproliferative assay demonstrated that **RCC** had an IC_{50} of 1.2 ± 0.2 µM after 48 h of treatment. Regarding the selective index (SI), the compound was 121.4 times more toxic towards the amastigotes than the macrophages. Whilst **C5** had an IC_{50} of 1 µM ± 0.3 and a SI higher than 1000 (Table 1).

Table 1. Activity of β-carboline derivatives against intracellular amastigotes of *L. amazonensis* (IC_{50}) and J774A.1 macrophages (CC_{50}) after 48 h of treatment.

Substances	IC_{50} (µM)*	CC_{50} (µM) **	SI[#]
RCC	1.2 ± 0.2	145.7 ± 10.1 [#]	121.4
C5	1.0 ± 0.3	>1000	>1000

IC_{50} = inhibitory concentration for 50 % of the parasites
CC_{50} = citotoxity concentration for 50% of the cells
SI = Selective index

3.2 Ultrastructural analysis of intracellular amastigotes after treatment with β-carboline derivatives

Considering the good activity and selectivity against *L. amazonensis* intracellular amastigotes, the ultrastructure after treatment with the β-carbolines was assessed by TEM and SEM. For TEM, the infected macrophages were treated for 48 h with the IC_{50} of miltefosine (2.4 µM), **RCC** (1.2 µM), and **C5** (1 µM). Untreated macrophages infected with amastigotes showed many parasites inside parasitophorous vacuoles with well-preserved structures of the amastigotes, such as the nucleus, kinetoplast, and internalized flagella (Figure 2, A-a). Infected macrophages treated with miltefosine showed empty parasitophorous vacuoles or few amastigotes, compared to untreated control (Figure 2, B-b). Those treated with **RCC** also showed several empty parasitophorous vacuoles. Amastigotes that remained showed mitochondrial swelling, lipid body accumulation, vacuoles, emergence of exosomes and intense cellular disorganization (Figure 2, C-c). Whilst treatment with **C5** showed alterations in the flagellar pocket, vacuoles and an accumulation of lipid bodies (Figure 2, D-d).

In SEM, it was possible to see fewer amastigotes in the macrophages treated with the β-carbolines when compared with untreated control (Figure 3). After treatment with miltefosine it is possible to observe a few remaining amastigote nests (Figure 3, B-b), however infected macrophages treated with **RCC** showed even fewer parasites (Figure 3, C-c). Furthermore, the SEM micrographs of RCC-treated macrophages clearly showed the empty parasitophorous vacuoles, corroborating the results of the antiproliferative activity and the TEM images. Macrophages treated with **C5** reduced the number of

intracellular amastigotes, however, it was not possible to observe empty parasitophorous vacuoles (Figure 3, D-d).

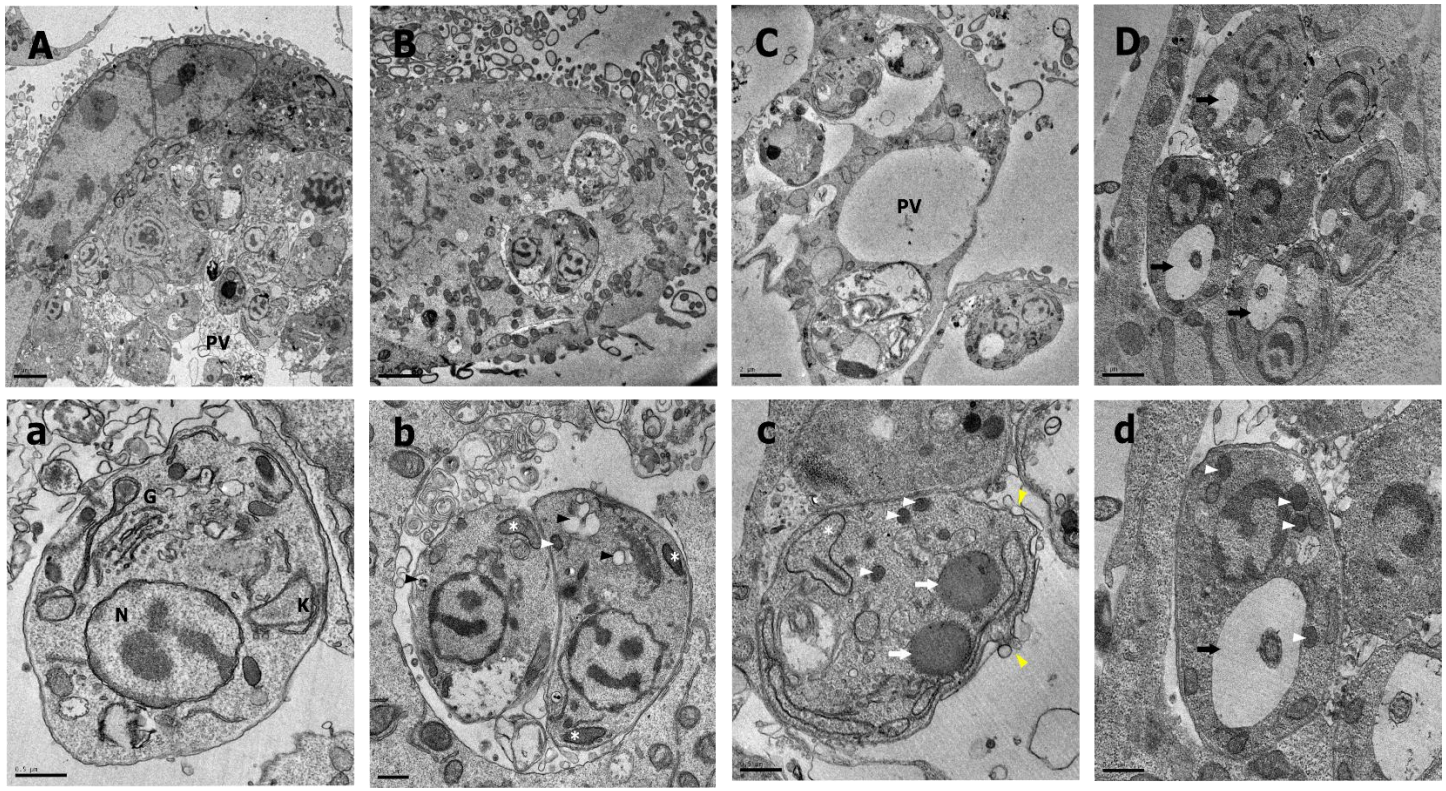

Figure 2. Ultrastructural alterations of intracellular amastigotes of *Leishmania amazonensis* in J774A.1 macrophages treated with **RCC** and **C5.** visualized by transmission electron microscopy. Control macrophages (infected and not treated) (A, a); infected macrophages treated with miltefosine (2.4 µM) (B-b), the IC_{50} of **RCC** (1.2 µM) (C,c) and the IC_{50} of **C5** (1 µM) (D,d) for 48 h. The macrophage parasitophorous vacuole (PV). Parasite structures and alterations are indicated as follows: nucleus (N); mitochondrion (K) and mitochondrial alteration; Golgi complex (G); (*); yellow arrow head, exosomes; white arrow head,lipid bodies; white arrow,reservosomes; black arrow head, vacuoles; black arrow, flagella pocket alterations. Bars A, B and D = 2 µm; a,b, c and d = 0.5 µm; C = 1µm.

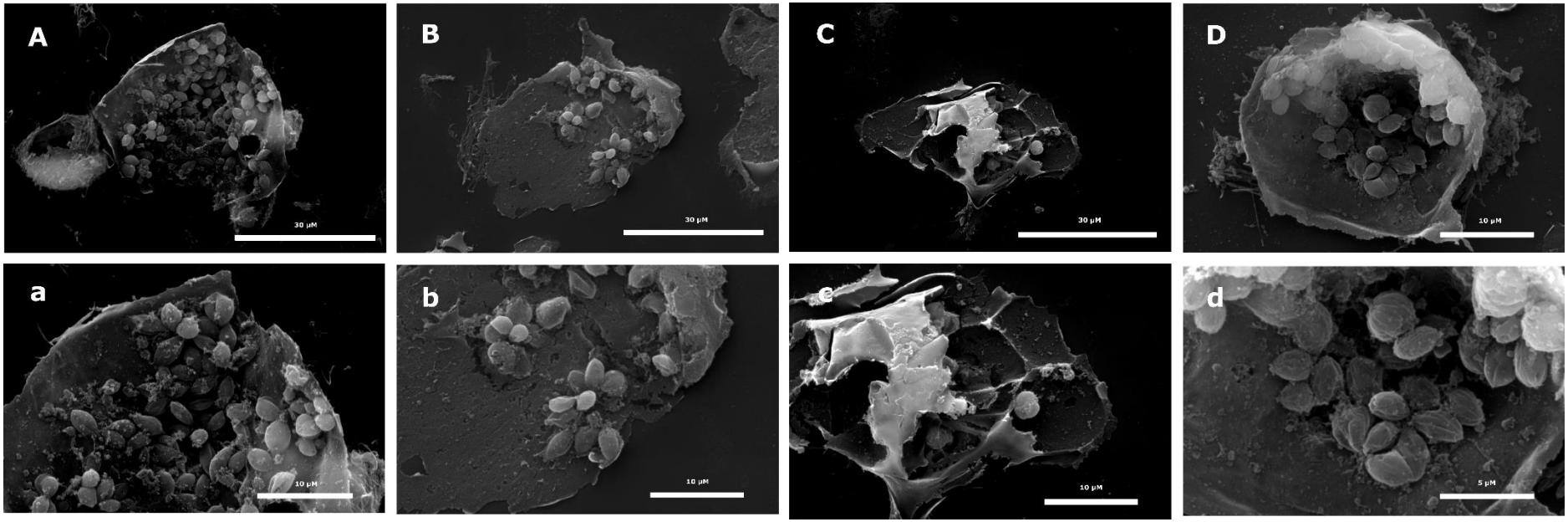

Figure 3. Morphological alterations of intracellular amastigotes of *Leishmania amazonensis* in J774A.1 macrophages treated with miltefosine, **RCC,** and **C5**, visualized by scanning electron microscopy. Control cells (not treated) (A-a); cells treated with miltefosine (2.4 µM) (B-b); cells treated with **RCC** (1.2 µM) (C-c) and cells treated with **C5** (1 µM) (D-d) for 48 h. Bars A, B and C = 30 µm; D, a, b and c = 10 µm; d = 5 µm.

3.3 Nitric oxide production in β-carboline-treated macrophages

In order to evaluate biochemical alterations in *L. amazonensis* and the host macrophages after treatment with the β-carboline derivatives, the DAF-FM was used for NO detection. The DAF-FM probe is a fluorochrome that acts in two steps: first it is hydrolyzed into DAF-2 by membrane esterase, then, in presence of nitric oxide, DAF-2 is converted into triazole fluorescein, DAF-2T. As a positive control, 4 µM H_2O_2 was used, which caused an 84% increase in the NO production by macrophages compared to negative control (NC). There was 57% more production of NO in the **C5**-treated macrophages infected compared to NC. Whilst miltefosine and **RCC** showed decrease of NO production of 35% and 21%, respectively, in comparison compared to the untreated control (Figure 4).

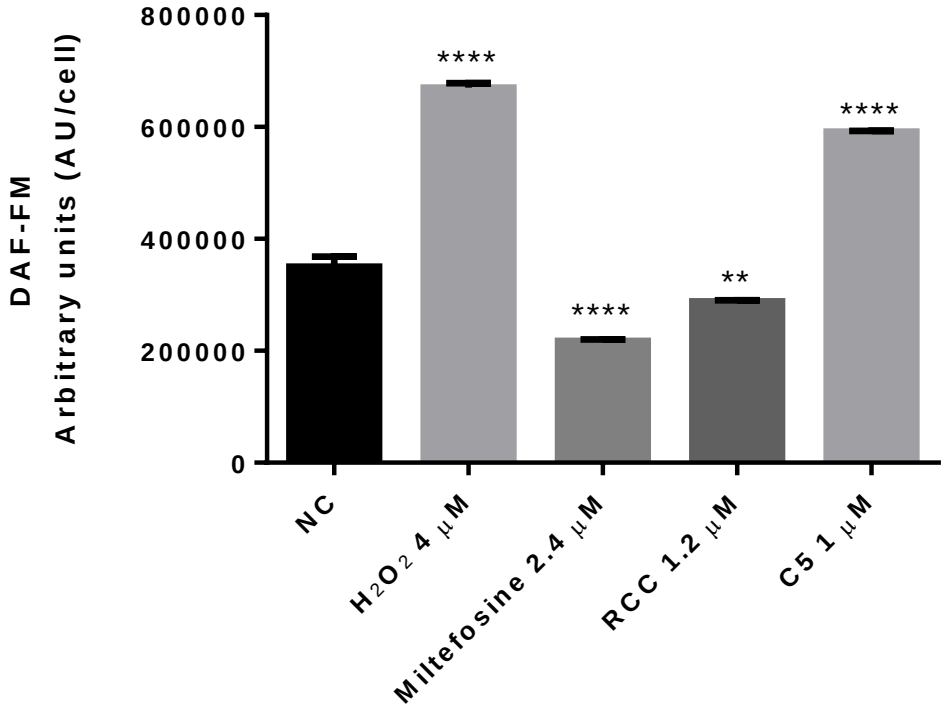

Figure 4. Production of nitric oxide from *L. amazonensis* infected-J774A.1 macrophages treated with miltefosine (2.4 µM), and **RCC** and **C5** (1.2 µM and 1 µM, respectively) for 48 h. H_2O_2 was used as a positive control. Untreated macrophages were used as a negative control (NC). Two-way ANOVA followed by Bonferroni post hoc test. $^{**}p \leq 0.01$; $^{****}p \leq 0.0001$.

3.4 Lipid body and ROS production in *L. amazonensis* amastigotes after treatment with RCC and C5

The fluorescent dye, Nile red, was used to investigate the accumulation of lipid bodies in isolated amastigotes treated with **RCC** and **C5**. The positive control, amastigotes treated with H_2O_2, showed a 50% increase in fluorescence compared to untreated control, indicating an increase in lipid body accumulation. Miltefosine did not show alterations, while the compounds **RCC** and **C5** caused an increase of 20 and 240%, respectively, compared to the untreated control (Figure 5 A).

To evaluate the effect of **RCC** and **C5** on the amastigotes, ROS production was also analyzed. Isolated amastigotes were treated for 48 h with 1.2 µM **RCC** and 1 µM **C5**, as well as 2.4 µM miltefosine and 4 µM H_2O_2 was used as a positive control. The results not showed alteration of ROS production for **RCC** and **C5.** However, treatment with **RCC** and **C5** did not induce alterations in ROS production (Figure 5 B).

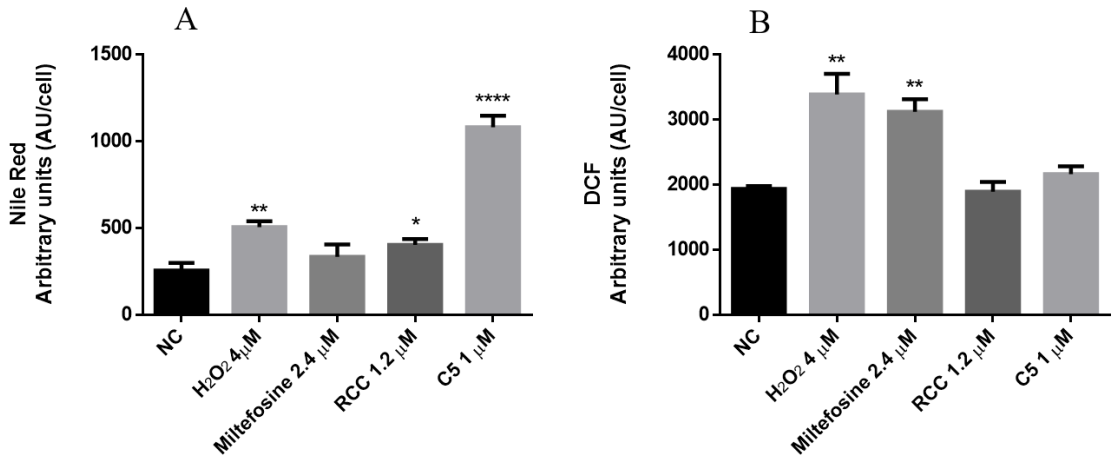

Figure 5. Accumulation of lipid bodies (A) and total ROS production (B) using the fluorescent probes Nile red and H_2DCFDA, respectively, in treated *L. amazonensis* amastigotes. Isolated amastigotes were treated with miltefosine (2.4 µM), **RCC** (1.2 µM) and **C5** (1 µM), and 4 µM H_2O_2 as a positive control, for 48 h. Untreated parasites were used as a negative control (NC). The data are expressed as relative fluorescence of at least three independent experiments. Two-way ANOVA followed by Bonferroni post hoc test. $*p \leq 0.05$; $**p \leq 0.01$; $****p \leq 0.0001$ compared to the negative control.

3.5. Formation of autophagic vacuoles in amastigotes treated with RCC and C5

As vacuoles were observed in the β-carboline-treated parasites, as analyzed by TEM analysis, the nature of these vacuoles was investigated. MDC is a probe that has affinity for autophagic vacuoles. The positive control (parasites without serum) showed an increase in autophagic vacuoles almost three times more than that of the negative control, while miltefosine had a small increase. Amastigotes treated with **RCC** and **C5**, however, showed a significant increase in autophagic vacuoles, almost one time higher than the untreated control (Figure 6).

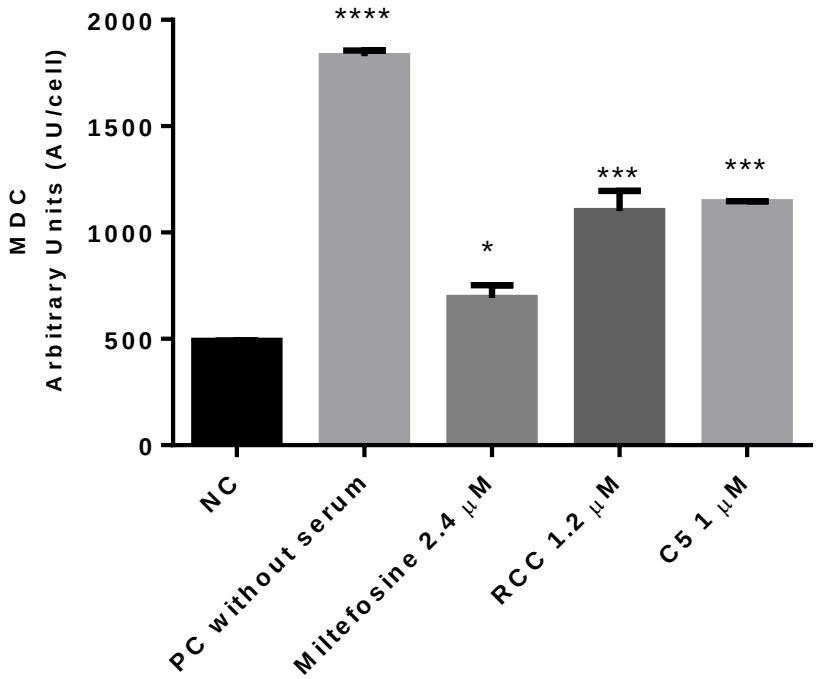

Figure 6. Accumulation of autophagic vacuoles in *L. amazonensis* amastigotes treated with miltefosine (2.4 µM), **RCC** (1.2 µM) and **C5** (1 µM) for 48 h, respectively. Assessed using the fluorescent probe, MDC. Parasites without serum were used for positive control (PC). The data are expressed as relative fluorescence of at least three independent experiments. Two-way ANOVA followed by Bonferroni post hoc test. *$p \leq 0.05$; ***$p \leq 0.001$; ****$p \leq 0.0001$ compared to untreated parasites (NC, negative control).

3.6. Mitochondrial assessment of membrane potential and intracellular ATP after treatment with RCC and C5

For the evaluation of mitochondrial membrane potential, treated parasites were incubated with Rh123 dye and analyzed by flow cytometry. For the positive control, parasites were treated with 100 µM CCCP and 37% mitochondrial depolarization occurred (Figure 7 A). Miltefosine did not show alteration at mitochondria (Figure 7 B). Parasites treated with β-carbolines **RCC** underwent mitochondrial hyperpolarization 83.3 % and depolarization in 33.3%. **C5** did not show hyperpolarization or depolarization (Figure 7, C-D).

To confirm the mitochondrial swelling observed by TEM and the hyperpolarization assessed by using the Rh123 dye, the intracellular ATP after treatment was also evaluated. The positive controls, 500 µM KCN and 100 µM CCCP, showed a decrease in intracellular ATP of 75% and 80%, respectively than compared with untreated control (Figure 7 E). Treatment with the β-carbolines, **RCC** and **C5**, showed a significant decrease compared to the untreated control but not to the same extent as the positive controls.

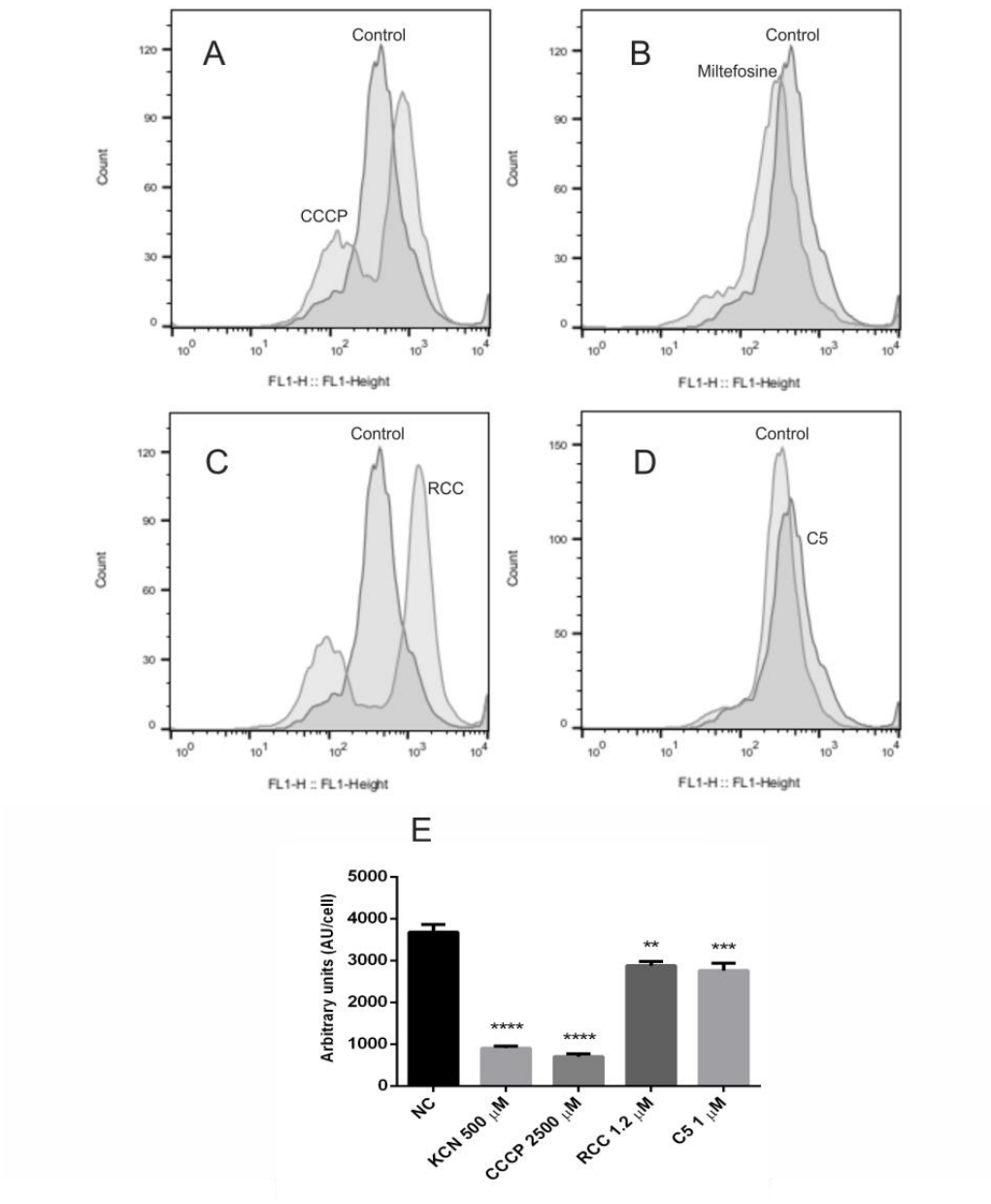

Figure 7. Determination of mitochondrial membrane potential (ΔΨm) (A-D) and intracellular ATP (E) of *L. amazonesis* intracellular amastigotes treated with 1.2 µM **RCC** and 1µM **C5** for 48 h. Flow cytometry histograms of Rh123-labeled untreated control parasites with parasites treated with (A) CCCP (100 µM) (positive control); (B) miltefosine (2.4 µM); (C) **RCC (**1.2 µM); and (D) **C5 (**1 µM). In (E) intracellular ATP of parasites after treatment with the positive controls, KCN and CCCP, and the β-carbolines, **RCC** and **C5**, as assessed using the CellTiter-Glo Luminescent Cell Viability Assay (Promega). Representative flow cytometry histograms of three independent assays are presented. Two-way ANOVA followed by Bonferroni post hoc test. $^{**}p \leq 0.01$; $^{***}p \leq 0.001$; $^{****}p \leq 0.0001$.

3.7 Assessment of PS exposure on the membranes of treated amastigotes

When the cell starts the process of death, membrane integrity is altered and phosphatidylserine (PS) is exposed on the cell surface. For the evaluation of PS exposure, annexin V conjugated with FITC was used. In addition, PI was used to assay cell viability. Both PI and annexin V are impermeable when the cell membrane is intact. Annexin V binds to PS exposed on the surface of the plasma membrane, which occurs during apoptosis, and fluorescence can be detected. PI is only able to intercalate DNA if the membrane is permeabilized. Annexin V-positive and PI-negative cells indicate PS exposure and early apoptosis. While annexin Vnegative and PI-positive cells suggests late apoptosis or necrosis.

The positive control, amastigotes incubated with digitonin, was used to permeabilize the cell membrane, leading to a 55% increase in fluorescence intensity of PI. Miltefosine, and the β-carbolines, **RCC** and **C5**, did not show a difference in PI fluorescence compared to the untreated control, indicating that the membrane integrity was intact. Amastigotes treated with the compounds, miltefosine, **RCC**, and **C5** showed PS exposure at 39.7%, 44.2% and 37.65%, respectively (Figure 8). The results indicate that treatment with these compounds induce PS exposure or change the membrane permeability of the amastigotes.

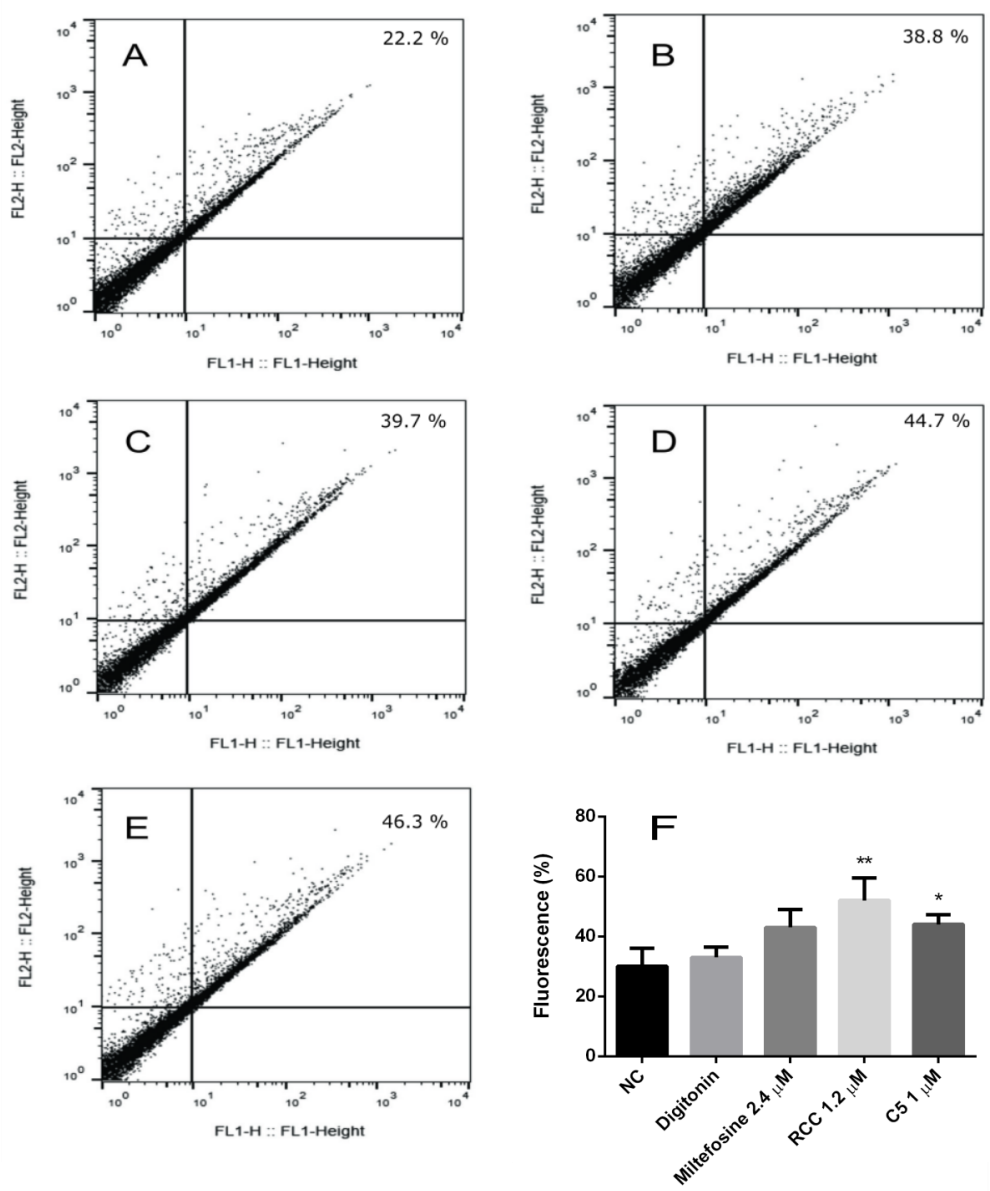

Figure 8. Exposure of the phosphatidylserine (PS) in treated *L. amazonensis* amastigotes. Flow cytometry dot plots of (A) untreated negative control (NC); (B) positive control, treated with digitonin; (C) amastigotes treated with miltefosine (2.4 µM); (D) amastigotes treated with **RCC (**1.2 µM); and (E) amastigotes treated with **C5 (**1 µM) for 48h. (F) Bar chart to show the percentage of parasites with fluorescence for annexin V. All the samples were marked with FITC-conjugated annexin V and PI. Representative dot plots of three independent assays are presented. Two-way ANOVA followed by Bonferroni post hoc test. *$p \leq 0.05$; **$p \leq 0.01$.

4. Discussion

The β-carboline derivatives are a group of alkaloids with an indole nucleus, a hydrogenated six-member pyridine ring that can have synthetic or natural origin. It has been demonstrated that these molecules are active against protozoa, bacteria, and tumor

cells (Daoud et al. 2014; Li et al. 2015; Nenaah 2010; Valdez et al. 2009). In this study, the β-carboline compounds, **RCC** and **C5**, exhibited strong activity against intracellular amastigotes of *L. amazonensis*, which was even greater than that of the anti-leishmanial drug, miltefosine. Previous studies have described the synthesis and biological activity of several β-carboline derivates, however, none of the tested substances presented activity higher than that of **RCC** and **C5** (Baréa et al. 2018; Mendes et al. 2016; Pedroso et al. 2011; Valdez et al. 2009; Volpato et al. 2013).

The results of cytotoxicity in J774A.1 macrophage and the anti-leishmanial activity against *L. amazonensis* showed that substances are more active against the protozoa with higher SIs. This corroborates previous results that have also demonstrated activity and selectivity against the other form of the parasite, the promastigote (Baréa et al. 2018; Pedroso et al. 2011). Based on the high activity and selectivity of **RCC** and **C5**, we further investigated the effects of these substances on the intracellular amastigotes. Through biochemical assays, it was possible to observe that **RCC** and **C5** induced amastigote death through metabolic alterations.

Both substances were able to enter the macrophages and induced death in the *L. amazonensis* amastigotes without drastically affecting macrophages. Treatment with the two compounds decreased the number of amastigotes inside the parasitophorous vacuole of the macrophage, as observed by light and electronic microscopy. Valdez et al. (2009) also described a reduction in the number of amastigotes after treatment of infected macrophages with C4 β-carboline. SEM enabled the visualization of some empty parasitophorous vacuoles within RCC- and C5-treated macrophages. Whilst cells that were treated with miltefosine also showed a decrease in the number of amastigotes.

TEM also revealed that amastigotes within β-carboline-treated macrophages had alterations in their mitochondria with mitochondrial swelling. This organelle is unique to trypanosomatids, with its own genetic material and being distinct to mitochondria of mammalian cell, therefore it is an important target for drug discovery studies (Mendes et al. 2016; Monzote et al. 2014; de Souza 2009). Changes in the mitochondria can be detrimental to the parasite, alterations to the flow of ions can affect ATP production, leading to death of this protozoa (Monzote et al. 2014; Mukherjee et al. 2002). In this study after treatment with **RCC** and **C5** there was depolarization and hyperpolarization of the mitochondrial membrane. This occurs due to the movement of electrons through

the mitochondrial respiratory chain during oxidative phosphorylation, generating an increase in the permeability of protons (Britta et al. 2014). The ATP levels is also affected because depolarization damages the ATP synthase complex and decreases the O_2 production (Alvarez et al. 2007).

Mitochondrial alterations may also be related to ergosterol synthesis. Several studies have shown that ergosterol and its analogues are essential for the organization and maintenance of the mitochondrial membrane (Rodrigues, Rodriguez, and Urbina 2002). Our results showed that treatment with **RCC** and **C5** increased lipid accumulation in the amastigotes, known as lipid-storage bodies, which are composed of ergosterol, fatty acids and phospholipids. This could be due to different perturbations or oxidative stress in the parasite (Rodrigues et al. 2008; Stefanello et al. 2014). These effects can lead to physical alterations in the membranes, membrane trafficking, cell signaling, abnormal metabolic production and production of proteins that regulate the activity of nitric oxide and arginase in the macrophages (Bozza et al. 2008; Kathuria et al. 2014; Santa-Rita et al. 2004). Although the results demonstrated mitochondrial depolarization and accumulation of lipid-storage bodies upon treatment with the β-carbolines, there was not an increase in ROS. The alterations in the mitochondria and lipids could be a secondary response of oxidative stress or due to an autophagic process occurring in the parasite leading to a decrease in the ROS levels. In fact, the production of ROS can be observed after the macrophages infection without treatment, as a normal mechanism to deal with the parasite and the stress (Manzano et al. 2017).

The formation of vacuoles with lysosomal activity, known as the autophagosomes, can be induced by cell stress, such as in response to a lack of nutrient, growth, development and cell division (Proto, Coombs, and Mottram 2013). In the TEM micrographs of the β-carboline-treated amastigotes, several vacuoles could be seen. To confirm these organelles as autophagic vacuoles, the MDC probe was implemented, an autofluorescent compound that labels these organelles (Munafó and Colombo 2001), which showed that the vacuoles are predominantly autophagic. It can be inferred that the induced lysosomal activity led to the accumulated degraded cellular material. Autophagic vacuoles are formed from a double membrane, sometimes, called of myelin-figure like (precursor structure), which participates in catabolic process such as protein degradation (Brooks and Striepen 2011; Proto, Coombs, and Mottram 2013). The autophagy process observed here could lead directly to death of the parasite, or influence the infectivity of

the parasite during remodeling of the *Leishmania* life cycle or mitochondrial function as has been shown for *Trypanosoma cruzi* (Meyer and Biofi 2008; Williams et al. 2006).

To determine whether the amastigote death was related to apoptosis, the membrane integrity and the PS exposure were evaluated. After treatment with **RCC** and **C5** no changes in membrane permeability and PS exposure were detected. Several studies showed that the PS exposure is a feature of early or late apoptosis (Kaplum et al. 2016; Lazarin-bidóia et al. 2016). However, a recent study reported that a transporter called LABCG-2 in *Leishmania* spp. is related with resistance to the antimonial and to protozoan virulence. Expression of LABCG-2 produced a defect in the external surface of PS during metacyclogenesis, which displayed levels of the molecules that occur during autophagy (Manzano et al. 2017).

Intracellular amastigotes treated with **RCC**, vesicles of around 100 nm could be observed at the surface of the amastigotes. These vesicles, known as exosomes, are essential for cellular communication, as they carry specific lipids, proteins, mRNA and miRNA from the cell (Lynn et al. 2010; Marshall et al. 2018; Torró, Moreira, and Osuna 2018). During the treatment, the amastigotes have undergone changes, which leads to the formation of more exosomes.

Parasites treated with **C5** had an alteration in the flagellar pocket, the site unique for exocytosis and important for the cytoskeleton of trypanosomatids (Santa-Rita et al. 2004). Changes in this region can be seen as a result of ergosterol synthesis inhibition (De Macedo-Silva et al. 2013); the accumulation of lipid bodies observed in this study support this hypothesis. This change usually leads to a lack of subpellicular microtubules, marking the region of the flagellar pocket more susceptible to morphological changes due to the action of substances (Almeida-Souza et al. 2016; Magaraci et al. 2003).

5. Conclusion

This study assessed two derivatives of β-carbolines, **RCC** and **C5**, against *L. amazonensis* intracellular amastigotes, highlighting the promising activity of these substances as potential anti-leishmanial drugs. The results suggest that both of these compounds are more efficient than miltefosine due to the significantly reduced number of amastigotes in the parasitophorus vacuoles of the host macrophages and the reduced

toxicity against the mammalian cells. Furthermore, the death of the parasites caused by these substances can be related to autophagy, and the initial changes in the amastigotes may be related to ergosterol synthesis accumulating lipid bodies, the formation of autophagosomes, and changes in the production of exovesicles (**RCC**) and in the flagellar pocket (**C5**). Further studies to find the molecular target of these β-carboline derivatives and *in vivo* assays are needed in order to confirm **RCC** and **C5** as potent and efficient substances against *Leishmania* parasites.

6. Authors' contributions

JCP contributed to the biological analysis and elaboration of the manuscript. NSF contributed with data analysis and elaboration of the manuscript. TKK contributed to the biological analysis. PB and MHS contributed with the synthesis of the substances. TUN and CVN designed the study, supervised the laboratory work and contributed to critical reading of the manuscript. All the authors have read the final manuscript and approved the submission.

7. Conflicts of interest

All authors declare no conflicts of interest.

8. References

Almeida-souza, Fernando et al. 2016. "Ultrastructural Changes and Death of *Leishmania infantum* Promastigotes Induced by *Morinda citrifolia* Linn . Fruit (Noni Juice Treatment." *Evidence-Based Complementary and Alternative Medicine* 2016: 1–10.

Alvarez, Noel et al. 2007. "Mitochondrial Superoxide Radicals Mediate Programmed Cell Death in *Trypanosoma cruzi* : Cytoprotective Action of Mitochondrial Iron Superoxide Dismutase Overexpression." *The journal of biological chemistry* 334: 323–34.

Baréa, Paula et al. 2018. "Synthesis, Antileishmanial Activity and Mechanism of Action

Studies of Novel β-Carboline-1,3,5-Triazine Hybrids." *European Journal of Medicinal Chemistry* 150: 579–90.

Bozza, Patrícia T. et al. 2008. "Induction of Autophagy Correlates with Increased Parasite Load of *Leishmania amazonensis* in BALB/c but Not C57BL/6 Macrophages." *Microbes and Infection* 11(2): 181–90.

Britta, Elizandra Aparecida et al. 2014. "Cell Death and Ultrastructural Alterations in *Leishmania amazonensis* Caused by New Compound 4-Nitrobenzaldehyde Thiosemicarbazone Derived from S-Limonene." *BMC Microbiology* 14(1): 1–12.

Brooks, Carrie F, and Boris Striepen. 2011. "Autophagy Protein Atg3 Is Essential for Maintaining Mitochondrial Integrity and for Normal Intracellular Development of *Toxoplasma gondii* Tachyzoites." *Plos Pathogens* 7(12).

Clemente, Wanessa Trindade et al. 2018. "Visceral and Cutaneous Leishmaniasis Recommendations for Solid Organ Transplant Recipients and Donors." *Journal of Medicinal Chemistry* 102(2).

Daoud, Abdelkader, Jing Song, Feiyang Xiao, and Jing Shang. 2014. "B-9-3 , a Novel β -Carboline Derivative Exhibits Anti-Cancer Activity via Induction of Apoptosis and Inhibition of Cell Migration in vitro." *European Journal of Pharmacology* 724: 219–30.

Ewa Grelaa, Joanna Kozłowskab, Agnieszka Grabowiecka. 2018. "Current Methodology of MTT Assay in Bacteria – A Review." *Acta Histochemica journal* 120(303–311): 21.

Hempel, Stephen L. et al. 1999. "Dihydrofluorescein Diacetate Is Superior for Detecting Intracellular Oxidants." *Free radical biology & medicine* 27(99): 146–59.

Kaplum, Vanessa et al. 2016. "In vitro and in vivo Activities of 2,3-Diarylsubstituted Quinoxaline Derivatives against *Leishmania amazonensis*." *Antimicrobial Agents and Chemotherapy* 60(6): 3433–44.

Kathuria, Manoj et al. 2014. "Induction of Mitochondrial Dysfunction and Oxidative Stress in *Leishmania donovani* by Orally Active Clerodane Diterpene." *Antimicrobial Agents and Chemotherapy* 58(10): 5916–28.

Lazarin-bidóia, Danielle et al. 2016. “Affect the *Trypanosoma cruzi* Redox System.” *Antimicrobial Agents and Chemotherapy* 60(2): 890–903.

Li, X et al. 2015. “Novel β -Carbolines against Colorectal Cancer Cell Growth via Inhibition of Wnt / β -Catenin Signaling.” *Cell Death Differentiation Association* (August): 1–9.

Lynn, M. A. et al. 2010. “Leishmania Exosomes Modulate Innate and Adaptive Immune Responses through Effects on Monocytes and Dendritic Cells.” *The Journal of Immunology* 185(9): 5011–22.

De Macedo-Silva, Sara Teixeira, Julio A. Urbina, Wanderley De Souza, and Juliany Cola Fernandes Rodrigues. 2013. “In vitro Activity of the Antifungal Azoles Itraconazole and Posaconazole against *Leishmania amazonensis*.” *PLoS ONE* 8(12).

Magaraci, Filippo et al. 2003. “Azasterols as Inhibitors of Sterol 24-Methyltransferase in Leishmania Species and *Trypanosoma cruzi*.” *Journal of Medicinal Chemistry* 46(22): 4714–27.

Manzano, José Ignacio et al. 2017. “*Leishmania* LABCG1 and LABCG2 Transporters Are Involved in Virulence and Oxidative Stress: Functional Linkage with Autophagy.” *Parasites and Vectors* 10(1): 1–12.

Marshall, Skye et al. 2018. “Extracellular Release of Virulence Factor Major Surface Protease via Exosomes in *Leishmania infantum* Promastigotes.” *Parasites and Vectors* 11(1): 1–10.

Mendes, Edevi Arbonelli et al. 2016. “Chemico-Biological Interactions C5 Induces Different Cell Death Pathways in Promastigotes of *Leishmania amazonensis*.” *Chemico-Biological Interactions* 256: 16–24.

Meyer, Hertha, and Instituto De Biofı. 2008. “Autophagy Is Involved in Nutritional Stress Response and Differentiation in *Trypanosoma cruzi*.” *The Journal of Biological Chemistry* 283(6): 3454–64.

Mitropoulos, Panagiotis, Pete Konidas, and Mindy Durkin-Konidas. 2010. “New World Cutaneous Leishmaniasis: Updated Review of Current and Future Diagnosis and

Treatment." *Journal of the American Academy of Dermatology* 63(2): 309–22.

Monzote, Lianet et al. 2014. "Experimental Parasitology Essential Oil from *Chenopodium ambrosioides* and Main Components : Activity against *Leishmania* , Their Mitochondria and Other Microorganisms." *Experimental Parasitology* 136(601): 20–26.

Mukherjee, Sikha Bettina, Manika Das, Ganapasam Sudhandiran, and Chandrima Shaha. 2002. "Increase in Cytosolic Ca2+ Levels through the Activation of Non-Selective Cation Channels Induced by Oxidative Stress Causes Mitochondrial Depolarization Leading to Apoptosis-like Death in *Leishmania donovani* Promastigotes." *Journal of Biological Chemistry* 277(27): 24717–27.

Munafó, Daniela B, and María I Colombo. 2001. "A Novel Assay to Study Autophagy : Regulation of Autophagosome Vacuole Size by Amino Acid Deprivation." *Journal of Cell Science*.

Nenaah, Gomah. 2010. "Fitoterapia Antibacterial and Antifungal Activities of (Beta) - Carboline Alkaloids of *Peganum harmala* (L) Seeds and Their Combination Effects." *Fitoterapia* 81: 779–82.

Pedroso, R B et al. 2011. "Beta-Carboline-3-Carboxamide Derivatives as Promising Antileishmanial Agents." *Annals of Tropical Medicine & Parasitology* 105(8): 549–57.

Proto, William R., Graham H. Coombs, and Jeremy C. Mottram. 2013. "Cell Death in Parasitic Protozoa: Regulated or Incidental?" *Nature Reviews Microbiology* 11(1): 58–66.

Rodrigues et al. 2008. "In vitro Activities of ER-119884 and E5700, Two Potent Squalene Synthase Inhibitors, against *Leishmania amazonensis*: Antiproliferative, Biochemical, and Ultrastructural Effects." *Antimicrobial Agents and Chemotherapy* 52(11): 4098–4114.

Rodrigues, Juliany C F, Carlos Rodriguez, and Julio A Urbina. 2002. "Ultrastructural and Biochemical Alterations Induced by Promastigote and Amastigote Forms of *Leishmania amazonensis*." *Antimicrobial Agents and Chemotherapy* 46(2): 487–99.

Santa-Rita, Ricardo M., Andréa Henriques-Pons, Helene S. Barbosa, and Solange L. de Castro. 2004. “Effect of the Lysophospholipid Analogues Edelfosine, Ilmofosine and Miltefosine against *Leishmania amazonensis*.” *Journal of Antimicrobial Chemotherapy* 54(4): 704–10.

de Souza, Wanderley. 2009. “Structural Organization of *Trypanosoma cruzi*.” *Memorias do Instituto Oswaldo Cruz* 104(SUPPL. 1): 89–100.

Stefanello, T. F. et al. 2014. “N-Butyl-[1-(4-Methoxy)Phenyl-9H-β-Carboline]-3-Carboxamide Prevents Cytokinesis in *Leishmania amazonensis*.” *Antimicrobial Agents and Chemotherapy* 58(12): 7112–20.

Sunter, Jack, and Keith Gull. 2017. “Shape, Form, Function and *Leishmania* Pathogenicity: From Textbook Descriptions to Biological Understanding.” *Open biology* 7(9).

Torró, Luis M De Pablos, Lissette Retana Moreira, and Antonio Osuna. 2018. “Extracellular Vesicles in Chagas Disease : A New Passenger for an Old Disease.” *Frontiers in Microbiology* 9(June): 1–11.

Valdez, Rodrigo Hinojosa et al. 2009. “Biological Activity of 1,2,3,4-Tetrahydro-β-Carboline-3-Carboxamides against *Trypanosoma cruzi*.” *Acta Tropica* 110(1): 7–14.

Volpato, Hélito et al. 2013. “Tetrahydro- -Carboline-3-Carboxamide against *Leishmania amazonensis* Are Mediated by Mitochondrial Dysfunction.” *Evidence-Based Complementary and AlternativeMedicine* 2013: 1–7.

Williams, Roderick A, Laurence Tetley, Jeremy C Mottram, and Graham H Coombs. 2006. “Cysteine Peptidases CPA and CPB Are Vital for Autophagy and Differentiation in *Leishmania mexicana*.” *Molecular Microbiology* 61(June): 655–74.

World Health Organization. Leishmaniasis epidemiological situation. http://www.who.int/leishmaniasis/burden/en/. Updated 2019. Accessed May,24, 2019.

Artigo Científico 2

Submissão: European Journal of Medicinal Chemistry

Fator de impacto: 4,876

Antiproliferative activity of the dibenzilidenoacetone derivate (E)-3-ethyl-4-(4-nitrophenyl)but-3-en-2-one in *Trypanosoma cruzi*

Jéssica Carreira de Paula[1], Amanda Beatriz Kawano Bakoshi[1], Danielle Lazarin-Bidóia[1], Zia Ud Din[2], Edson Rodrigues-Filho[2], Tania Ueda-Nakamura[1], Celso Vataru Nakamura[1, a]

[1] Programa de Pós-graduação em Ciências Biológicas, Laboratório de Inovação Tecnológica no Desenvolvimento de Fármacos e Cosméticos, Universidade Estadual de Maringá, Bloco B-08, Av. Colombo 5790, Maringá, PR CEP 87020-900, Brazil

[2] LaBioMMi, Departamento de Química, Universidade Federal de São Carlos, CP 676, São Carlos, SP 13.565-905, Brazil

[a] email address: cvnakamura@gmail.com

Abstract

Chagas' disease is one of the most prevalent neglected diseases in the world. It is found in 21 countries and affect approximately 8 million people. The illness is caused by *Trypanosoma cruzi*, a protozoan parasite with a complex life cycle and three morphologically distinct evolutionary forms. Nowadays, the treatment is based only in two nitroderivative drugs, benznidazole and nifurtimox, which cause serious side effects. Since the treatment is limited, the search for new treatment options for patients with Chagas' disease becomes necessary. In this study we analyzed the substance **A11K3**, a dibenzilidenoacetone (DBA). These group of substances have an acyclic dienone attached to aryl groups in both β-positions and several studies showed that DBA's has biological activity against tumors cells, bacteria and protozoa as *T. cruzi* and *Leishmania spp.* **A11K3** was active against epimastigotes, tripomastigotes and intracellular amastigotes forms with IC_{50} = 3.3 ± 0.8, EC_{50} = 24 ± 4.3 and IC_{50} = 9.3 ± 0.5 µM. Citotoxity assay in $LLCMK_2$ cells showed CC_{50} of 239.2 ± 15.7 µM, so the selectivity index (CC_{50}/IC_{50}) was of 72.7 for epimastigotes, 9.9 for trypomastigotes and 25.9 for intracellular amastigotes. The morphological and ultrastructural analysis by TEM and SEM of the parasites treated

with **A11K3** induced alterations in Golgi complex, mitochondria, plasma membrane, cell body, increase of autophagic vacuoles and lipid bodies. Biochemical assays of *T. cruzi* generated increase of ROS, plasma membrane ruptures, lipid peroxidation, mitochondrial membrane depolarization with ATP decrease and autophagic vacuoles. The results obtained lead us to believe that **A11K3** lead the protozoan to death cellular collapse and death similar to ferroptosis.

Keywords: Chagas disease, *Trypanosoma cruzi*, dibenzilidenoacetone, ferroptosis.

1. Introduction

Chagas disease is a neglected tropical disease caused by the protozoan *Trypanosoma cruzi*, affecting 6-7 million people worldwide (WHO, 2018). This protozoan displays three distinct evolutionary relevant forms. Epimastigotes, found inside the hematophagous insect; trypomastigotes, the infective form, found in the insect vector and in the blood circulation of the mammalian; and amastigotes, found intracellularly in tissues of mammalian host. Epimastigotes and amastigotes are the replicative forms of the parasite (Alves et al. 2007; Nogueira et al. 2007).

The infection by *T. cruzi* has two clinical phase: acute phase characterized by high parasitemia; and the chronic phase, a long and progressive phase that can manifest symptoms after some years. The treatment of Chagas' disease is performed with two drugs, nifurtimox or benznidazole. However, they have several side effects and limited therapeutic potential (Coura 2009; Izumi et al. 2011).

Several studies have shown that synthetic compounds have great potential for the treatment of Chagas' disease. The 1,5-Diarylpentanoid dibenzylideneacetone and their derivatives are substance that have an acyclic dienone attached to aryl groups in both β-positions. These substances demonstrated antiproliferative, anti-inflammatory and apoptotic effects in cancer cell lines (Bhandarkar et al. 2008; Prasad et al. 2011; Ud et al. 2014; H-j Yu et al. 2013). Others studies reported the anti-leishmanial and anti-trypanosomal effects of the dibenzylideneacetones (Garcia et al. 2017; Lazarin-Bidóia et al. 2016). Based in the context, the aim of this study is to elucidate the possible mechanism of action of the substance against epimastigotes and intracellular amastigotes of *T. cruzi*.

2. Material and Methods

2.1. Chemicals

The following chemicals were used: carbonylcyanide m-chlorophenylhydrazone (CCCP), rhodamine 123 (Rh 123), dancylcadaverine (MDC), Nile Red, Digitonin, methylphenazinium methyl sulfate (PMS), dihydrochlorofluorescein (H_2DCFDA), wortinmanin, potassium cyanate (KCN), dimethylsulfoxide (DMSO), hemin and folic acid were purchase from Sigma-Aldrich (St. Louis, MO, USA). The 3-[4,5-dimethylthiazol-2-yl]-2,5phenyltetrazolium bromide (MTT), 2,3-Bis(2-methoxy-4-5-5sulfophenyl)-2H-tetrazolium-5-carboxanilide (XTT), propidium iodide (PI) and Annexin V conjuged with FITC of the Invitrogen. Dulbecco's modified medium (DMEM), Fetal bovine serum (FBS) and Giemsa were purchase from Gibco, Invitrogen (Grand Island, NY, USA). Sodium Cacodylate buffer (CaCo), solution of 1% osmium tetroxide (OsO_4), 0.8% potassium ferrocyanide, and 10 mM $CaCl_2$, lead citrate, uranyl acetate, 25% glutaraldehyde and EPON resin were purchase from EMS – Electron microscopy Sciences. The diphenyl-1-pyrenylphosphine (DPPP) of the Molecular Probes. Cell Titer-Glo® Luminescent Cell Viability Assay were purchase from Promega.

2.2. Synthesis and preparation of the dibenzylideneacetones derivate A11K3

The synthesis of the substance (E)-3-ethyl-4-(4-nitrophenyl)but-3-en-2-one (**A11K3**), was performed by deuterated solvents of Apolo and were used for the NMR analysis. Thin layer chromatography was performed with precoated silica gel G-25-UV254 plates and detection was carried out at 254 nm under UV, and by vanillin in H_2SO_4 solution. ^{1}H NMR, ^{13}C NMR were performed on a Brüker AVANCE 400 operating at 400.15 MHz and 100.62 MHz, respectively; $CDCl_3$ was used as solvent and tetramethylsilane (TMS) as internal reference. All compounds were dissolved in organic solvents at about 5-10 mg mL^{-1} each and shifted into a 5-mm NMR tube. Chemical shifts (δ in ppm) were measured with accuracy of 0.01 (^{1}H) and 0.1 ppm (^{13}C).

2.2.1. (3E)-3-[(4-nitrophenyl)methylene]-2-Pentanone

p-Nitrobenzaldehyde (1 g, 6.6 mmol) and 2-pentanone (1.05 g, 12.2 mmol) were taken in a 50 mL two - necked round bottomed flask. Dry HCl gas was passed via the content of the flask until it was saturated and coloration appeared. The reaction mixture was stirred for 8 hrs. The crude product was dilute with toluene and washed with $NaHSO_3$ solution. The organic layer was separated, dried with anhydrous Na_2SO_4 and evaporated in vacuo. The residue was distilled under reduced pressure to give pure substance, which was solidified by keeping in a refrigerator for 24 hours. Percent yield: 83 %; Mp: 122-124 °C; ^{1}H NMR (400 MHz, $CDCl_3$) δ 8.24 (d, *J* = 8.9 Hz, 2H), 7.52 (d, *J* = 8.4 Hz, 2H), 7.45 (s, 1H), 2.47 (q, *J* = 7.5 Hz, 4H), 2.46 (s, 3H), 1.07 (t, *J* = 7.5 Hz, 3H). ^{13}C NMR (101 MHz, $CDCl_3$) δ 199.85 (1C), 144.51 (1C), 137.88 (1C), 134.50 (1C), 134.18 (1C), 130.49 (2C), 128.82 (2C), 26.15 (1C), 19.60 (1C), 13.69 (1C).

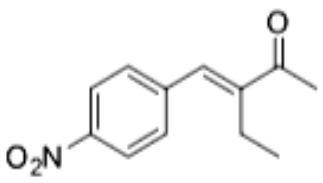

Figure 1. Chemical structure of dibenzilidenoacetone derivated (E)-3-ethyl-4-(4-nitrophenyl)but-3-en-2-one (**A11K3**).

2.3. Parasites and cell culture

Epimastigotes of *T. cruzi*, Y strain (TcIV), were maintained at 28 °C in LIT (liver infusion tryptose, pH 7.4) medium supplemented with 10% FBS heat-inactivated. Trypomastigotes and intracellular amastigotes were obtained from infected monolayers of $LLCMK_2$ cells (*Macaca mulata* kidney epithelials cells); CCL-7; American Type Culture Collection, Rockville, MD, USA) in DMEM medium supplemented with 2 mM L-glutamine and 10% FBS and buffered with sodium bicarbonate in a 5% CO_2-air mixture at 37 °C.

2.4. Activity in epimastigotes, trypomastigotes and intracellular amastigotes

Epimastigotes (1 x 10^6 parasites/mL), were treated with different concentrations (1, 5, 10, 50 and 100 µM) of **A11K3** for 96 h at 28 °C. After incubation was added 50 µL of solution of XTT/PMS (0.5 and 0.3 mg/mL) in the absence of light for 4 h. The absorbance was read in a spectrophotometer at 450 nm. The concentration that decreased 50% (IC_{50}) of the epimastigotes was determined by linear regression analysis of the data. Trypomastigotes (1x10^7 parasites/mL) were obtained from supernatant of infected cells, treated with the substance **A11K3** in increase concentrations (1, 5, 10, 50, 100 µM) and incubated at 37 °C with the 5% atmosphere CO_2 for 24 h. After that, the viable trypomastigotes were counted and the EC_{50} were determined. For the antiproliferative assay against intracellular amastigotes, $LLCMK_2$ (2.5 x 10^5 cells/mL) were added in the plate with coverslips and incubated for 24 h at 37 °C. After that, trypomastigotes (1 x 10^7 parasites/mL) were added in the culture of $LLCMK_2$ and incubated at 37 °C. After 24 h, they were treated with **A11K3** (1, 5, 10, 50 and 100 µM) and incubated for 96 h. For the determination of IC_{50}, the infected cells were fixed with methanol and stained with Giemsa and the number of infected cells and amastigotes were determined under a light microscope by counting randomly 200 cells in duplicate cultures. The results were expressed as the survival index (%). The survival index was obtained by multiplying the percentage of infected cells by the number of amastigotes per infected $LLCMK_2$ cell. The survival index observed in the control without treatment was considered as 100%, the results for treated groups were comparatively evaluated.

2.5. Citotoxicity in $LLCMK_2$ cells

$LLCMK_2$ cells (2.5 x 10^5 cells/mL) were added in 96 wells plate with FBS 10% and incubated at 37 °C with 5% CO_2 atmosphere. After 24 h, the culture was treated with the concentrations 1, 5, 10, 50 and 100 µM of the compound **A11K3**. The cells were incubated as described before. The results were obtained by MTT reduction method (2 mg/mL), that consist on the ability of viable cells to convert tetrazolium yellow salt into a purple compound, formazan, soluble in DMSO (Grela, Kozłowska, and Grabowiecka 2018). The samples were read in spectrophotometer (Power Wave XS - Bio-Tek) at 570 nm and the cytotoxic concentration for 50% of the LLCMK2 (CC_{50}) was determined.

2.6. Electron microscopy

Epimastigotes and intracellular amastigotes were treated or not (control) with benznidazole and **A11K3** IC_{50}, incubated for 24 and 96 h, respectively. After the treatment, the samples were fixed with 2.5% glutaraldehyde in 0.1M cacodylate buffer for 1 h. For the scanning electron microscopy (SEM), the samples were adhered in coverslips with poli-L-lisine and, after fixation, dehydrated in increasing concentrations of ethanol, submitted to critical point and metalized with gold. Lastly, the samples were observed on FEI Quanta 250 SEM. For the ultrastructural analysis, after the fixation, the samples were post fixed in a solution of 1% OsO4, 0.8% potassium ferrocyanide, and 10 mM $CaCl_2$ in 0.1 M cacodylate buffer, dehydrated in increasing concentrations of acetone and embedded in EMbed 812 resin. Ultrathin sections of the 60 nm were obtained, contrasted with uranyl acetate and lead citrate, and observed on a JEOL JM 1400 TEM.

2.7. Biochemical assays

Epimastigotes (1 x 10^6 parasites/mL) were treated or not with 3.3 and 6.6 µM **A11K3** and incubated for 24 h and 96 h at 28 ^oC.

For the analysis of intracellular amastigotes, $LLCMK_2$ cells were infected with trypomastigotes, as described above (Section 2.4). After the treatment or not (control), with benznidazole, 3.3 or 6.6 µM **A11K3**, the samples were incubated for 24 h and 96 h. After, intracellular amastigotes were isolated by rupture of $LLCMK_2$ cells membrane and differential centrifugation by 1,000 rpm for 3 min. Supernatant was collected and then, centrifuged at 3,000 rpm for 5 min. Amastigotes were standardized in the concentration of 1 x10^6 parasites/mL. Amastigotes not treated were used as negative control.

2.7.1. Detection of total reactive oxygen species (ROS)

Epimastigotes and amastigotes were labelled with the probe 10 µM H_2DCFDA in the dark for 45 min. In the parasite, H_2DCFDA is hydrolyzed by esterases giving to compound dihydrochlorofluorescein (H_2-DCF). This compound is converted at diclorofluorescein (DCF) generating fluorescence in presence the ROS (Crow 1997;

Hempel et al. 1999). The fluorescence was determined in a Victor X3 spectrophotometer at λ_{ex} of 488nm and λ_{em} of 530 nm.

2.7.2. Detection of storage lipid bodies

Epimastigotes and intracellular amastigotes treated with A11K3 were labelled with the probe 10 µg/mL Nile red in the dark for 30 min. The probe Nile red is a pigment liposelective, which associates with neutral lipid molecules. It is used in assays for quantitative and qualitative analysis of intracellular lipids in several cells types (Greenspan 1985). The fluorescence was observed in Olympus BX51 fluorescence microscope (Olympus, Tokyo, Japan) and quantified in a Victor X3 spectrophotometer at λ_{ex} of 490 nm and λ_{em} of 535 nm.

2.7.3. Determination of cell membrane integrity

After the treatment with **A11K3**, the epimastigotes were incubated with 0.2 µg/mL PI in the dark for 5 min. Digitonin (40 µM) was used as positive control. The acquisition of data was performed using a FACSCalibur flow cytometer equipped with CellQuest software and10,000 events were acquired. Alterations in the fluorescence of PI of treated parasites were compared with the fluorescence of untreated parasites.

2.7.4. Phosphatidylserine exposure (PS)

Phosphatidylserine exposure was determined using the probe Annexin V conjugates with FITC. The epimastigotes were incubated in presence of the probe for 15 min. After the incubation, PI was added. Data acquisition was performed using a FACSCalibur flow cytometer equipped with CellQuest software and 10.000 events were acquired and the phosphatidylserine exposure of parasites treated was compared with the untreated parasites.

2.7.5. Lipid peroxidation assay

After the treatment with **A11K3**, the epimastigotes were labeled with 50 µM DPPP in the dark for 15 min. DPPP is not fluorescent until it is oxidized to a phosphine oxide (DPPP-O) by peroxides. The fluorescence was quantified in a Victor X3 spectrophotometer at λ_{ex} of 380 nm and λ_{em} of 460 nm.

2.7.6. Determination of membrane mitochondrial potential (ΔΨm)

The epimastigotes treated with **A11K3** were incubated with rhodamine 123 (5 µg/mL) in the dark for 30 min. CCCP (100 µM) was used as a positive control. After the incubation, the samples were washed twice with PBS, for remove the excess of the probe and incubated for another 15 min. The acquisition of data was realized using FACSCalibur flow cytometer equipped with CellQuest software. A total 10,000 events were acquired. Alterations in Rh123 fluorescence were determined using the index of variation (MT - MC)/MC, where MT is the median fluorescent for the treated parasites and MC is the median fluorescence for the untreated control.

2.7.7. Detection of intracellular ATP

The epimastigotes treated or not treated with **A11K3** were incubated with 50 µL of the Cell Titer-Glo® Luminescent Cell Viability Assay and the luminescence was determined in a Victor X3 spectrophotometer at 590 nm. For the positive control, it was used 50 µM KCN and 100 µM CCCP.

2.7.8. Evaluation of autophagy vacuoles

The epimastigotes treated or not treated with **A11K3** were labelling with 0.05 mM of MDC in the dark for 60 min. This probe has affinity by autophagy vacuoles due to the combination and imprisonment of ions and interactions with lipid membrane. For the positive control, it was used parasites without serum. Additionally, parasites were pretreated with 0.5 µM of wortmannin, a potent inhibitor of PI3 kinase. The fluorescence was quantified in a Victor X3 spectrophotometer at λ_{ex} of 380 nm and λ_{em} of 525 nm.

3. Results

3.1.Preparation of the derivate A11K3

The reaction of *p*-nitrobenzaldehyde (A_{11}) with 2-pentanone (K_3), using gaseous HCl as catalyst, as outlined in Scheme 1, was performed at room temperature by stirring the reaction mixture and passing dry gaseous HCl until the reaction mixture turned white-yellow.

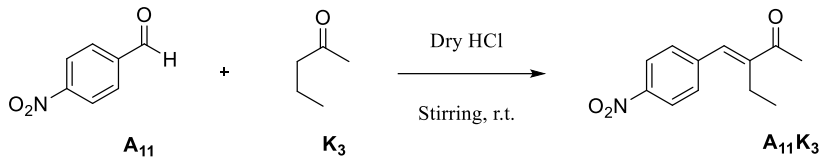

Scheme 1. Acid catalyzed aldol condensation of aldehydes A_{11} with ketones K_3.

3.2. Epimastigotes, trypomastigotes and intracellular amastigotes activity

In the present study, we analyzed the activity of a dibenzilidenoacetone, **A11K3** on epimastigotes, trypomastigotes and intracellular amastigotes. The compound showed a IC_{50} of 3.3 ± 0.8 µM, EC_{50} of 24.0 ± 4.3 and IC_{50} of 9.2 ± 0.57, respectively. In $LLCMK_2$ cells, **A11K3** presented a CC_{50} of 239.2 ± 15.7 µM. The selective index (SI) was calculated (ratio: CC_{50} of cells divided by IC_{50} of the **A11K3** in the parasites). The SI for epimastigotes was 72.5, for trypomastigotes 10.0, and for amastigotes 26.0, showing that the **A11K3** was more toxic to the protozoan than to mammalian cells (Table 1).

Table 1. Activity of DBA **A11K3** in epimastigotes, trypomastigotes e amastigotes of *Trypanosoma cruzi* and citotoxicity in epitelials cells $LLCMK_2$.

	Epimastigotes ***(IC_{50})****	***Trypomastigotes*** ***(EC_{50})****	***Amastigotes*** ***(IC_{50})****	***$LLCMK_2$*** ***(CC_{50})****
A11K3	3.3 ± 0.8	24.0 ± 4.3	9.2 ± 0.6	239.3 ± 15.7
SI	72.6	10.0	26.0	

IC_{50} = inhibitory concentration of 50% of the parasites

EC_{50} = effective concentration of 50 % of the parasites

*results expressed in µM

SI = CC_{50}/IC_{50} or EC_{50}

3.3. Ultrastructural and morphological evaluation in epimastigotes and intracellular amastigotes after treatment with A11K3

Ultrastructural and morphological alterations were evaluated by TEM and SEM. Untreated epimastigotes exhibited nucleus, mitochondria, flagellar pocket, Golgi apparatus and others structure preserved (Figure 2, A). Epimastigotes treated with 3.3 and 6.6 µM **A11K3** for 24 h showed changes in the production of reservosomos (Figure 2, B), presence of autophagic vacuoles, increase of Golgi vesicles and concentric membranes can also be observed (Figure 2, C). The treatment with **A11K**3 for 96 h showed an increase of autophagic vacuoles (Figure 2, D) and accumulation of lipid bodies and nuclear alteration (Figure 2, F).

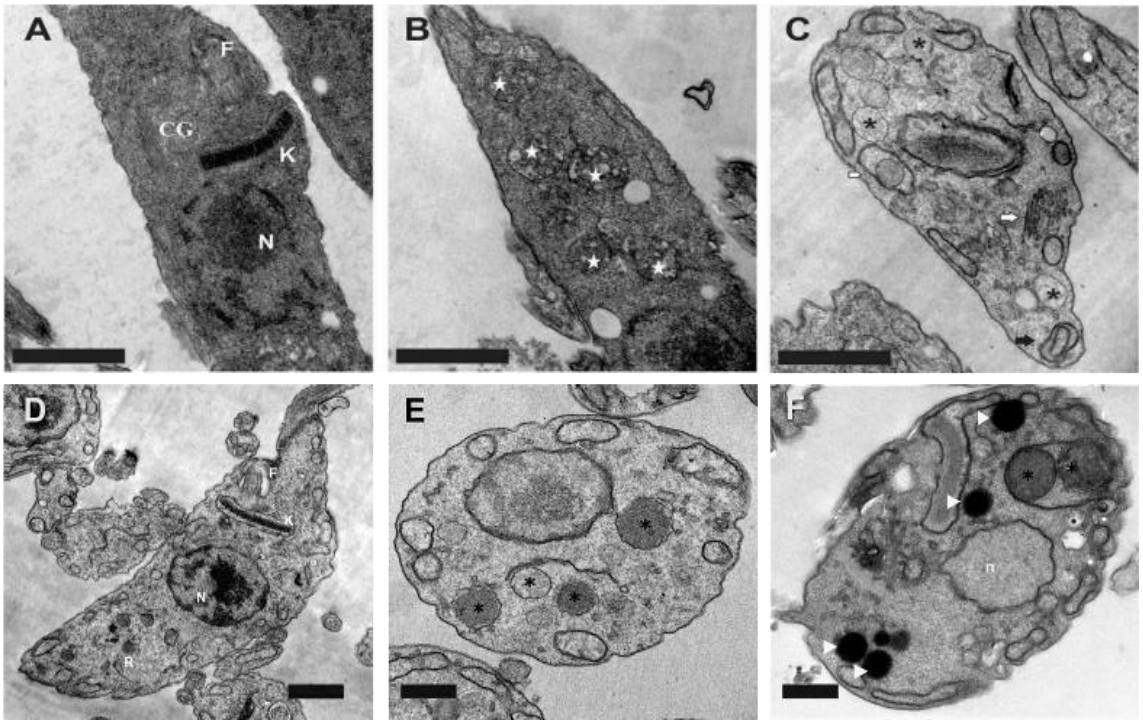

Figure 2. Ultrastructural alterations in epimastigotes of *Trypanosoma cruzi* treated with 3.3 and 6.6 µM **A11K3** for 24 h (A-C) and 96 h (D-F), visualized by transmission electron microscopy. Negative control (A and D) with normal morphology. In (B) and (E) epimastigotes treated with 3.3 µM **A11K3** for 24 and 96 h. In (C) and (F) epimastigotes treated with 6.6 µM **A11K3** for 24 and 96 h. Flagellum: F; Nucleous: N; Kinetoplast: K; Golgi complex: (CG). Reservosomos (White star), autophagy vacuoles (*), vesicles of Golgi complex (White arrow), concentric membrane (black arrow) and Lipid bodies (white arrow head). Bars = 5 µM.

In the SEM images, it was observed that untreated epimastigotes has the bodies, flagellum and size without alterations (Figure 3, A and D). The parasites treated with 3.3 µM **A11K3** for 24 h showed rounding bodies (Figure 3, B). For the treatment with 6.6 µM of **A11K3, it** was observed flagella length reduction (Figure 3, C). Epimastigotes treated for 96 h showed emergence of extra flagellum (Figure 3, E), and loss of membrane integrity (Figure 3, F), after exposure with 3.3 and 6.6 µM **A11K3**, respectivelly.

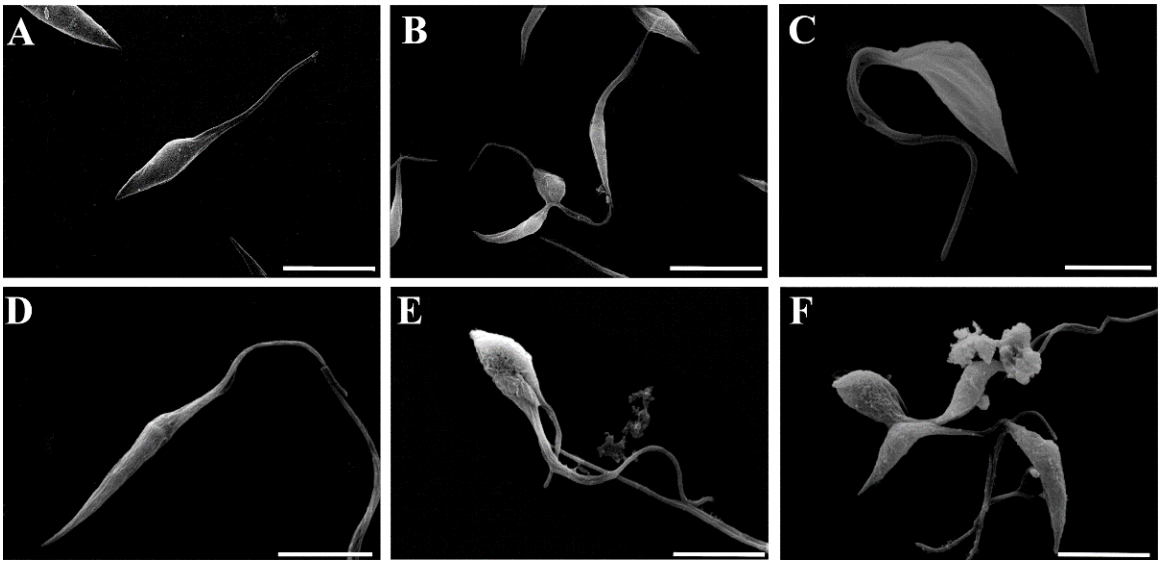

Figure 3. Morphological alterations in epimastigotes of *Trypanosoma cruzi* treated with 3.3 and 6.6 µM **A11K3** for 24 and 96 h. (A, D) Untreated epimastigotes. (B, C) Epimastigotes treated with 3.3 and 6.6 µM **A11K3** for 24 h. (E, F) Epimastigotes treated with 3.3 and 6.6 µM **A11K3** for 96 h. Bars: 5 µm (A, D-F), 10 µm (B), 3 µm (C).

In amastigotes treated with 9.2 and 19 µM of **A11K3** for 24 h and processed for TEM it was observed that the negative control, without treatment showed $LLCMK_2$ cells infected with amastigote forms (Figure 4). The parasites showed normal morphology (Figure 4, A and B). The treatment with 9.2 µM of **A11K3**, demonstrated a decrease of parasites number inside the cells, accumulation of vacuoles, nuclear alterations and mitochondrial alterations in the amastigotes (Figure 4, C, D, E and F).

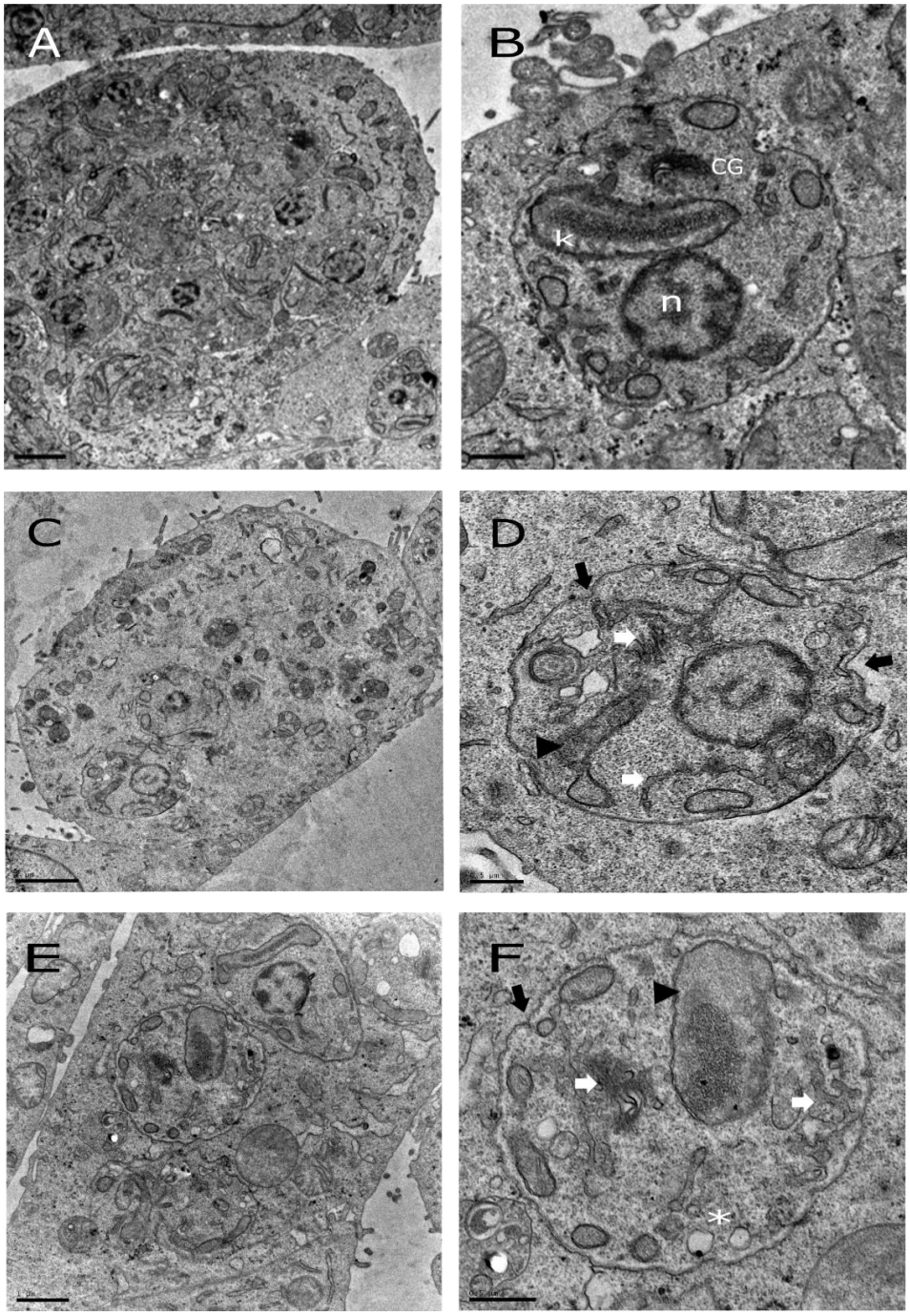

Figure 4. Ultrastructural alterations in amastigotes of *Trypanosoma cruzi* treated with 9.2 (C-D) and 19 µM (E-F) **A11K3** for 24 h, visualized by transmission electron microscopy. Negative control (A and B) with normal morphology. In (C) and (D) intracellular amastigotes treated with 9.2 µM **A11K3** for 24 h. In (E) and (F) intracellular amastigotes treated with 19 µM **A11K3** for 24 h. Nucleous: N; Kinetoplast: K; Golgi complex: (CG). Autophagy vacuoles (*), vesicles of Golgi complex (White arrow), swelling mitochondrial (black arrow head) and membrane rupture (black arrow). Bars A, C and E = 2 µM. Bars B, D and F = 0.5 µM.

3.4. Production of ROS

For evaluation of the production of ROS, epimastigotes and amastigotes were treated with H_2O_2 (positive control) or **A11K3** (Figure 5). After the incubation, epimastigotes treated with 4 µM H_2O_2 and 6.6 µM **A11K3** showed an increase in the production of ROS of 400 and 120%, respectively (Figure 5 A). Intracellular amastigotes treated with H_2O_2 generated an increase of 90% in the ROS production. Protozoa treated with **A11K3** did not show an increase in the production of ROS when compared with the control group (Figure 5 B).

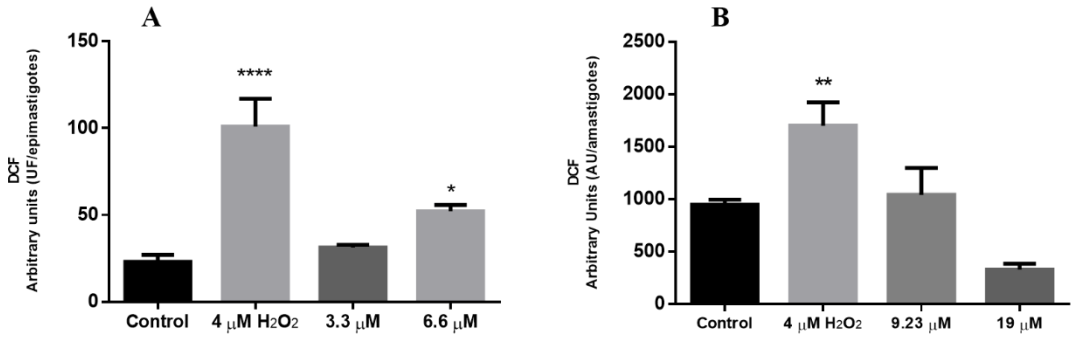

Figura 5. Total ROS production using the probe H_2DCFDA in epimastigotes (A) and intracellular amastigotes (B) of *Trypanosoma cruzi* treated with 3.3 and 6.6 µM **A11K3** for 24 h. The data are expressed as relative fluorescence of at least three independent experiments. H_2O_2 was used as a positive control. Two-way ANOVA followed by Bonferroni post hoc test. *$p \leq 0.05$; **$p \leq 0.01$; ****$p \leq 0.0001$ compared to untreated parasites (control).

3.5. Detection of lipid bodies

Nile red was used for detection of lipid bodies accumulation in epimastigotes and intracellular amastigotes (Figure 6). Epimastigotes treated with 4 µM H_2O_2 showed fourfold increase in the accumulation of lipids when compared with the control group (Figure 6 A). The treatment with 3.3 and 6.6 µM of **A11K3** did not change lipids bodies accumulation, compared with control. In the intracellular amastigotes, the H_2O_2 treated parasites had twofold more lipid bodies when compared with negative control (Figure 6 B). The treatment with 9.2 and 19 µM **A11K3** produced a threefold increase in accumulation of lipids (Figure 6).

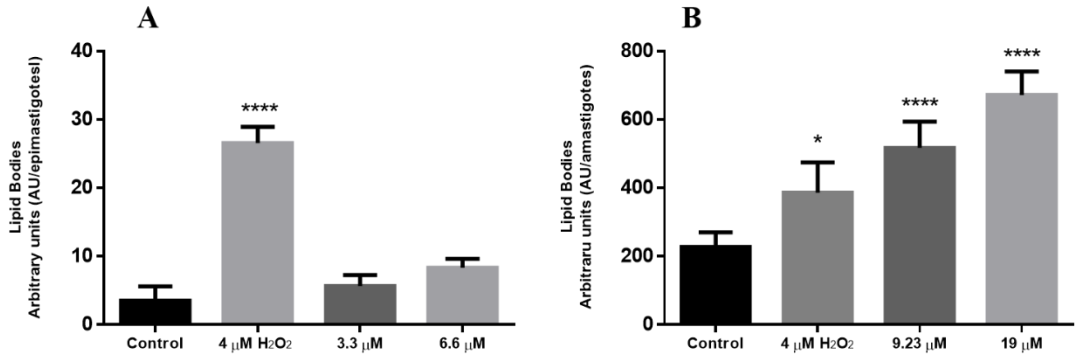

Figure 6. Lipid bodies accumulation with fluorescent probe Nile red in *Trypanosoma cruzi*. In (A) epimastigotes treated with 3.3 and 6.6 µM **A11K3** for 24 h. In (B) amastigotes treated with 9.2 and 19 µM **A11K3** for 24 h. The data are expressed as relative fluorescence of at least three independent experiments. Hydrogen peroxide was used as a positive control. Two-way ANOVA followed by Bonferroni post hoc test. $*p \leq 0.05$; $****p \leq 0.0001$ compared to untreated parasites (control).

3.6. Evaluation of membrane integrity and phosphatidelserine exposure (PS)

The PS exposure affect the membrane integrity and might be an indicative of necrosis or apoptosis-like in the protozoa. After the treatment for 24 h with digitonin (as positive control), 3.3 and 6.6 µM of **A11K3** was possible to observed that digitonin showed an increase in fluorescence of 53%, while the treatment with **A11K3** did not induce any alterations in epimastigotes (Figures 7, A-D).

For the evaluation of plasma membrane integrity, epimastigotes treated with digitonin it was observed a lack of membrane integrity in 77% of the parasites, when compared with the control group (Figure 7 E). Epimastigotes treated with 3.3 and 6.6 µM **A11K3** exhibit an increase in the intensity of PI fluorescence of 55 and 66%, respectively (Figure 7, E).

Reactive Oxigen Species production in cells can be affect the membrane fatty acids through lipid peroxidation. After the treatment for 24 h, epimastigotes were incubated with DPPP for detection of lipid peroxidation (Figura 7, F). The positive control with 4 µM H_2O_2 showed an increase in lipid peroxidation of 400% when compared to the control. Epimastigotes treated with 3.3 and 6.6 µM **A11K3** showed an increase of 19.1 and 112.7% in of lipid peroxidation, respectively.

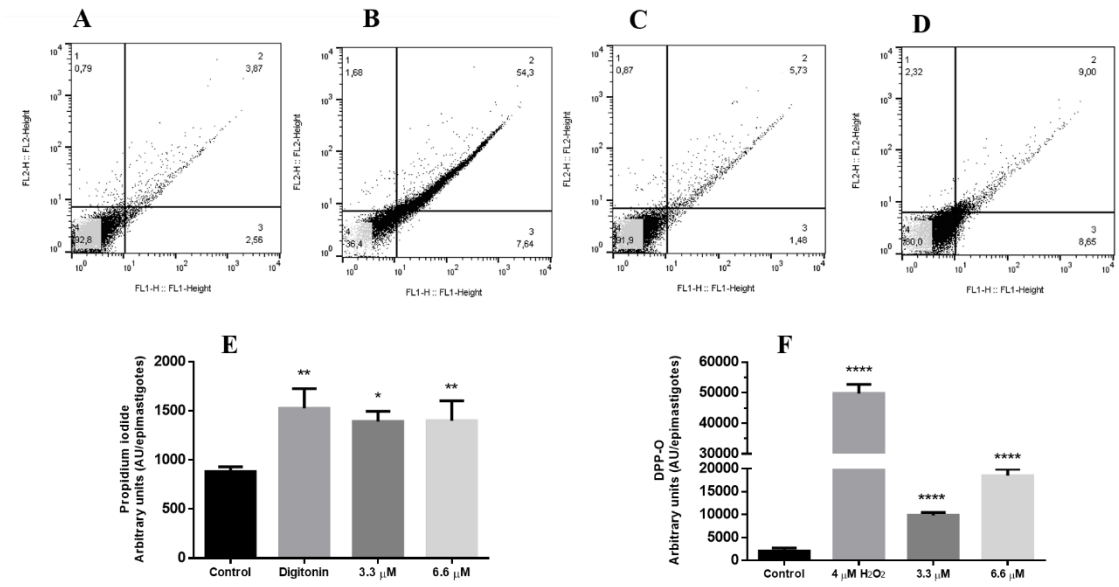

Figure 7. Phoshatidylserine exposure using Annexin V and PI, cell membrane integrity assay using PI staining and lipid peroxidation using probe DPPP in epimastigotes of *Trypanosoma cruzi* treated with 3.3 and 6.6 µM **A11K3** for 24 h. A to D, PS: in (A) negative control, (B) epimastigotes treated with 40 µM digitonin, (C) epimastigotes treated with 3.3 µM **A11K3** and (D) epimastigotes treated with 6.6 µM **A11K3**. In (E) evaluation of membrane integrity and in (F) evaluation of lipid peroxidation. Two-way ANOVA followed by Bonferroni post hoc test. $*p \leq 0.05$; $**p \leq 0.01$; $****p \leq 0.0001$ compared to untreated parasites (control).

3.7. Detection of mitochondrial potential and intracellular ATP

Rh123 was used to determine the membrane mitochondrial potential. In this assay, after 24 h of incubation at 28 °C, epimastigotes treated with 100 µM CCCP showed a decrease of membrane mitochondrial potential of 173% when compared with the control. The treatment with 3.3 and 6.6 µM **A11K3** showed a decrease in total Rh123 fluorescence intensity in 13 and 55%, respectively, indicating mitochondrial depolarization (Figure 8, A).

To evaluated the intracellular ATP, it was used as positive control 50 µM KCN and 100 µM CCCP. Intracellular ATP decreased in 70 and 71%, for the controls, respectively. The treatment for 24 h with 3.3 and 6.6 µM **A11K3** showed small decrease however, not significant, when compared with the control (Figure 8, B).

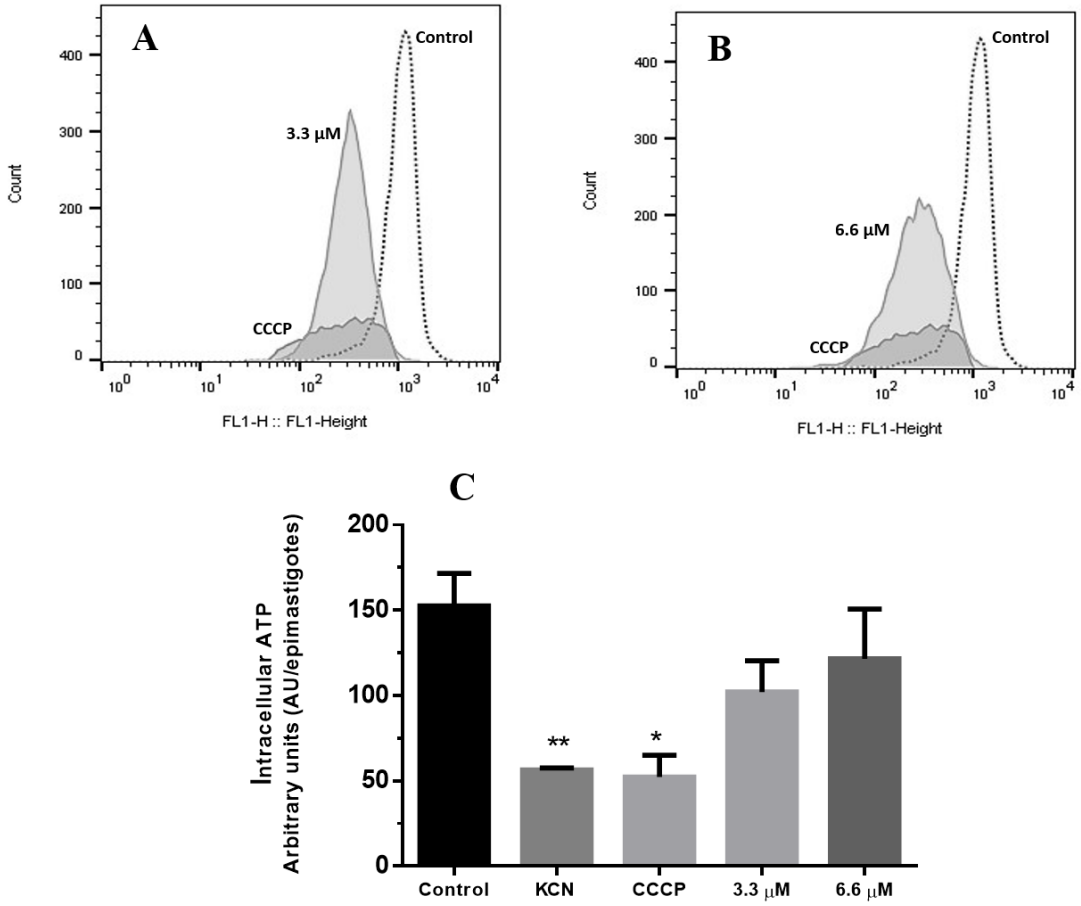

Figure 8. Determination of mithocondrial membrane potential in epimastigotes of *Trypanosoma cruzi* treated with **A11K3** for 24 h. In (A) protozoa not treated, treated with 100 µM CCCP and treated with 3.3 µM **A11K3**; (B) untreated protozoa, treated with 100 µM CCCP and treated with 6.6 µM **A11K3.** In (C) intracellular ATP of protozoa after the treatment. For cell mitochondrial membrane potential, the samples were loaded with Rhodamine123 and for determination of ATP production was used the Celltiter-Glo kit (Promega). Representative dot plot of three independents assays are presented. Two-way ANOVA followed by Bonferroni post hoc test. In the graphical. $*p \leq 0.05$; $**p \leq 0.01$.

3.8. Accumulation of autophagic vacuoles

Epimastigotes treated with **A11K3** were, incubated with MDC for 1 h. The positive control with epimastigotes without serum had fourfold increase in autophagic vacuoles. Epimastigotes treated with 3.3 and 6.6 µM **A11K3** produced fourfold and twofold increase in autophagic vacuoles, respectively. The samples pretreated with wortmannin had a decrease in the autophagic vacuoles even after the treatment with 3.3 and 6.6 µM **A11K3** (Figure 9).

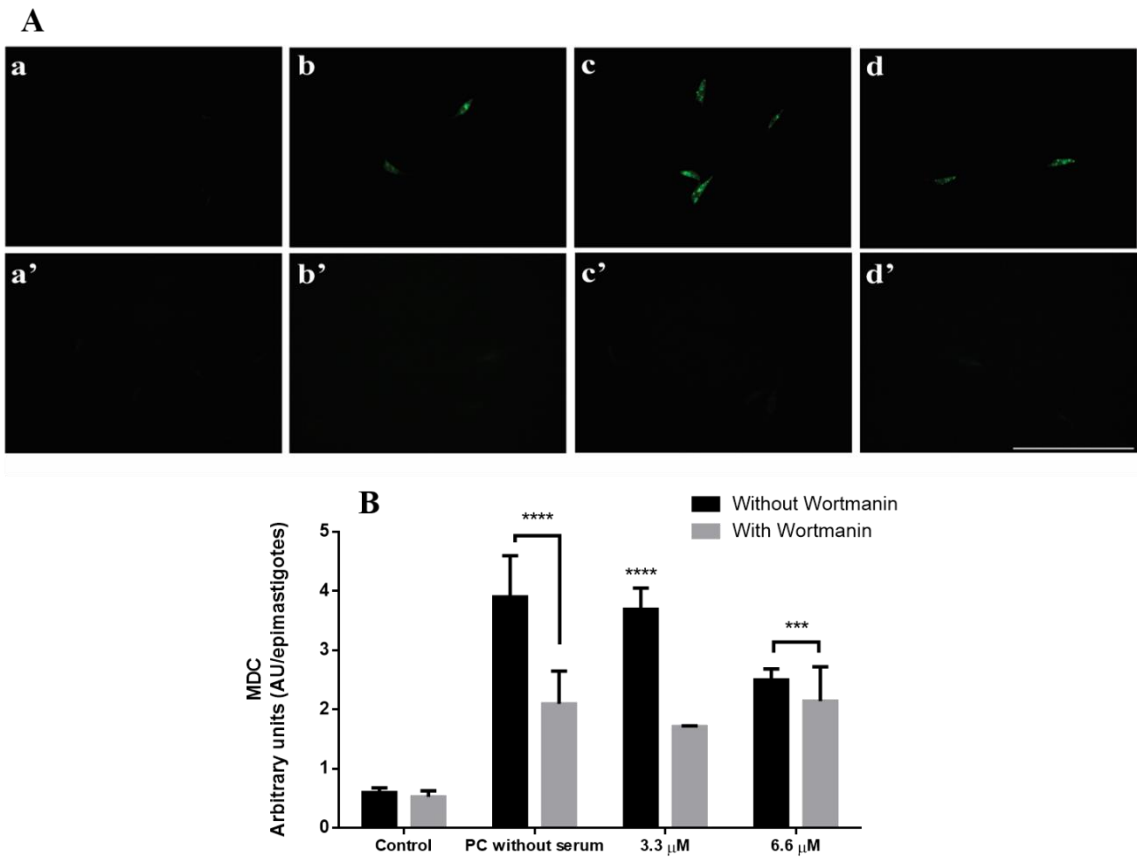

Figure 9. Autophagic vacuoles in *Trypanosoma cruzi* treated with 3.3 and 6.6 µM **A11K3** for 24 h using MDC labeling. (A) Fluorescence microscopy images: (a) untreated epimastigotes, (a') untreated epimastigotes plus wortmannin, (b) positive control (without serum), (b') positive control (without serum) plus wortmannin, (c, d) epimastigotes treated with 3.3 and 6.6 µM, respectively, (c', d') epimastigotes treated with 3.3 and 6.6 µM plus wortmannin, respectively. Bars 50 µm. (B) Fluorescence intensity was obtained by fluorimetry. Asterisks indicate significant differences of the groups with and without wortimannin.

4. Discussion

During our recent studies on synthesis of curcumin analogues, or diaryalkadienones, we have reacted many different aldehydes (An) with ketones (Km) in condition to produces the aldols intermediaries following by its condensation on pot (Din et al. 2018). The reaction of *p*-nitrobenzaldehyde (A11) with 2-pentanone (K3) occurs via the thermodynamic enolate giving good regiochemistry control, letting to almost 100% of **A11K3** without detectable amount of aldol condensation via kinetic enolate.

Dibenzilidenoacetones are substances that have an acyclic dienone attached to aryl groups in both β-positions. These molecules are active in several organisms, such as protozoa and tumoral cells (Garcia et al. 2017; Lazarin-Bidóia et al. 2016; Prasad et al. 2010; H-j Yu et al. 2013). In this study, **A11K3** exhibited activity against the three forms of *T. cruzi*, epimastigotes, trypomastigotes and intracellular amastigotes. Besides that, **A11K3** substance did not show toxicity in $LLCMK_2$ cells, being less toxic than benznidazole, the standard drug for treatment during acute and chronic phases (Izumi et al. 2008). These results prove the strong efficacy, since the selectivity index is favorable in all forms tested. **A11K3** was able to induce epimastigotes and intracellular amastigotes death in low concentration.

By SEM and TEM, it was possible to note a collapse on epimastigotes that indicate alterations in flagellum, cell body and release of intracellular content. These alterations were confirmed by staining the parasites with PI, where it was observed alterations in plasma membrane integrity, a sign of necrosis. The membrane alteration may be caused by lipid peroxidation due enzymes and proteins inactivation and oxidative modification environment of macromolecules (Stark 2005). Besides that, the lipid peroxidation can generate a process call ferroptosis, one type of necrosis, characterized by iron-dependent lipids peroxide accumulation and lipophilic antioxidants suppression. In this type of death, occurs ROS production in the first moment of treatment and the mitochondria can suffer a shrinkage or swelling and cause mitochondrial membrane depolarization (Gaschler and Stockwell 2017; Haitao Yu et al. 2017)**.** Those type of features were observed here in epimastigotes and intracellular amastigotes treated with **A11K3**. The iron is essential for survival of several organisms and is the fourth component more abundant in the world. Studies with *T. cruzi* and *Leishmania* spp. proves that iron has an important role for parasite-host interaction, however depletion and excessive decrease of iron can be toxicity and cause a cellular collapse and death of the parasite (Bogacz and Krauth-Siegel 2018; Mesquita-Rodrigues et al. 2013; Rea et al. 2013; Reyes-lópez, Piña-vázquez, and Serrano-luna 2015).

By TEM, it was possible observed that epimastigotes and intracellular amastigotes treated with **A11K3** had an increase of Golgi vesicles. The Golgi complex is responsible for targeting cell proteins and the alteration cause the disruption of protein trafficking (Engel et al. 1998). These changes are connected with the accumulation of lipid bodies and swelling and mitochondrial depolarization, also observed during the assays. This could be due to physical alterations in all membranes, abnormal intermediate metabolic

production and cell signally alteration induced by the treatment with **A11K3** (Bozza et al. 2008; Kathuria et al. 2014; Santa-Rita et al. 2004).

Epimastigotes treated with **A11K3** have undergone mitochondrial changes. In kinetoplastids, the mitochondria is an unique organelle, has its own genetic material and is distinct of mammalian mitochondria, being an important target for drug discovery studies (Mendes et al. 2016; Monzote et al. 2014; de Souza 2009). Alterations in mitochondria can be harmful and alter the flow of ions, affecting the intracellular ATP and leading the protozoa to death (Monzote et al. 2014; Mukherjee et al. 2002) . In our results with Rh123 dye, the mitochondria membrane is depolarized, the electrons move through the mitochondrial respiratory chain during the oxidative phosphorylation and generate an increase in the permeability of protons (Britta et al. 2014). The ATP levels is affect due to depolarization that damages the complex of ATP synthase and decrease the O_2 production (Alvarez et al. 2007).

We found that the amastigotes treated with **A11K3** generated lipid bodies. This event occurs because the cell was submitted at stress that triggers lipid droplets accumulation (Jin et al. 2018). The biogenesis of the lipid bodies plays an essential role in many cellular homeostasis events in different eukaryotes (Guedes-Da-Silva et al. 2016; De Macedo-Silva et al. 2013). They are dynamic organelles composed of triglycerides surrounded by phospholipid monolayers, associated with metabolism and signally. Hence, they are indicative of cellular equilibrium (Boren and Brindle 2012; Guedes-Da-Silva et al. 2016). It was reported the accumulation of these structures in the cytoplasm of *L. amazonensis* treated with inhibitors of squalene synthase and ergosterol synthesis enzyme, attributing this accumulation of lipids to the sterol content in the parasite membrane (Rodrigues et al. 2008). It has also been shown that drugs such as taxol, synthetic compounds and β-carboline alkaloids induced lipid accumulation in *L. amazonensis* and *T. cruzi*, suggesting that changes not related to lipid synthesis also induce the formation of lipid droplets (Scariot et al. 2017; Stefanello et al. 2014).

Vacuoles production occur in response to several stress and can be related to uncontrolled lysosomal activity due to the lack of nutrient, growth, development and cell division (Proto, Coombs, and Mottram 2013). It is well described that the autophagy is a natural process of recycling components of the cell under stress conditions. However, the increase or prolonged exposure to stress, such as toxins or absence of nutrients can be harmful and led to cell death (Galluzzi et al. 2018). For confirmation of the presence of vacuoles, it was used the probe MDC, that is an auto fluorescent compound that label

these organelles (Munafó and Colombo 2001). The results obtained showed that the vacuoles are predominantly autophagic due to the increase in the fluorescence after treatment and MDC incubation. **A11K3** was able to induce the lysosomal activity and degraded cellular material. (Brooks and Striepen 2011; Proto, Coombs, and Mottram 2013).

5. Conclusion

The study with dibenzilidenoacetone derivated **A11K3** demonstrated that the compound is efficient on epimastigotes, trypomastigotes and intracellular amastigotes. The results suggest that **A11K3** is less toxicity for mammalian cell and induces death of protozoan by several perturbations as in the Golgi complex, membrane plasma and mitochondrial. All the features observed resemble a type of cell death called ferroptosis, leading protozoan to a cellular collapse. Further assays are necessary to evaluate the molecular targets of the compound and suggest a possible new treatment for Chagas disease patients.

6. Reference

Alvarez, Noel et al. 2007. “Mitochondrial Superoxide Radicals Mediate Programmed Cell Death in *Trypanosoma cruzi* : Cytoprotective Action of Mitochondrial Iron Superoxide Dismutase Overexpression.” *The journal of biological chemistry* 334: 323–34.

Alves, C.R. et al. 2007. “*Trypanosoma cruzi*: Attachment to Perimicrovillar Membrane Glycoproteins of Rhodnius Prolixus.” *Experimental Parasitology* 116(1): 44–52.

Bhandarkar, Sulochana S et al. 2008. “Cancer Therapy : Preclinical Ris (Dibenzylideneacetone) Dipalladium , a N -Myristoyltransferase-1 Inhibitor , Is Effective against Melanoma Growth In vitro and In vivo.” *Clinical Cancer Reseacher* 1(18): 5743–49.

Bogacz, Marta, and R Luise Krauth-Siegel. 2018. “Tryparedoxin Peroxidase-Deficiency Commits Trypanosomes to Ferroptosis-Type Cell Death.” *eLife* 7: 1–29.

Boren, J., and K. M. Brindle. 2012. “Apoptosis-Induced Mitochondrial Dysfunction

Causes Cytoplasmic Lipid Droplet Formation." *Cell Death & Differentiation* 19(9): 1561–70.

Bozza, Patrícia T. et al. 2008. "Induction of Autophagy Correlates with Increased Parasite Load of *Leishmania amazonensis* in BALB/c but Not C57BL/6 Macrophages." *Microbes and Infection* 11(2): 181–90.

Britta, Elizandra Aparecida et al. 2014. "Cell Death and Ultrastructural Alterations in *Leishmania amazonensis* Caused by New Compound 4-Nitrobenzaldehyde Thiosemicarbazone Derived from S-Limonene." *BMC Microbiology* 14(1): 1–12.

Brooks, Carrie F, and Boris Striepen. 2011. "Autophagy Protein Atg3 Is Essential for Maintaining Mitochondrial Integrity and for Normal Intracellular Development of *Toxoplasma gondii tachyzoites*." *Plos Pathogens* 7(12).

Coura, José Rodrigues. 2009. "Present Situation and New Strategies for Chagas Disease Chemotherapy: A Proposal." *Memórias do Instituto Oswaldo Cruz* 104(4): 549–54.

Crow, John P. 1997. "Dichlorodihydrofluorescein and Dihydrorhodamine 123 Are Sensitive Indicators of Peroxynitrite in vitro: Implications for Intracellular Measurement of Reactive Nitrogen and Oxygen Species." *Nitric Oxide - Biology and Chemistry* 1(2): 145–57.

Din, Zia Ud et al. 2018. "Symmetrical and Unsymmetrical Substituted 2,5-Diarylidene Cyclohexanones as Anti-Parasitic Compounds." *European Journal of Medicinal Chemistry* 155: 596–608.

Engel, Juan C et al. 1998. "Cysteine Protease Inhibitors Alter Golgi Complex Ultrastructure and Function in *Trypanosoma cruzi*." *Journal of cell science* 111 (Pt 5: 597–606.

Galluzzi, Lorenzo et al. 2018. "Molecular Mechanisms of Cell Death: Recommendations of the Nomenclature Committee on Cell Death 2018." *Cell Death & Differentiation* 25(3): 486–541.

Garcia, Francielle Pelegrin et al. 2017. "A3K2A3-Induced Apoptotic Cell Death of *Leishmania amazonensis* Occurs through Caspase- and ATP-Dependent Mitochondrial Dysfunction." *Apoptosis* 22(1): 57–71.

Gaschler, Michael M, and Brent R Stockwell. 2017. “Biochemical and Biophysical Research Communications Lipid Peroxidation in Cell Death.” *Biochemical and Biophysical Research Communications* 482(3): 419–25.

Greenspan, P. 1985. “Nile Red: A Selective Fluorescent Stain for Intracellular Lipid Droplets.” *The Journal of Cell Biology* 100(3): 965–73.

Grela, Ewa, Joanna Kozłowska, and Agnieszka Grabowiecka. 2018. “Current Methodology of MTT Assay in Bacteria – A Review.” *Acta Histochemica* 120(4): 303–11.

Guedes-Da-Silva, F. H. et al. 2016. “In vitro and in vivo Trypanosomicidal Action of Novel Arylimidamides against *Trypanosoma cruzi*.” *Antimicrobial Agents and Chemotherapy* 60(4): 2425–34.

Hempel, Stephen L. et al. 1999. “Dihydrofluorescein Diacetate Is Superior for Detecting Intracellular Oxidants.” *Free radical biology & medicine* 27(99): 146–59.

Izumi, Erika et al. 2008. “*Trypanosoma cruzi*: Antiprotozoal Activity of Parthenolide Obtained from *Tanacetum parthenium* (L.) Schultz Bip. (Asteraceae, Compositae) against Epimastigote and Amastigote Forms.” *Experimental Parasitology* 118(3): 324–30.

Izumi, Erika et al. 2011. “Natural Products and Chagas’ Disease: A Review of Plant Compounds Studied for Activity against *Trypanosoma cruzi*.” *Natural Product Reports* 28(4): 809.

Jin, Yi et al. 2018. “Reactive Oxygen Species Induces Lipid Droplet Accumulation in HepG2 Cells by Increasing Perilipin 2 Expression.” *International Journal of Molecular Sciences* 19(11): 3445.

Kathuria, Manoj et al. 2014. “Induction of Mitochondrial Dysfunction and Oxidative Stress in *Leishmania donovani* by Orally Active Clerodane Diterpene.” *Antimicrobial Agents and Chemotherapy* 58(10): 5916–28.

Lazarin-bidóia, Danielle et al. 2016. “Affect the *Trypanosoma cruzi* Redox System.” *Antimicrobial Agents and Chemotherapy* 60(2): 890–903.

De Macedo-Silva, Sara Teixeira, Julio A. Urbina, Wanderley De Souza, and Juliany

Cola Fernandes Rodrigues. 2013. “In vitro Activity of the Antifungal Azoles Itraconazole and Posaconazole against *Leishmania amazonensis.*” *PLoS ONE* 8(12).

Mendes, Edevi Arbonelli et al. 2016. “Chemico-Biological Interactions C5 Induces Different Cell Death Pathways in Promastigotes of *Leishmania amazonensis*.” *Chemico-Biological Interactions* 256: 16–24.

Mesquita-Rodrigues, C et al. 2013. “Cellular Growth and Mitochondrial Ultrastructure of *Leishmania (Viannia) braziliensis* Promastigotes Are Affected by the Iron Chelator 2 , 2-Dipyridyl.” *PLoS Neglected Tropical Diseases* 7(10).

Monzote, Lianet et al. 2014. “Experimental Parasitology Essential Oil from Chenopodium Ambrosioides and Main Components : Activity against *Leishmania* , Their Mitochondria and Other Microorganisms.” *Experimental Parasitology* 136(601): 20–26.

Mukherjee, Sikha Bettina, Manika Das, Ganapasam Sudhandiran, and Chandrima Shaha. 2002. “Increase in Cytosolic Ca2+ Levels through the Activation of Non-Selective Cation Channels Induced by Oxidative Stress Causes Mitochondrial Depolarization Leading to Apoptosis-like Death in *Leishmania donovani* Promastigotes.” *Journal of Biological Chemistry* . 277(27): 24717–27.

Munafó, Daniela B, and María I Colombo. 2001. “A Novel Assay to Study Autophagy : Regulation of Autophagosome Vacuole Size by Amino Acid Deprivation.” *Journal of Cell Science*.114 (20).

Nogueira, Nadir F S et al. 2007. “*Trypanosoma cruzi* : Involvement of Glycoinositolphospholipids in the Attachment to the Luminal Midgut Surface of Rhodnius Prolixus.” 116: 120–28.

Prasad, Sahdeo, Vivek R Yadav, Jayaraj Ravindran, and Bharat B Aggarwal. 2011. “ROS and CHOP Are Critical for Dibenzylideneacetone to Sensitize Tumor Cells to TRAIL through Induction of Death Receptors and Downregulation of Cell Survival Proteins.” *Cancer Research* 71(2): 538–49.

Proto, William R., Graham H. Coombs, and Jeremy C. Mottram. 2013. “Cell Death in Parasitic Protozoa: Regulated or Incidental?” *Nature Reviews Microbiology* 11(1):

58–66.

Rea, Alexandre et al. 2013. “Soulamarin Isolated from *Calophyllum brasiliense* (Clusiaceae) Induces Plasma Membrane Permeabilization of *Trypanosoma cruzi* and Mytochondrial Dysfunction.” *PLoS Neglected Tropical Diseases* 7(12): 1–8.

Reyes-lópez, Magda, Carolina Piña-vázquez, and Jesús Serrano-luna. 2015. “Transferrin : Endocytosis and Cell Signaling in Parasitic Protozoa.” *BioMed Research International* 2015.

Rodrigues et al. 2008. “In vitro Activities of ER-119884 and E5700, Two Potent Squalene Synthase Inhibitors, against *Leishmania Amazonensis:* Antiproliferative, Biochemical, and Ultrastructural Effects.” *Antimicrobial Agents and Chemotherapy* 52(11): 4098–4114.

Rodrigues, Juliany C F, Carlos Rodriguez, and Julio A Urbina. 2002. “Ultrastructural and Biochemical Alterations Induced by Promastigote and Amastigote Forms of *Leishmania amazonensis*.” *Antimicrobial Agents and Chemotherapy* 46(2): 487–99.

Santa-Rita, Ricardo M., Andréa Henriques-Pons, Helene S. Barbosa, and Solange L. de Castro. 2004. “Effect of the Lysophospholipid Analogues Edelfosine, Ilmofosine and Miltefosine against *Leishmania amazonensis.*” *Journal of Antimicrobial Chemotherapy* 54(4): 704–10.

Scariot, Débora B. et al. 2017. “Induction of Early Autophagic Process on *Leishmania amazonensis* by Synergistic Effect of Miltefosine and Innovative Semi-Synthetic Thiosemicarbazone.” *Frontiers in Microbiology* 8(FEB): 1–16.

de Souza, Wanderley. 2009. “Structural Organization of *Trypanosoma cruzi*.” *Memorias do Instituto Oswaldo Cruz* 104(SUPPL. 1): 89–100.

Stark, G. 2005. “Functional Consequences of Oxidative Membrane Damage.” *Journal of Membrane Biology* 205(1): 1–16.

Stefanello, T. F. et al. 2014. “N-Butyl-[1-(4-Methoxy)Phenyl-9H-β-Carboline]-3-Carboxamide Prevents Cytokinesis in *Leishmania amazonensis.*” *Antimicrobial Agents and Chemotherapy* 58(12): 7112–20.

Ud, Zia et al. 2014. “Bioorganic & Medicinal Chemistry Evaluation as Antiparasitic Agents.” *Bioorganic & Medicinal Chemistry* 22(3): 1121–27.

Yu, H-j et al. 2013. “Apoptotic Effect of Dibenzylideneacetone on Oral Cancer Cells via Modulation of Specificity Protein 1 and Bax.” *Oral Diseases* 19(8): 767–74.

Yu, Haitao et al. 2017. “Ferroptosis , a New Form of Cell Death , and Its Relationships with Tumourous Diseases Definition and Discovery of Ferroptosis Differences between Ferroptosis and Apoptosis / Necrosis.” *Journal Cellular Molecular Medicine* 21(4): 648–57.

WHO, 2018. Chagas Diseases. In: Chagas diseases. Acessed in September, 22, 2019.

APÊNDICE 1: Doutorado Sanduíche – PDSE/2018-19

Universidade de Granada – Granada/ Espanha

GERAÇÃO DE LINHAGENS CELULARES DE *Trypanosoma cruzi* COM EXPRESSÃO ENDÓGENA DE MARCADORES MOLECULARES

1. INTRODUÇÃO

Devido a toxicidade e ineficácia do benznidazol e nifurtimox encontrada na fase crônica da doença de Chagas é necessário buscar novas substâncias para o tratamento. Para se avaliar novas substancias, é necessário conhecer a biologia do organismo em estudo. Assim, existe um grande interesse em estudos envolvendo imunologia, sequenciamento de RNA e DNA, espectrometria de massas e bioinformática a fim de identificar a função de milhares de genes encontrados em *T. cruzi*. Dean e colaboradores 2015, desenvolveram técnicas que fornecem um conjunto de plasmídeos modulares com protocolos para a marcação de genes, sendo uma abordagem fácil, rápida e reprodutiva. O interessante nessa técnica é a ausência de clonagem bacteriana, sendo todo processo realizado por reações de PCR, aumentando a velocidade do processo. Ainda neste artigo, foi demonstrado que a eficiência de transfecção em *Leishmania spp* é proporcional ao tamanho do gene em relação ao tamanho do gene repórter (marcador) (obtendo poucas chances de recombinação com homologias inferiores à 100 pb). Para isso, os autores criaram uma estratégia que inclui uma PCR de fusão capaz de vincular uma sequência de interesse (gene de interesse + marcador) com duas regiões de flanqueamento (FRs) até 500 pb.

Para anelar os FRs com o gene, ambos os FRs possuem uma extensão oligonucleotídica de poucos nucleotídeos (incorporados nos iniciadores para amplificar

as extremidades 5’ e 3’ dos FRs) que são complementares das extremidades 5’ e 3’ da sequência do gene de resistência aos antibióticos, dependendo da estratégia (N-, Ctagging (ou nocaute)). Assim, os três elementos (gene, 5’FR e 3’FR) são capazes de hibridar, polimerizar e fazer cópias da sequência de genes completas. Para realizar a PCR, são criados modelos longos, utilizando 5 ciclos de amplificação (tipicamente 1500-2500 pb, dependendo do comprimento do gene marcador + gene de resistência) que será novamente re-amplificado (30 ciclos) na mesma reação e após são adicionados dois iniciadores alinhados. Portanto, as construções de marcação podem ser realizadas sem a etapa de clonagem bacteriana. Deve-se ressaltar que as construções para a marcação N- não modificou o 3'UTR endógeno do gene de interesse (GOI), permitindo a regulação endógena da expressão de mRNA, enquanto a marcação em C- substitui a UTR endógena de 3 ' do GOI, resultando em uma alteração dos níveis endógenos de mRNA. Os mesmos autores criaram uma ferramenta web para o projeto de iniciadores com base em DND ou IDs de TritrypDB para marcação N ou C com um conjunto definido de plasmídeos. Além disso, os autores expandiram o repertório de vetores (pPOTv6, pPOTv7), para permitir a marcação com diferentes proteínas ou enzimas fluorescentes (mNeongreen, mScarlet ou BirA*) (Dean et al., 2015).

Considerando a importância da função das proteínas e um tratamento eficaz, pesquisas com alvos moleculares e compostos naturais ou sintéticos crescem a cada ano, possibilitando a inserção de genes no genoma do parasito através de plasmídeos endógenos (expressão constitutiva) utilizando a PCR de fusão e posteriormente a avaliação de compostos frente às modificações.

Dessa forma, este estudo teve como objetivo, gerar linhagens celulares de *T. cruzi* com expressão endógena de marcadores e posteriormente avaliar o mecanismo de substancias, frente a novas linhagens de *T.cruzi*. Para tanto, foram utilizadas diferentes

abordagens *in vitro* com substâncias ativas, a fim de sugerir novas metodologias para o trabalho com *T. cruzi*.

2. MATERIAIS E MÉTODOS

2.1. MEIOS DE CULTURA E SOLUÇÕES

2.1.1. Meio LB (Luria Bertani)

O meio de cultura Luria Bertani (LB) foi utilizado para cultivar as bactérias recombinantes de *Escherichia coli*. Para o preparo de 1 litro de meio foi utilizado 950 mL de água destilada, 10 gramas de triptona, 10 gramas de NaCl e 5 gramas de extrato de levedura. O pH e o volume da solução foram ajustados para 7.0 e 1L, respectivamente. Para realizar a transformação das bactérias (item2.3) foi utilizado o LB ágar. Para isso, foi adicionado ao meio LB liquido 15 gramas de ágar.

O meio foi esterilizado em autoclave e armazenado em temperatura ambiente. Quando se fez necessário o uso de antibióticos em LB ágar, o meio foi resfriado até 50 °C, o antibiótico de interesse foi adicionado e o meio distribuído em placas de petri. Após a solidificação, o meio foi armazenado à 4 °C.

2.1.2. Solução Tris-Acetato-EDTA (TAE) 50X

A solução TAE 50X foi o tampão utilizado durante a eletroforese e na preparação do gel de agarose para a separação de ácidos nucleicos (RNA e DNA). Para o preparo de 1 litro, primeiramente foi preparada uma solução de 100 mL de etilenodiamino tetra-acético (EDTA), onde pesou-se 22,6 gramas de EDTA e solubilizou-se em 100 mL de água destilada. O pH da solução foi ajustado para 8,3. Pesou-se 22,6 gramas de Tris-

base e solubilizou-se em 850 mL de àgua destilada. Após, foi adicionada a solução de EDTA e 57,1 mL de ácido Glacial Acético. Por fim, o volume foi ajustado para 1 litro.

2.1.3. Solução de Cloreto de Cálcio 1M

A solução de cloreto de cálcio foi utilizada para preparação de bactérias competentes. Foram pesados 11,1 gramas de $CaCl_2$ anidro e solubilizado em 80 mL de agua MiliQ. Após, o volume foi ajustado para 100 mL. A solução foi esterilizada em autoclave ou em filtro com poros de 0,22 µM. A solução de trabalho utilizada durante os experimentos foi de 0,1 M, então, 10 mL da solução estoque foi diluída em 90 mL de água MiliQ e por fim esterilizada.

2.1.4. Soluções Alcalinas de Lise

As soluções alcalinas de lise foram utilizadas durante as extrações de DNA dos plasmídeos (item 2.2.3).

- Solução alcalina de lise I: 50 mM glucosa 25 mM Tris-Cl (pH 8.0) 10 mM EDTA (pH 8.0). Esterilizar em Autoclave. Armazenado à 4 °C.
- Solução alcalina de lise II: 0.2 N NaOH (diluído recentemente a partir da solução de 10N) 1% (w/v) SDS. Armazenado à temperatura ambiente.
- Solução alcalina de lise III: 5 M acetato de potássio, 60.0 ml ácido acético glacial, 11.5 ml H_2O, 28.5 ml. Armazenado à 4 °C.

2.2. PCR DE FUSÃO

A PCR de fusão foi proposta por Dean e colaboradores 2015 e permite a inserção de genes em tripanosomatídeos sem a etapa de clonagem bacteriana. Para tal metodologia, foram realizados os passos abaixo.

2.2.1. Amplificação do gene de interesse

Para a obtenção da Clatrina, o gene foi amplificado a partir de DNA genômico de *T.cruzi*, utilizando PCR. O DNA genômico foi extraído seguindo o protocolo do kit de extração comercial DNeasy Blood & Tissue (QIAGen).

Para PCR foi preparado um mix de reação como indica o fabricante Canvax (Figura 1).

Recommended PCR assay (20 µl assay)

Components	Volume	Final con.
10X PCR buffer	2 µL	1X
$MgCl_2$ 25 mM	2 µL	2.5 mM
dNTPs 8 mM mixture	2 µL	0.8 mM
Primer Forward (15 mm)	1 µL	0.75 µm
Primer Reverse (15 mm)	1µL	0.75 µm
Template DNA	0.2-10 µL	1.75-2.5 ng/µL
Horse-Power-Taq DNA polymerase (5 U/µL)	0.2 µL	0.05 U/µL
Autoclaved distilled water	to 20 µL	-

Cycling instructions:94 °C 5:00, 25-30x (95 °C 0:30, Tm 0:30, 72 °C 1'/kb), 72 °C 10:00, 4 °C ∞

Figura 1. Instruções de preparação de mix de PCR Canvax.

Primeiramente, foi adicionado a água MiliQ autoclavada em um eppendorf livre de DNAse e RNAse e, em seguida, os outros componentes. Em todas as PCR realizadas, usou-se um controle negativo, ou seja, não foi adicionado o DNA. No caso de Clatrina foram utilizados os primers 16b e17b para a extreminadade 5' e 18b e 19b para a extremidade 3' (anexo 1).

Com o auxílio de uma plataforma online, TM calculator (https://www.thermofisher.com/br/pt/home/brands/thermo-scientific/molecular-

biology/molecular-biology-learning-center/molecular-biology-resource-library/thermo-scientific-web-tools/tm-calculator), foi calculada a temperatura de hibridação ideal de cada primer.

O mix de reação foi levado ao termociclador onde as amostras foram submetidas à etapa de desnaturação inicial à 95 °C por 5 min. Para a hibridação dos primers na fita de DNA desnaturada a temperatura foi de 55 °C por 30 segundos. Em seguida, a *Taq* polimerase iniciou sua atividade, estendendo o molde de DNA a uma temperatura de 72 °C por 40 segundos. As etapas de desnaturação, hibridação e extensão foram repetidas por 34 ciclos. As amostras passaram pela etapa de elongação final à 72 °C por 5 min e a temperatura final foi 10 °C. Ao final da reação, as amostras foram submetidas à eletroforese (item 2.2.2).

2.2.2. Confirmação da PCR e obtenção do gene – Eletroforese em Gel de Agarose

Foi realizada eletroforese em gel de agarose para obtenção dos genes de interesse e confirmação das integrações destes nos plasmídeos. Para preparação de 100 mL da solução de agarose, foram pesados 1 g de agarose e adicionados em água destilada. Juntamente, foi acrescentado 2 mL de tampão TAE 50X. A solução foi levada ao micro-ondas por aproximadamente 2 min, até que a solução se mostrou completamente límpida. Após, foi adicionado 10 µL de SyberSafe (ThermoFisher). A solução foi depositada em uma cuba de eletroforese onde esperou-se a solidificação.

Foi adicionado o tampão TAE 50X na cuba de eletroforese após a solidificação do gel. As amostras obtidas por PCR foram preparadas adicionando o tampão de amostras (Invitrogen) (1:1) e, em seguida, aplicadas nos poços do gel. A corrida foi realizada à 80 V, por aproximadamente 45 min. Após a eletroforese, as imagens foram adquiridas por

um ChemiDoc Imaging Systens (Life Sciences Reseach – Bio Rad). Em todas as corridas foram utilizadas 5 µL do padrão molecular Hiperladder para 1 Kb (Invitrogen) (Figura 2).

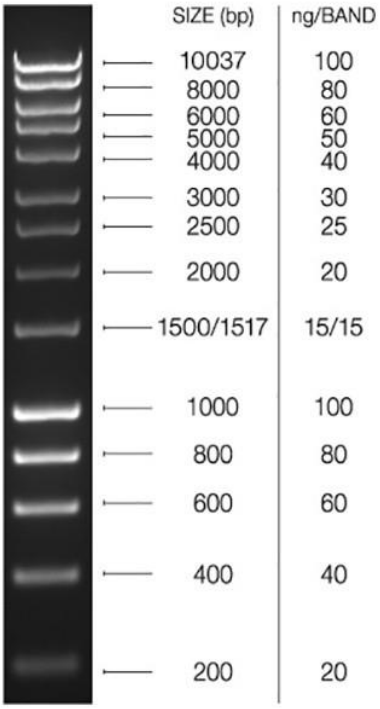

Figura 2. Hiperladder do padrão molecular de 1 kb utilizado durante as eletroforeses.

O fragmento de interesse após ser visualizado no gel, foi extraído utilizando o QIAprep gel extraction kit (QIAGen) de acordo com o fabricante.

2.2.3. Obtenção do gene repórter

Os genes repórteres mScarlet e E2crimsom foram obtidos a partir de plasmídeos bacterianos. Para isso, bactérias *Escherichia coli*, cepa DH5α, contendo os plasmídeos pPOTV7mScarlet Blast e pNUSE2crimsom foram inoculadas em 20 mL de meio LB contendo 2 µg/Ml DE ampicilina por 24 h à 37 °C com agitação de 200 rpm. Após, as bactérias foram centrifugadas à 2000 g por 10 minutos. Os pellets foram ressuspendidos em 400 µL de solução alcalina I. Em seguida, foi adicionado 800 µL de solução alcalina

II, agitou-se o eppendorf cinco vezes (sem vórtex). Em seguida, foi adicionado 600 µL solução alcalina III e o eppendorf foi agitado cinco vezes e incubado por 5 min em gelo.

As amostras foram centrifugadas à 15.000 rpm por 5 min, o sobrenadante foi coletado em um novo eppendorf de 2 mL e foi adicionada RNAse (2 µg/mL) (para degradação de RNA bacteriano). As amostras foram incubadas por 40 min à 37 °C.

Após a incubação, um volume igual de fenocloroformio foi adicionado, homogeneizado em vórtex e centrifugado 15.000 rpm por 5 min à 4° C. A fase aquosa foi coletada (cerca de 600 µL) em um novo eppendorf e adicionado 600 µL de isopropanol com o intuito de precipitar o DNA. Os eppendorfs foram homogeneizados e incubados à temperatura ambiente por 2 min.

As amostras foram centrifugadas a 15.000 rpm por 5 min à 4 °C, o sobrenadante foi descartado, adicionado 1mL de etanol 70% gelado e as amostras centrifugadas novamente à velocidade máxima (> 16.000 rpm) por 2 min. O etanol foi descartado por aspiração e o pellet contendo o DNA plasmidial foi ressuspendido em água deionizada esterilizada, contendo RNAase (2µg/mL). O DNA foi quantificado em nanodrop, confirmado por eletroforese e gel de agarose e armazenado à -20°C.

Para a obtenção dos genes repórteres mScarlet e E2-crimsom os plasmídeos foram submetidos a digestão com enzimas de restrição.

Para mScarlet foi utilizado o plasmídeo pPOTV7mScarlet Blast, e utilizadas as enzimas de restrição *Apa*1 e *Eco53ki* (New England Bio Lab) (tabela 1). Primeiramente foi preparada uma reação somente com a enzima Apa1 e a amostra foi incubada a 25 °C por 30 min. Após este período a enzima *Eco53ki* foi adicionada e incubada novamente a 37 °C por 30 min.

Tabela 1. Reação de digestão para o plasmídeo pPOTV7mScarlet Blast com a enzimas Apa1 e EcoKi53.

COMPONENTES	CONCENTRAÇÃO	QUANTIDADE (µL)
pPOTV7mScarlat Blast	10 ug	4
Enzima *Apa*I (50.000 u) - 25 °C	10U/µL 10%	1
Enzima *Eco53ki* (10.000 u) - 37 °C Ou *Bam*Hi (20.000 u) - 37 °C	10U/µL 10%	5
Tampão 10x	--	5
Água Miliq	--	35
TOTAL		**50**

Para a obtenção do gene repórter E2-crimsom, o plasmídeo pNUSE2-crimsom Blast foi submetido a digestão com as enzimas de restrição *Apa*1 e *Bam*HI. A reação de digestão foi realizada como descrito na tabela 1. Após a digestão, as amostras forma submetidas à eletroforese como descrito anteriormente (item 2.2.2).

Após a amplificação do gene de interesse, Clatrina, e a digestão dos genes repórteres, mScarlet e E2-crimsom (marcadores fluorescentes), foi preparada uma reação para unir os fragmentos 5' e 3' de Clatrina ao fragmento de mScarlet e E2crimsom. Para isso, foram utilizados primers desenhados através da plataforma www.richardwheeler.net/interactive/bioinf/dnatools (primers 20b e 21b). Foram usados 5 ciclos de amplificação em termociclador com temperaturada de 55 °C por 30 segundos, para gerar os moldes e estes posteriormente foram re-amplificados (30 ciclos, temperatura e tempo), na mesma reação adicionando os primers específicos para cada gene. Por fim, as amostras foram submetidas à eletroforese para a verificação do fragmento corresponde ao plasmídeo gerado contendo o gene de interesse fusionado ao gene repórter (Figura 3).

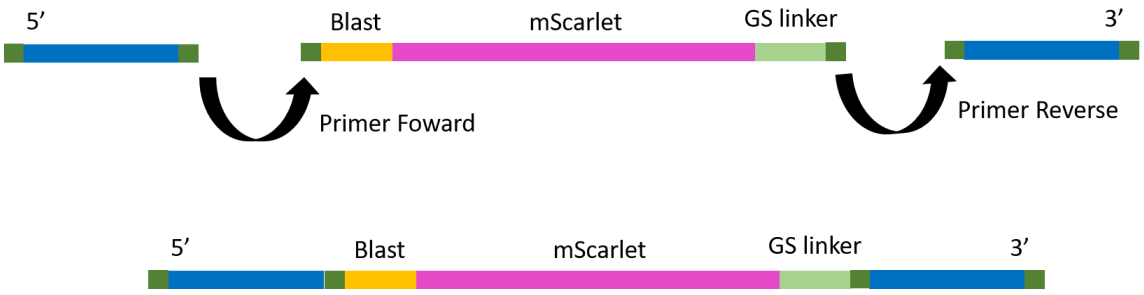

Figura 3. Esquema representativo de PCR de fusão com as extremidades 5' e 3' para clatrina e fragmento de mScarlet com gene de resistência para blasticidina.

2.3. GERAÇÃO DO PLASMÍDEO pPOTV7E2CRIMSOM BLAST

O plasmídeo pPOTV7E2crimsomBlast foi desenhado no software Serial Cloner. Após o desenho *in silico*, bactérias *E.coli* contendo o plasmídeo pPOTV7mscarlet Blast foram cultivadas para a extração do DNA do plasmídeo assim como descrito no item 2.2.3. Após a extração do plasmídeo, o mesmo foi submetido à digestão com as enzimas *Bam*HI e *Hind*III. O fragmento contendo o plasmídeo sem o mScarlet foi extraído do gel de agarose, quantificado em nanodrop e armazenado à -20 °C.

O fragmento de E2-crimsom foi adquirido c omo descrito no item 2.4.3. Uma reação de ligação com o vetor comercial pGEM T-easy (Promega) foi preparada como sugere o fabricante (Figura 4).

Reaction Component	Standard Reaction	Positive Control	Background Control
2X Rapid Ligation Buffer, T4 DNA Ligase	5µl	5µl	5µl
pGEM®-T or pGEM®-T Easy Vector (50ng)	1µl	1µl	1µl
PCR product	Xµl*	–	–
Control Insert DNA	–	2µl	–
T4 DNA Ligase (3 Weiss units/µl)	1µl	1µl	1µl
nuclease-free water to a final volume of	**10µl**	**10µl**	**10µl**

*Molar ratio of PCR product:vector may require optimization.

Figura 4. Reação de ligação com pGEM T-easy Promega.

Após a preparação da reação, as amostras foram inseridas em bactérias competentes (descrita no item 2.3.1). A reação foi adicionada junto às bactérias competentes e incubadas à 42 °C por 1:30 min, em seguida incubados em gelo por 5 min. Por fim, foi adicionado 100 µL da solução de bactérias em placas contendo LB ágar com ampicilina. As amostras foram incubadas por 24 h à 37 °C.

As colônias com crescimento positivo, foram submetidas à PCR com os primers 22b e 23b (para detecção de E2-crimsom –Anexo 1), inoculadas em meio LB liquido com ampicilina e incubadas à 37 °C sob agitação de 200 rpm. Após 24 h, foi realizado a extração de DNA das bactérias (item 2.2.3) para obter o pGEME2-crimsom. Os plasmídeos foram submetidos a uma nova PCR para amplificação do fragmento de E2-crimsom e então, purificado com o kit QIAquick gel extraction de acordo com o fabricante.

Com o plasmídeo pPOTV7 e o fragmento de E2-crimsom foi realizada uma ligação com DNA T4 ligase (Promega) com diferentes proporções entre os fragmentos, como sugere o fabricante (Tabela 2). A reação foi incubada em gelo por 5 min, submetidas ao choque térmicos à 42 °C durante 1:30 e incubados novamente em gelo por 5 min. A solução foi inoculada em LB ágar e incubadas à 37 °C. As colônias positivas foram submetidas a PCR para a verificação do fragmento E2-crimsom (Figura 5).

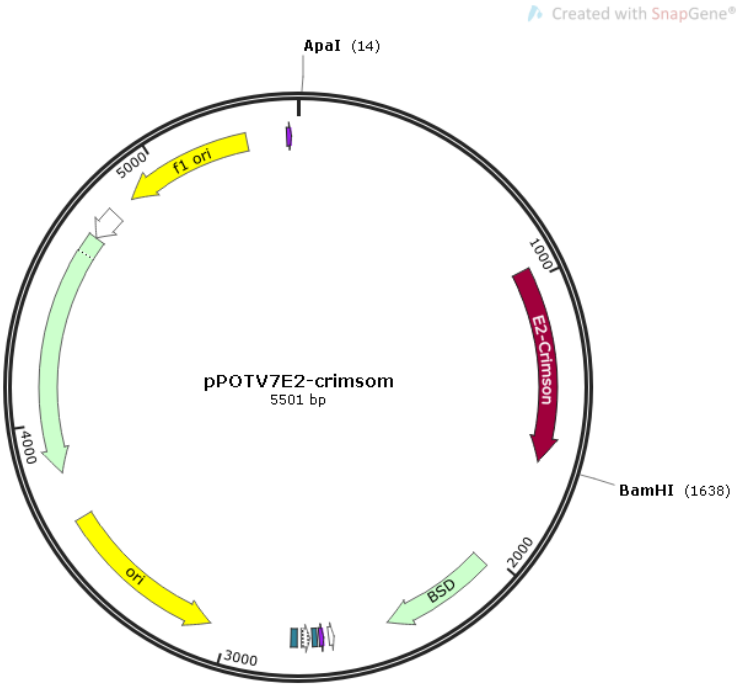

Figura 5. Plasmídeo pPOTV7E2-crimsom *in silico* após a ligação do pPOTV7 e o E2-crimsom usando o software Serial Cloner.

Tabela 2. Reação de ligação de fragmentos com T4 ligase.

Componente	Concentração	Razão 1:1	Razão 1:3	Razão 1:6	Razão 3:1
Vetor DNA	50ng	2.5ul	2.5	2.5	7.5
Inserto DNA	9ng	0.7ul	2	4.2	0.7
Tampão Ligase 10X	1µl	1ul	1	1	1
T4 DNA ligase	0.1u-1u	0.5ul	0.5	0.5	0.5
Água MiliQ	Para 10 µl	5.3ul	4	1.8	0.3

2.3.1. Bactérias competentes

E. coli, da cepa DH5α selvagem proveniente de uma única colônia foi inoculada em meio LB sem antibiótico. As bactérias foram incubadas por 24 h com

agitação de 200 rpm. Após, foi adicionado 4 mL de cultivo bacteriano em 100 mL de LB sem antibiótico e então as s bactérias foram incubadas novamente durante 1:30 h à 37 °C sob agitação ou até o crescimento bacteriano atingir a densidade óptica de 0.5 a 600 nm (após 1h de incubação a leitura foi realizada em espectrofotômetro a cada 10 min).

Uma vez alcançada a densidade óptica, o cultivo foi transferido para tubos falcons previamente resfriados e incubados em gelo por 10 min com o intuito de cessar o crescimento. Em uma centrifuga previamente refrigerada à 4 °C as bactérias foram centrifugadas à 3300 por 10 min. O sobrenadante foi descartado e acrescentado 20 mL de $CaCl_2$ 0,1M. Os pellets foram homogeneizados e centrifugados sob as mesmas condições.

As bactérias foram congeladas para uso futuro. Para isso, foi preparada uma solução de congelamento com 3mL de $CaCl_2$ 0,1M e 15% de glicerol estéril. O pellet bacteriano foi ressuspendido na solução de congelamento e as amostras foram aliquotadas em eppendorfs previamente resfriados (50-100 µL). As amostras foram congeladas em freezer à -80 °C imediatamente.

3. RESULTADOS

3.1. PCR DE FUSÃO

A proteína clatrina de *T. cruzi* executa um importante papel durante a formação de vesículas, colaborando para o transporte de diversas moléculas como lipídeos e proteínas, transporte trans-Golgi para o retículo endoplasmático e endocitose. Portanto, tendo proteína clatrina fusionada à um gene repórter (marcador), seria possível observar o controle da expressão e localização no protozoário após um tratamento, por exemplo (Kalb et al., 2014).

Foram obtidos fragmentos de clatrina de *T. cruzi* da extremidade 5’ e 3’ a partir da PCR e purificação do gel de agarose (Figura 6). Para a extremidade 5’ foram utilizados os primers 16b e 17b e para a extremidade 3’ os primers utilizados foram 18b e 19b (sequências anexo). Os fragmentos obtidos apresentaram tamanho de aproximadamente 480 pares de bases (pb). As purificações desses fragmentos foram quantificadas em nanodrop resultando em volumes de 26,1 ηg/µL de clatrina 5’ e 65 ηg/µL de clatrina 3’.

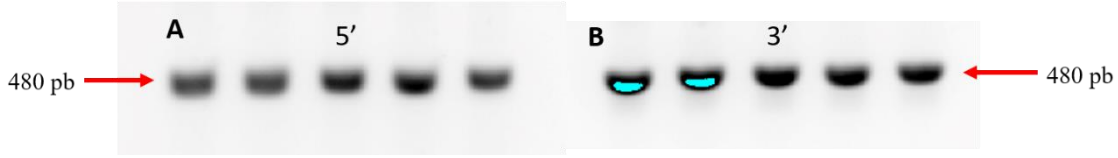

Figura 6. Perfil eletroforético em gel de agarose 1% dos produtos de PCR das extremidades 5’ e 3’ do gene que codifica a clatrina. Em (A) fragmentos 5’ com os primers 16b e 17b contendo 480 pares de bases. Em (B) fragmentos 3’ contendo 480 pb utilizando os primers 18b e 19b. A seta indica a massa molecular de 480 pb.

Para a obtenção dos genes repórteres, *E. coli* contendo os plasmídeos pPOTV7mScarlet Blast e pNUSE2-crimsom Blast, foram extraídos e quantificados em nanodrop. Foi extraído 4232,4 ηg/µL de pPOTV7mScarlet Blast e 4533,6 ηg/µL de pNUSE2-crimsom. Os plasmídeos foram submetidos a digestão em sítios específicos com as enzimas de restrição para a aquisição dos genes repórteres mScarlet e E2-crimsom.

O pPOTV7mScarlet Blast tem 5516 pb e foi digerido com as enzimas de restrição *Apa*1 e *Eco53ki*. O fragmento obtido com 1682 pb, indicou que o mScarlet e o gene de resistência para a blasticidina foram cortados nas regiões desejadas (Figura 7). Na união de um gene repórter e uma proteína de interesse é importante obter junto aos fragmentos um gene de resistência a antibióticos, pois quando inseridos em micro-

organismo como o *T. cruzi*, o antibiótico será a forma de seleção de população com o gene de interesse.

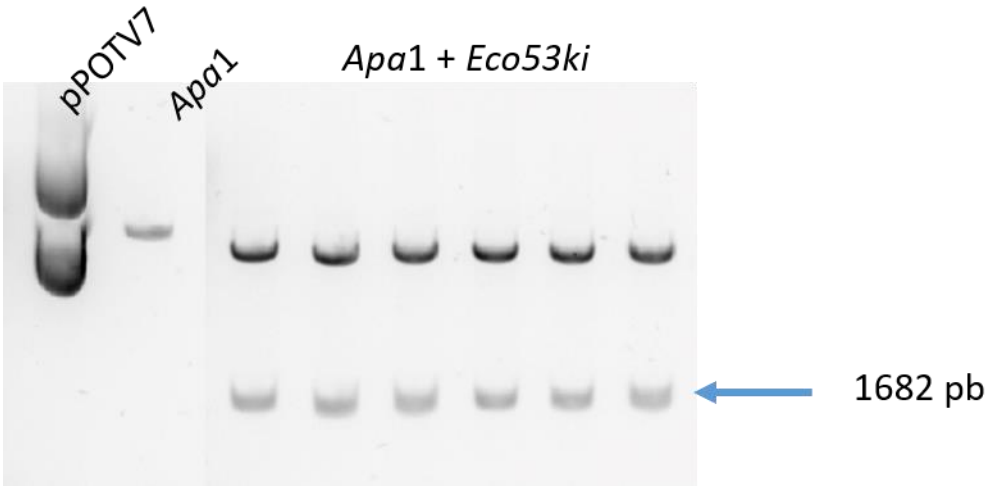

Figura 7. Perfil eletroforético em gel de agarose 1% dos produtos da extração de DNA do plasmídeo pPOTV7mScarlet Blast digerido com as enzimas de restrição *Apa*1 e *Eco53ki*.

O plasmídeo pNUSE2-crimsom Blast foi digerido com as enzimas *Bam*HI e *Hind*III. O fragmento obtido com 1720 pb, indicou que o E2-crimsom e o gene de resistência para a blasticidina foram cortados nas regiões desejadas (Figura 8).

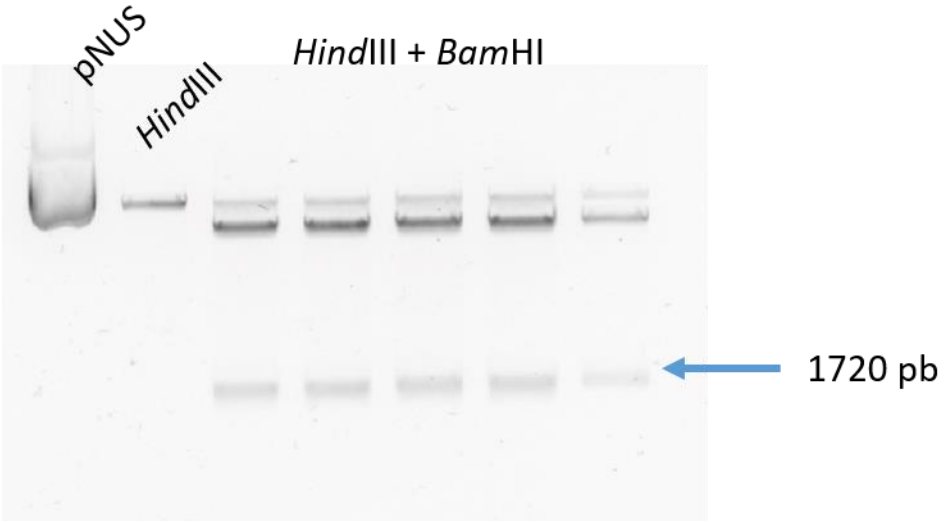

Figura 8. Perfil eletroforético em gel de agarose 1% dos produtos da extração de DNA do plasmídeo pNUSE2-crimsom Blast digerido com as enzimas de restrição *Hind*III e *Bam*Hi.

A PCR de fusão entre a clatrina e a o gene repórter mScarlet teria que gerar um fragmento de 2680 pb. No entanto, o fragmento não foi obtido. Como protocolos alternativos para tentativa de realizar a fusão, foram realizadas PCR's com diferentes concentrações de $MgCl_2$ (1,5, 2,5 e 3,5 mM), pois é um importante co-fator da DNA polimerase. Outra alteração foi a quantidade de gene repórter inserido, de 20 ŋg, foram realizadas PCR de fusão com 20 e 40 ŋg. A fusão não ocorreu em nenhum dos casos, tando para mScarlet + Clatrina quanto pra E2-crimsom + Clatrina. Visto que a metodologia utilizada neste trabalho é relativamente nova (Dean et al., 2015), seria ideal aperfeiçoar a metodologia para cada protozoário e gene de interesse (tentar achar artigos que usaram a técnica). Como o tempo de doutorado sanduíche foi de 6 meses, optou-se por testar outra metodologia para obtenção dos protozoários modificados.

3.2. GERAÇÃO DO PLASMÍDEO pPOTV7E2Crimsom BLAST

A geração do plasmídeo pPOTV7E2-crimsom é interessante pois possibilita estudos *in vivo* com maior clareza e facilidade (Strack et al., 2009). A inserção de E2-crimsom no plasmídeo possibilita análises com maior qualidade, pois não interfere com a autofluorescência dos animais pois tem excitação de 611 nm e emissão de 646 nm. Diferente da proteína mScarlet que tem excitação de 569 e emissão de 594 nm e por isso, gera interferência com pelos de camundongos que produzem autofluorescência verde. Ainda, o E2-crimsom apresenta alta fotoestabilidade, alta solubilidade, baixa citotoxicidade e é facilmente detectável (Goyard et al., 2014).

O plasmídeo pPOTV7mScarlet foi extraído a partir de bactérias *E. coli*, DH5α, onde foram adquiridos 4430,0 ng/µL. A digestão com as enzimas *Bam*Hi e *Hind*III

possibilitou a linearização do plasmídeo e a retirada da proteína fluorescente mScarlet. O plasmídeo linearizado foi obtido com 60 ng/µL.

O E2-crimsom foi amplificado por PCR com os primers 22b e 23b e inserido por uma reação de ligação em um vetor comercial, o pGEM T-easy, a fim de aumentar a eficiência durante a clonagem. Por transformação bacteriana foi possível obter colônias com pGEME2-crimsom (Figura 9). O plasmídeo pGEME2-crimsom foi extraído de bactérias, linearizado com enzimas *Bam*Hi e *Hind*III e o fragmento de E2-crimsom foi purificado do gel de agarose e obtido 37, 2 ng/µL do fragmento.

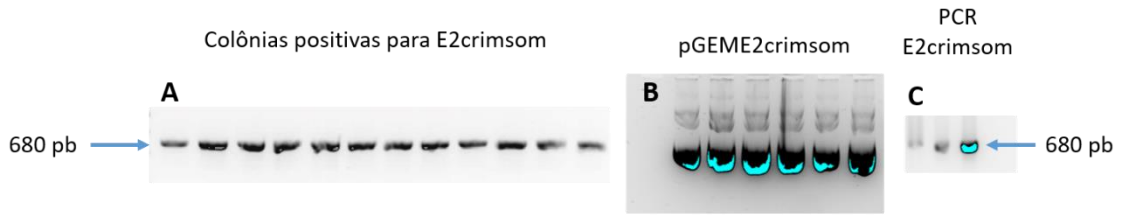

Figura 9. Perfil eletroforético em gel de agarose dos produtos da PCR para obtenção do plasmídeo pGEME2-crimsom. Em (A) colônias positivas para E2-crimsom após a ligação em pGEM T-easy. Em (B) extração de DNA do pGEME2-crimsom. Em (C) confirmação de E2-crimsom em colônias de bactéria E. coli, DH5α contendo o plasmídeo pGEME2-crimsom.

Para inserção do gene que codifica a proteína E2-crimsom, foi utilizada uma reação de ligação com a DNAT4 ligase, pois facilita a união das cadeias de DNA. Após a ligação o plasmídeo foi inserido em bactérias competentes e após 24h foi verificado por PCR que as colônias presentes continham o E2-crimsom (Figura 10).

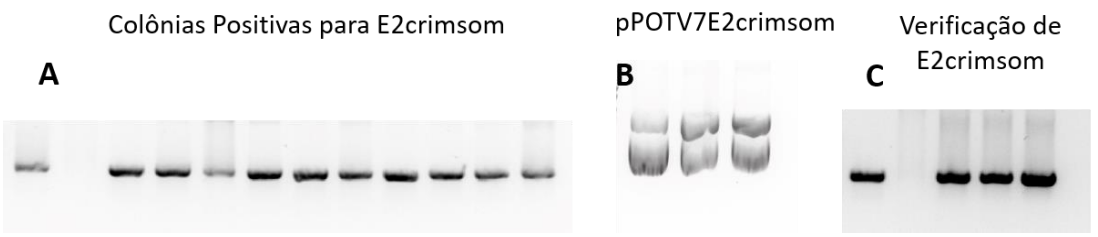

Figura 10. Perfil eletroforético em gel de agarose dos produtos da PCR para obtenção do plasmídeo pPOTV7E2-crimsom. Em (A) colônias positivas para E2crimsom após a ligação em pPOTV7E2-crimsom. Em (B) extração de DNA do pPOTV7E2-crimsom. Em (C) confirmação de E2-crimsom no plasmídeo em bactérias *E. coli*, DH5α contendo o pPOTV7E2-crimsom.

4. CONCLUSÕES E PERSPECTIVAS

As técnicas aplicadas durante o doutorado sanduiche possibilitaram obter conhecimento sobre maquinaria molecular de *T.cruzi*, assim como o aprendizado de diversas técnicas de biologia molecular.

A técnica de PCR de fusão seria de grande importância no estudo de mecanismo de ação de substâncias. No entanto, são necessários ajustes de protocolo para novas tentativas, pois essa técnica é relativamente nova e seria necessário mais tempo para padroniza-la para utilização com os genes escolhidos.

Com o plasmídeo pPOTV7E2-crimsom será realizado a transfecção de acordo com Pacheco-Lugo 2017 em formas epimastigotas de *T. cruzi* para uso em futuros projetos de pesquisas (Pacheco-Lugo, 2017).

5. REFERENCIAS

Dean, S., Sunter, J., Wheeler, R. J., Hodkinson, I., Gluenz, E., & Gull, K. (2015). A toolkit enabling efficient, scalable and reproducible gene tagging in trypanosomatids. *Open Biology*, *5*(1).

Goyard, S., Dutra, P. L., Deolindo, P., Autheman, D., D'Archivio, S., & Minoprio, P. (2014). In vivo imaging of trypanosomes for a better assessment of host–parasite relationships and drug efficacy. *Parasitology International*, *63*(1), 260–268.

Kalb, L. C., Antunes Frederico, Y. C., Batista, C. M., Eger, I., Fragoso, S. P., & Soares, M. J. (2014). Clathrin expression in *Trypanosoma cruzi*. *BMC Cell Biology*, *15*(1).

Pacheco-Lugo, L., Díaz-Olmos, Y., Sáenz-García, J., Probst, C. M., & DaRocha, W. D.

(2017). Effective gene delivery to *Trypanosoma cruzi* epimastigotes through nucleofection. *Parasitology International*, *66*(3), 236–239.

Strack, R. L., Hein, B., Bhattacharyya, D., Hell, S. W., Keenan, R. J., & Glick, B. S. (2009). A Rapidly Maturing Far-Red Derivative of DsRed-Express2 for Whole-Cell Labeling. *Biochemistry*, *48*(35), 8279–8281.

ANEXOS

- **Sequencias de primers (Invitrogen)**
- *Para a fusão de pPOTV7mScarlet Blast e proteína Clatrina*

5'
16b - 5´TF Tc00.1047053503449.30: CTTAAGGATGAGAATACAGC
17b - 5´TR Tc00.1047053503449.30: gctgtgcccctagcttGGCTCAAGTTCCTACCC

3'
18b - 3´TF Tc00.1047053503449.30:
gatcaggatcgggtagtATGAATGTGAAAGATTCTAATG
19b - 3´TR Tc00.1047053503449.30: CTCCAAACGATTATCAACAC

20b - ATACAGCCCTTCGGAAAC
21b - TGCCTCCTGTGAAATTGC

- *E2 crimson para inserir no pPOTv7 mscarlet Blast*

22b (*Hind*III): aagcttATGGATAGCACTGAGAACGT
23b (*Bam*HI): ggatccCTGGAACAGGTGGTGGC

APÊNDICE 2 – Ensaios *in vivo* das substâncias C5 e A11K3 em camundongos Balb/c infectados com os protozoários *Leishmania amazonensis* e *Trypanosoma cruzi*

INTRODUÇÃO

Doenças Tropicais Negligenciadas, por serem um relevante problema de saúde pública, estão atraindo a atenção mundial (WHO, 2019).

A doença de Chagas, causada pelo protozoário *Trypanosoma cruzi*, encontrada em 21 países, afeta cerca de 8 milhões de pessoas com uma incidência de aproximadamente 50.000 novos casos por ano (WHO, 2019). A américa latina concentra maior número de casos da doença de Chagas que se tornou problema mundial de saúde em decorrência da migração para países não endêmicos afetando Austrália, Europa, USA e Canadá, resultando em um custo de tratamento anual de aproximadamente $600 milhões (Lee et al., 2013).

A patogênese da doença de Chagas subdivide-se em fase aguda caracterizada por inflamações inespecíficas, seguida fase indeterminada assintomática ou progride para fase crônica onde cerca de 30-40% dos casos desenvolve lesões cardiovasculares, gastrointestinais e neurológicas irreversíveis (Barret et al.,2003; Rassi et al., 2012).

Tradicionalmente, a transmissão da doença de Chagas ocorre por meio da picada e defecação de insetos contaminadas da subfamília T*riatominae* (Hemiptera, Reduviidae), entretanto pode decorrer de transfusão sanguínea, transmissão congenita e oral com alimentos contaminados (Rassi et al., 2010; Lescure et al., 2010).

A leishmaniose é endêmica em 98 países em todo mundo, com cerca de 350 milhões de pessoas em risco de contágio e 12 milhões de pessoas infectadas. Provocada por mais de 20 espécies do protozoário *Leishmania sp.* as manifestações clínicas subdivide-se em cutânea, mucocutânea e visceral. A leishmaniose cutânea é a forma clínica mais comum com 1,5 milhões de novos casos por ano, as espécies que se destacam são *L. amazonensis, L. braziliensis e L. guyanensis* (Herwaldt et al. 1999; Murray et al., 2005; WHO 2019).

Dentre os casos mundiais de leishmaniose cutânea 70 a 75% concentram-se em 10 países, dentre estes encontra-se o Brasil, com cerca de 30.000 casos somente em 2010 (Alvar et al., 2012). A transmissão ocorre pela picada da fêmea de flebotomínio, dos gêneros é *Phlebotomus* e *Lutzomyia* (Goto et al., 2012). As manifestações clínicas

caracterizam-se por lesões únicas ou múltiplas geralmente localizadas em pernas, braços e cabeça, inicialmente como pápulas, progridem para nódulo até atingirem lesão ulcerosa (Olliaro, 2013).

Atualmente, compostos nitroderivados como benzonidazol e nifurtimox são responsáveis pelo tratamento da doença de Chagas, porém apresentam eficácia limitada na fase crônica da patologia e as reações adversas são comuns em cerca de 40% dos pacientes (Buckner et al., 2010, Izumi et al.,2011). A leishmaniose tem como tratamento antimoniais pentavalentes (antimoniato de meglumina e estibogluconato de sódio), anfotericina B, pentamidina e miltefosina, do qual também possuem eficácia variada devido a toxicidade e; dificuldade de tratamento devido ao alto custo das aplicações intravenosas (Reithinger et al.,2007; Oliveira et al.,2011; Tiuman et al., 2011).

Para ambas as doenças o tratamento apresenta severos efeitos colaterais, longo tempo de tratamento e variabilidade na eficácia. Esses fatores fomentam a busca por novas alternativas terapêuticas (Barret et al., 2012). Dessa forma, o estudo avaliou a atividade *in vivo* da substâncias **C5** em camundongos infectados com *L. amazonensis* e a substância **A11K3** em camundongos infectados com *T.cruzi*, afim de avaliar o potencial anti-protozoários em camundongos Balb/c.

MÉTODOS E RESULTADOS

1. Avaliação *in vivo* de camundongos BALB/*c* infectados com *L. amazonensis* e tratados com C5

Os camundongos foram cedidos pelo biotério da Universidade Estadual de Maringá com o projeto aprovado pelo comitê de ética (CEUA-UEM) com o projeto intitulado ‘’Atividade de β- carbonilico **C5** em modelo murinho de leishmaniose cutânea’’ com número de aprovação 7542040717.

Os camundongos foram infectados com formas promastigotas de *L. amazonensis* na pata esquerda. Após o aparecimento das lesões (aproximadamente 8 semanas) o tratamento foi iniciado.

Os 7 grupos foram compostos por 5 animais:

1. Controle negativo: não infectado e não tratado
2. Controle positivo: infectado e não tratado
3. Infectado e tratado com Miltefosina
4. Infectado e tratado com **C5** oral 20 mg/kg/dia

5. Infectado e tratado com **C5** oral 50 mg/kg/dia
6. Infectado e tratado com **C5** tópico 50 mg/kg/dia
7. Toxicidade: não infectado e tratado com **C5** oral 50 mg/kg/dia

O tratamento foi realizado durante 30 dias. Após esse período, foi coletado o sangue por punção cardíaca e então, os camundongos foram sacrificados e realizado a coleta da lesão e órgãos. Com o sangue foram analisados níveis de colesterol, glicose, creatinina, TGO, TGP (tabela 1). As patas foram diariamente medidas e no final do experimento o exudato foi coletado para a análise de parasitemia (figura 1).

Tabela 1. Análises do soro do sangue de camundongos Balb/C infectados com *Leishmania amazonensis* e tratado com o β-carbonílico **C5**.

PARÂMETROS	**GLICOSE**	**COLESTEROL**	**CREATININA**	**TGO/AST**	**TGP/ALT**
Grupos	**mg/dL**	**mg/dL**	**mg/dL**	**U/ml**	**U/ml**
G1-CN	90,6±10,2	196,7±17,2	0,43±0,03	86,5±11,9	369,1±10,9
G2-CP	57,2±7,5	200,6±4,2	0,20±0,05	108,3±38	348,1±9,1
G3-MIL	85,7±15,3	225,5±8,4	0,56±0,03	61,4±10,21	335,8±6,8
G4-C5O 20mg	87,5±16,2	232,2±37,2	0,16±0,04	56,2±17,7	354,6±7,5
G5-C5O 50mg	64,6±12,1	198,7±19,7	0,46±0,03	78,9±13,7	336,7±5,4
G6-C5T 50mg	86,1±12,9	195,8±13	0,76±1,2	68,1±10,2	347,4±8,6
G7-CPT creme	95,1±24,9	193,2±60,3	0,52±0,04	62,5±4,1	345,4±11,3
G8-TOX 50mg	76,8±22,3	172,9±40,4	0,86±1,45	59,8±5,8	348,2±12,9
Soro negativo	61,2±0	224,2±0	0,54±0	380,4±0	357,4±0
Soro Patológico	170,7±0	372,3±0	2,31±0	113,8±0	346±0
Referencia	92,7	119,2	0,27	24,2	27,0

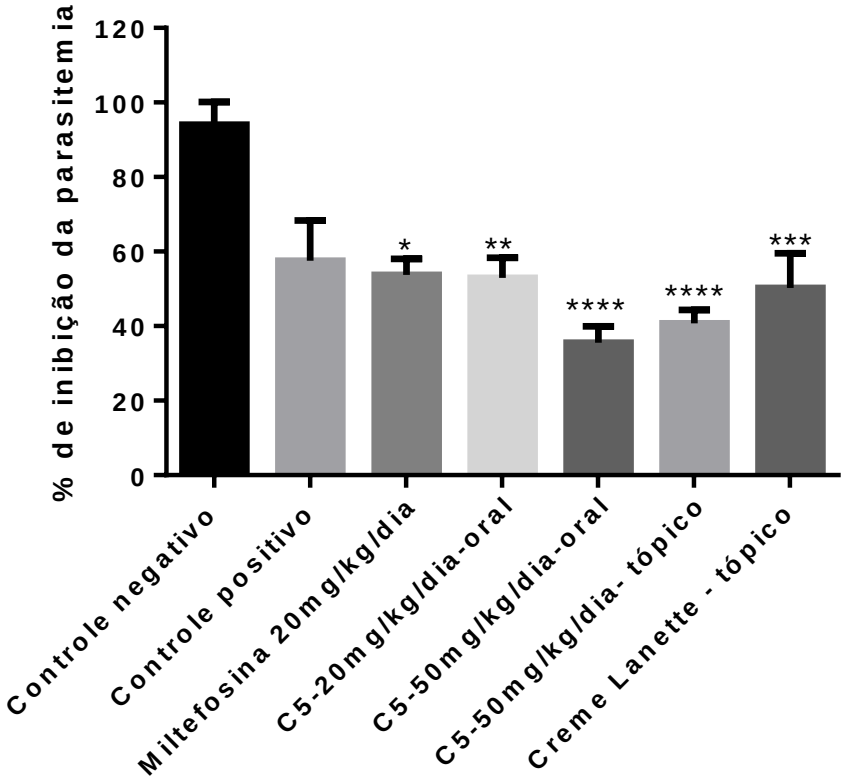

Figura 1. Percentual de inibição da parasitemia de camundongos Balb/C infectados com *L. amazonensis* e tratados com a substância C5. Os asteriscos indicam diferentes significâncias comparado com o controle negativo; Two-way ANOVA seguindo o Bonferronifoi utilizado onde *$p \leq 0.05$; **$p \leq 0.01$; *** $p \leq 0.001$; ****$p \leq 0.0001$.

Durante o decorrer do experimento não foram observadas alterações significativas no peso dos animais (figura 2). O tamanho da lesão diminui em ambos tratamentos, assim como a carga parasitária (oral e tópico), com 88,9% de redução nos grupos tratados com **C5** de 50 mg/kg/dia e 11,2% de redução nas patas tratadas com **C5** topicamente (figura 3).

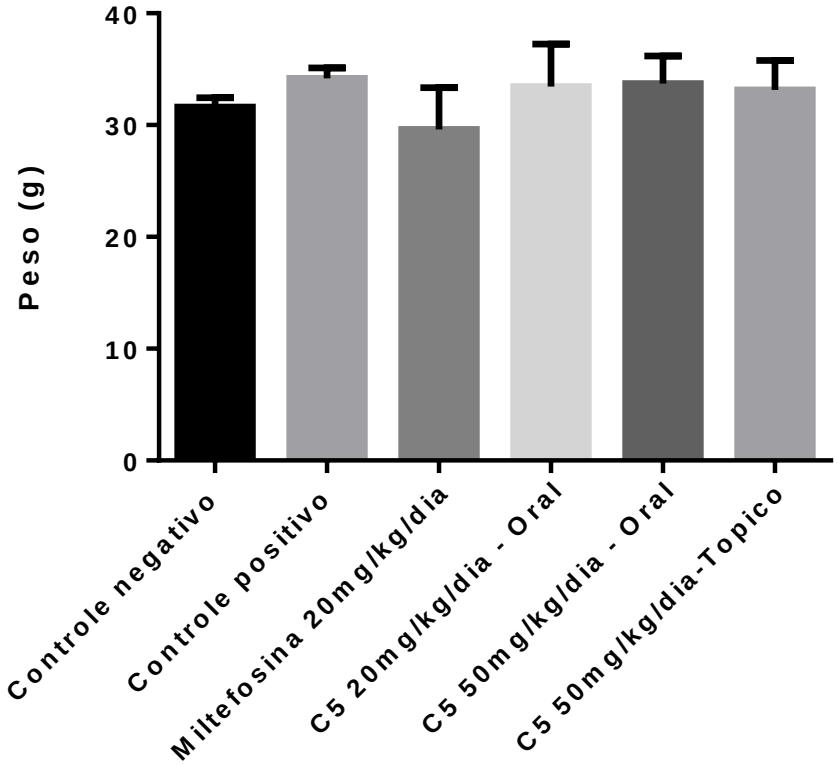

Figura 2. Variação de peso de camundongos infectados com L. amazonensis e tratados com a substâncica C5 por 30 dias.

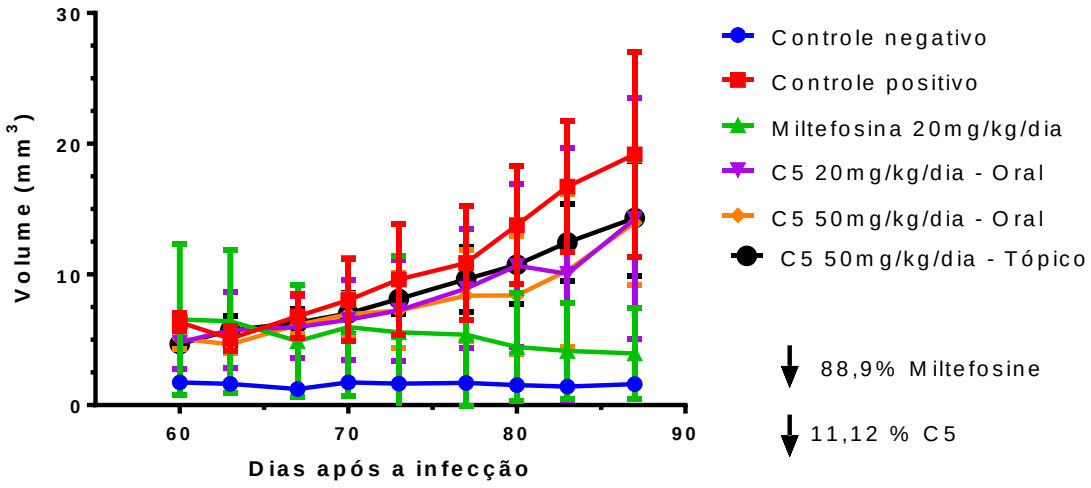

Figura 3. Volume da lesão da pata de camundongos infectados com *L. amazonensis* e tratados com a substância C5 oral e tópico por 30 dias.

2. Avaliação *in vivo* de camundongos BALB/*c* infectados com *Trypanosoma cruzi* e tratados com A11K3

Os camundongos foram cedidos pelo biotério da Universidade Estadual de Maringá com o projeto aprovado pelo comitê de ética (CEUA-UEM) com o projeto intitulado ‘’Atividade Biológica da Dibenzilidenoacetona **A11K3** em camundongos infectados com *Trypanosoma cruzi’’* com número de aprovação 3323040717.

Os camundongos foram infectados com formas tripomastigotas de *T. cruzi* na pata esquerda. Após três dias de infecção (d.p.i.).

o tratamento foi iniciado e contagem de parasitemia foi determinada todos os dias.

Os 6 grupos foram compostos por 5 animais:

1. Controle negativo: não infectado e não tratado
2. Controle positivo: infectado e tratado com 1% de DMSO
3. Infectado e tratado com benznidazol oral 5mg/kg/dia
4. Infectado e tratado com benznidazol oral 100mg/kg/dia
5. Infectado e tratado com **A11K3** oral 5mg/kg/dia
6. Infectado e tratado com **A11K3** oral 100 mg/kg/dia

O tratamento mostrou toxicidade, pois o percentual de sobrevivência após 12 dias de tratamentos para os grupos tratados com a substância **A11K3** foi de 33,3 %, enquanto que os camundongos tratados com benznidazol tiveram um índice de sobrevivência de 100% (Figura 1).

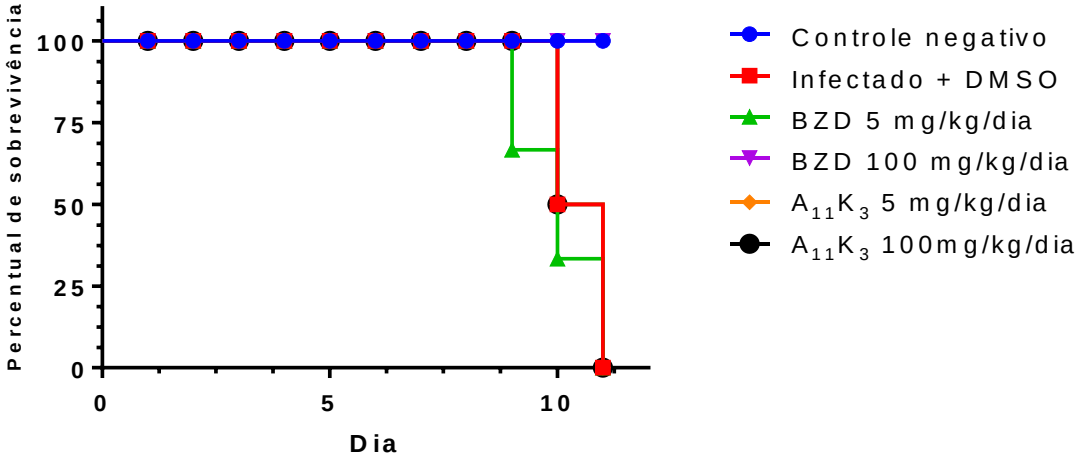

Figura 1. Percentual de sobrevivência de camundongos Balb/c infectados com *T. cruzi* e tratados com a substância A11K3 por 12 dias.

O tratamento com benzonidazol gerou uma diminuição significativa na parasitemia durante os dois picos de infecção (7 e 14 dias após a infecção) com 33,8 e 44,6 % para o tratamento com 5 mg/kg/dia e 100 mg/kg/dia no sétimo dia e 35,7 e 10,0 % no décimo quarto d.p.i. Os grupos tratados com **A11K3** mostraram resultados significativos no segundo pico de infecção (14 dias) com diminuição da parasitemia de 52,8 % no grupo tratado com 5 mg/kg/dia de **A11K3**.

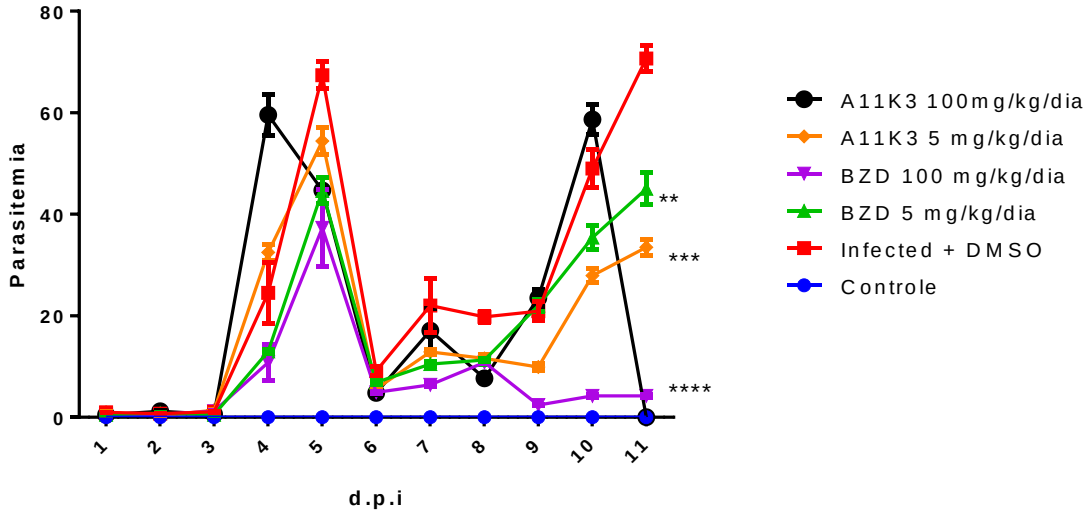

Figura 2. Parasitemia do sangue de camundongos Balb/c infectados com *T. cruzi*. Os asteriscos indicam diferentes significâncias comparado com o controle positivo; Two-way ANOVA seguindo o Bonferronifoi utilizado onde: $^{**}p \leq 0.01$; $^{***}\ p \leq 0.001$; $^{****}p \leq 0.0001$.

CONCLUSÕES

As substâncias analisadas *in vivo* foram parcialmente eficazes na diminuição da parasitemia de *L. amazonensis* e *T. cruzi*, porém mais estudos são necessários para aumentar a solubilidade das substâncias, aumentando a atividade contra os protozoários e diminuindo de acumulo em órgãos. Além disso, estudos futuros com aplicações de nanopartículas são de extrema importância, pois a tecnologia permite a diminuição da toxicidade e permanência da atividade.

REFERÊNCIAS

Alvar, J. Et Al. Leishmaniasis Worldwide And Global Estimates Of Its Incidence. Plos One, V. 7, P. E35671, 2012.

Barret, M. P. Et Al. The Trypanosomiases. The Lancet, V. 362, P. 1469-1480, 2003.

Buckner, F. S.; Navabi, N. Advances In Chagas Disease Drug Development: 2009-2010. Current Opinion In Infectious Diseases, V. 23, P. 609-616, 2010.

Herwaldt, B. L. Leishmaniasis. Lancet, V. 354, P. 1191-1199, 1999.

Izumi, E. Et Al. Natural Products And Chagas'disease: A Review Of Plant Compounds Studied For Activity Against Trypanosoma Cruzi. Natural Product Reports, V. 28, P. 809-823, 2011.

Goto, H.; Lindoso, J. A. L. Cutaneous And Mucocutaneous Leishmaniasis. Infectious Disease Clinics Of North America, V. 26, P. 293-307, 2012.

Lee, S. B. Et Al. 2,3,6-Trisubstituted Quinoxaline Derivative, A Small Molecule Inhibitor Of The Wnt/Beta-Catenin Signaling Pathway, Suppresses Cell Proliferation And Enhances Radiosensitivity In A549/Wnt2 Cells. Biophysical Research Communications, V. 431, P. 746-752, 2013.

Lescure, F.-X. Et Al. Chagas Disease: Changes In Knowledge And Management. The Lancet Infectious Diseases, V. 10, P. 556-570, 2010

Murray, H. W. Et Al. Advances In Leishmaniasis. The Lancet, V. 366, P. 1561-1577, 2005.

Olliaro, P. Et Al. Methodology Of Clinical Trials Aimed At Assessing Interventions For Cutaneous Leishmaniasis. Plos Neglected Tropical Diseases, V. 7, P. E2130, 2013.

Oliveira, L. F. Et Al. Systematic Review Of The Adverse Effects Of Cutaneous Leishmaniasis Treatment In The New World. Acta Tropica, V. 118, P. 87-96, 2011.

Rassi Jr., A.; Rassi, A.; Rezende, J. M. D. American Trypanosomiasis (Chagas Disease). Infectious Disease Clinics Of North America, V. 26, P. 275-291, 2012.

Rassi Jr., A.; Rassi, A.; Marin-Neto, J. A. Chagas Disease. The Lancet, V. 375, P. 1388-1402, 2010.

Reithinger, R. Et Al. Cutaneous Leishmaniasis. The Lancet, V. 7, P. 581-596, 2007.

Tiuman, T. S. Et Al. Recent Advances In Leishmaniasis Treatment. International Journal Of Infectious Diseases, V. 15, P. 525-532, 2011.

Who, Neglected Tropical Diseases, Hidden Successes, Emerging Opportunities. Department Of Control Of Neglected Tropical Diseases. 2019.